AN ELECTRON SPIN RESONANCE STUDY OF Cu(II) PEPTIDE COMPLEXES

by

Dennis C. Gould, B.S.

A THESIS
Presented to the Department of Biochemistry
and the Graduate Division of
The University of Oregon Medical School
in partial fulfillment of
the requirements for the degree of
Doctor of Philosophy
June 1966

APPROVED: [redacted]

Professor in Charge of Thesis

[redacted]

Chairman, Graduate Council

Financial support through a National Institutes of Health predoctoral fellowship and through grants from the United States Public Health Service and through a Woodrow Wilson fellowship is gratefully acknowledged.

For his confidence in me and guidance during the course of this research and for much needed assistance during my training I am greatly indebted to Professor H. S. Mason. His efforts are appreciated.

Dedication

To My Wife

TABLE OF CONTENTS

LIST OF FIGURES

LIST OF TABLES

APPENDICES

I INTRODUCTION

1. Statement of Problem

This thesis is concerned with the determination of the structure of the Cu(II)-peptide complexes in solution.

While the nature and disposition of four ligand atoms about iron in heme proteins is known, the groups which bind copper to copper proteins are unidentified; none of the possible two to six ligand atoms binding copper has been determined in any copper protein (72).

The identification of the atoms binding the iron atom in the heme proteins is facilitated by the stability of the hematin system, but no such stable structure exists in copper proteins. For this reason, the characterization of active sites containing copper has proved both difficult and exceptionally challenging.

Structural studies on biochemical systems explain biochemical function and mechanism of action. Structure can be defined operationally; certain measurable properties of a specific system are associated with specific structural features. The systems to be discussed in this thesis are Cu(II)-peptides and the measurable properties are characteristics of their ESR absorption spectra. The structural features that can be drawn from the ESR absorption spectra will be considered in the Discussion.

In general, the problem of structure determination could be solved by either a direct or an indirect method. The direct method would be the determination of the structure of the protein by x-ray analysis.

Several indirect approaches are possible, most involving chemical characteristics of the binding groups and selective chemical modification of these groups. In the present study, an attempt has been made to approach the problem by characterizing simple model chelates of Cu(II) and peptides of increasing complexity, using a technique which is highly sensitive to ligand-copper interaction, namely, electron spin resonance. This experimental approach to the determination of the copper-protein structure is based on the assumption that the ESR characteristics of the model complexes, identified in copper proteins, may establish the structure of the latter.

The direct determination of structure, x-ray analysis, gives the three dimensional arrangement of the atoms making up a system, with a resolution of about 2 Å. However, determination of the spacial arrangements of the atoms in this manner is not sufficient to establish a biochemical structure-function relationship because the structural equivalence of the crystalline and dissoved states is uncertain. In addition, the determination of the spacial arrangement of the atoms about the Cu(II) atom may not provide a significant structure-function relationship. The fact that the iron atom is bound at the center of the porphyrin ring in the heme proteins has given little indication of why the heme protein is better suited for rapid electron transport than uncomplexed iron atoms. A calculation of electronic energy levels in heme by quantum mechanical methods (91) has given a significant structure-function correlation in that the binding of the iron by the porphyrin ring alters the energy levels of the iron atom in such a way that it

is better suited for rapid electron transport than is the uncomplexed iron atom. The calculation gave results which show that the highest lying orbital of ferroporphyrin has an energy generally associated only with excited states. Thus the energy needed to remove an electron will be less than for the uncomplexed iron atom and ferroporphyrin will possess strong electron donor properties. The disposition of the energy levels in the ferriporphyrin molecule is such that the compound possesses pronounced electron acceptor properties. It is on such a basis that determination of electron distributions and energy levels increases the possibility of making structure-function correlations. While it is possible, in principle, to calculate electron probability distributions and energy levels from the spacial arrangements of the atoms, the approximations necessary to make such a calculation make its value doubtful. Orgel has emphasized this point in discussing Ingraham's calculations for oxyhemoglobin (47).

As will be shown, however, ESR gives experimental data from which electron probability distributions can be calculated under certain conditions.

The use of model compounds for the study of structure and mechanism of action in biological systems is a commonly used technique. The shortcoming of such a study is that the relationship between the biological system and the model may be poor. However, the model systems are relatively simple and straightforward. The crucial experiment then becomes the establishment of the relationship of the model system to the biological system.

As most results dealt with in the review are obtained from ESR measurements, a review of ESR theory will first be given. A review of structural studies on Cu(II) peptide complexes, model Cu(II) proteins, and the naturally occurring copper proteins, with emphasis being given ESR studies, will complete the Introduction.

2. ESR Theory*

A. General Considerations

In 1885 Balmer showed that the spectral series for atomic hydrogen from 6562 Å to ~3500 Å could be expressed by a simple formula. However, even before 1916 it was apparent that this formula could not account for the further splitting of many of these spectral lines; the fine structure of the spectra (89). Of the early explanations offered to explain this phenomenon, all contained contradictions. However, the proposal of Uhlenbeck and Goudsmit (107), made in 1926, resolved the previous difficulties by attributing to the electron the properties of angular momentum and magnetic moment. These are properties that would be associated with a charged body spinning about an axis passing through it. Thus their postulate is often described as a postulate of electron spin.

As required by experimental data, only two values of the spin angular momentum are allowed, $1/2(h/2\pi)$ and $-1/2(h/2\pi)$ (89). The spin angular momentum must be multiplied by the factor $2(e/2m_oc)$ to obtain the spin magnetic moment. The orbital angular momentum is multiplied by the factor $e/2m_oc$ to obtain the orbital magnetic moment; this is the result expected from classical electromagnetic theory. The extra factor 2 in the expression for the spin magnetic moment is called the Lande g factor.

* The articles of Androes and Calvin (3), Wertz (113), Carrington (21), Sogo and Tolbert (101), or Beinert and Palmer (8) should be consulted for a thorough review of ESR and its applications to biological systems.

Using methods of relativistic quantum mechanics, Dirac derived equations in which the spin and anomalous g factor 2 of the electron are automatically given; no separate postulate of spin was needed.

If the spin magnetic and angular moments are not affected by any external fields, the two orientations of the electron, corresponding to the magnetic moments $\pm 2eh/8m_o c\pi$, will be degenerate; that is, they will be of equal energy. If the system is then placed in a magnetic field H, the interaction energy between the magnetic dipole and the magnetic field is given by $(2eh/8m_o c\pi)H$ and $-(2eh/8m_o c\pi)H$ (49). The negative sign is associated with a magnetic moment anti-parallel to the field H and will be the high energy state. Thus the application of a field H removes the spin degeneracy and transitions between the two energy levels are possible. This energy difference is $2(eh/4m_o c\pi)H$ where the factor $eh/4m_o c$ is called the Bohr magneton and is denoted by β. Using the relationship $E=h\nu$, the transition between the lower and the upper energy level will occur when $h\nu = g\beta H$, where $g\beta H$ is separation of the two energy levels. (The Lande g factor 2 has been replaced by the more general term g.) Thus, for the simple system described, the absorption of energy (the absorption curve) will consist of a single line occurring where the value of ν and H satisfy the resonance condition given above. At a ν of 9,000 Mc/sec resonance will occur at H = 3,200 gauss for g=2.

In the model discussed above, electron spin resonance would provide little information since the resonance absorption would consist of a single line occurring at the same position regardless of the sample

used. In practice, the above description of ESR is, fortunately, inadequate. For one thing, the Lande g factor is not confined to the value 2 and deviations from this value provide information about the environment of the unpaired electron. Secondly, the field H "felt" by the electron is modified by the system in which the electron resides; interpretation of these ESR spectral modifications provides further information about the environment of the unpaired electron.

The methods of quantum mechanics must be used in describing the effects of the field and the deviation of the g values from 2 as seen in ESR absorption spectra. While it is beyond the scope of this thesis (and the author) to provide a rigorous discussion of the quantum mechanical methods involved, certain aspects of the theory must be given for an understanding of the experimental results obtained.

Of fundamental importance in the development of the theory is the approximation method of perturbation theory. In brief, since the wave equation for only the most simple molecular systems can be solved exactly, a method of approximation must be used. Certain factors contained in the total Hamiltonian* of the system under consideration are disregarded so that an equation simple enough to be solved is obtained. The factors which were disregarded are then considered as perturbations of the simple system. The wave functions and energy levels of the simple

* The Hamiltonian is the classical mechanical expression for the total energy of a system and is the kinetic plus the potential energy. For use in quantum mechanical calculations it is converted to operator form (63).

system are altered (corrected) by these perturbations and perturbation theory quantitates these effects. Pauling and Wilson (89) give a detailed development of the theory. It is an essential part of the theory that the perturbation effect be small; that is, the energy values and wave functions for the perturbed system will be only slightly altered over those of the unperturbed system. The energy for the perturbed system can then be expressed as $E=E^{o}+E^{1}+E^{2}+\ldots\ldots$ $(E^{o} \gg E^{1}, E^{2}, \ldots.)$ where E^{o} is the energy of the unperturbed system and E^{1}, E^{2}, etc. are the perturbation energies. For a system of non-degenerate levels these perturbation energies are given by (63)

$$(1) \qquad E_i = \int \psi_i^{o*} \mathcal{H}_i \psi_i^{o} \, d\tau$$

where the ψ_i^{o} are the solutions to the unperturbed Schrödinger equation and $\mathcal{H}_i$ is the Hamiltonian of the perturbation.

The interaction between the magnetic moment of an electron and a magnetic field H can be regarded as perturbing the electronic energy levels obtained in the absence of a field. Classically, this energy of interaction is given by $\vec{\mu}.\vec{H}$ in which $\vec{\mu}$ represents the magnetic moment of the electron and $\vec{H}$ represents the external magnetic field (63). In quantum mechanical notation the Hamiltonian for this perturbation is the operator $\mathcal{H}_i = g\beta \vec{S}_i \cdot \vec{H}$ (63). Taking $\vec{H}$ to be along the z-axis, $H=H_x\vec{i}+H_y\vec{j} + H_z\vec{k}$ where $H_x=H_y = 0$, gives $\mathcal{H}_i = g\beta S_{z_i} \cdot H_z$.
The spin only portion of the wave function for an unpaired electron can be either α, corresponding to $m_s = 1/2$ or β, corresponding to $m_s = -1/2$. Substitution into (1) then gives $E_\alpha = \int \alpha (g\beta S_z H_z) \alpha \, d\tau =$
$= \frac{1}{2} g\beta H_z \int \alpha^2 d\tau = \frac{1}{2} g\beta H_z$ and $E_\beta = \int \beta (g\beta S_z H_z) \beta \, d\tau = -\frac{1}{2} g\beta H_z$

Thus the energy level E^o will be split into two levels $E^o \pm 1/2g\beta H_z$ by the interaction between the electronic magnetic moment and the external magnetic field H_z. If an excited energy level exists it will also be split into two levels. Transitions between these two levels will then result in two absorption lines rather than just a single line. Electron spin resonance could be studied in this way. However, the situation can be simplified; energy sufficient to induce transitions only between the energy levels E_α and E_β can be used eliminating the complication of higher energy transitions. This then describes the technique of electron spin resonance; energy $h\nu$ is used such that only transitions between the α and β states are observed.

For a system of two electrons occupying the same electronic orbital (i.e. for paired electrons) the spin state is given by $\alpha_1\beta_2 - \alpha_2\beta_1$ (49). The other three possible spin states result in unpairing of the electron spins and give triplet states. These are, however, not allowed by consideration of the Pauli exclusion principle. The spin magnetic moment-magnetic field interaction Hamiltonian for a system of two electrons is $\mathcal{H} = \sum_i g\beta S_{z_i} H_z$ where the summation is over electrons. Thus the interaction energy is (ignoring the constants g, β, and H_z), for the allowed state,

$$E = \int (\alpha_1\beta_2 - \alpha_2\beta_1)[S_{z_1} + S_{z_2}](\alpha_1\beta_2 - \alpha_2\beta_1)\, d\tau_1 d\tau_2 =$$

$$\int (\alpha_1\beta_2 - \alpha_2\beta_1)(\tfrac{1}{2}\alpha_1\beta_2 + \tfrac{1}{2}\alpha_2\beta_1 - \tfrac{1}{2}\alpha_1\beta_2 - \tfrac{1}{2}\alpha_2\beta_1)\, d\tau_1 d\tau_2 = 0.$$

This gives the quantum mechanical basis for the statement that ESR detects only unpaired electrons, for any pairing of electrons will result in no interaction between the electronic magnetic moments and the external magnetic field.

The wave function(s) associated with these energy levels will also be altered over those for the unperturbed system. The new wave functions are given by

$$\psi_k' = \psi_k^\circ - \sum_{j=0}^{\infty} \frac{\int \psi_j^{\circ *} \mathcal{H} \psi_k^\circ \, d\tau}{E_j^\circ - E_k^\circ} \psi_j^\circ$$

(the term in the summation for j = k is neglected). This is the equation for a non-degenerate level and, strictly speaking, is not correct since the spin functions β and α are degenerate. The results are, however, the same as those obtained by first order perturbation theory for a degenerate level and are the same for the same reason; the quantity $\int \psi_j^{\circ *} \mathcal{H} \psi_k^\circ \, d\tau$, corresponding to $\int \alpha S_z \beta \, d\tau$, is zero and the wave functions for the perturbed energy levels are just the functions α and β; α corresponding to the ground state and β to the excited state. However, if the quantity $\int \psi_j^{\circ *} \mathcal{H} \psi_k^\circ \, d\tau$ was not zero then the perturbed wave function ψ_k' would be made up of the functions ψ_j° as well as ψ_k°; a small amount of the functions ψ_j° are said to "mix" with the function ψ_k°. This "mixing" becomes important when the unpaired electron is placed in a crystal field. This effect will be discussed later.

While the above discussion provides the basis for the following theoretical development it is oversimplified. As given by Bleaney and Stevens (12) the following interactions, in addition to the spin magnetic moment-external magnetic field interaction, will affect the energy levels of an unpaired electron and consequently will alter the observed ESR absorption spectrum: 1. the magnetic interactions between electron spins (spin magnetic moment) and orbits (orbital magnetic moments). 2. interaction with an external magnetic field (not only with the spin

magnetic moment as discussed above but with the orbital magnetic moment as well). 3. the interaction between the magnetic moment of the nucleus and the magnetic field set up by the orbital and spin moments of the electrons. 4. the electrostatic interaction between the electrons and the nuclear quadrupole. 5. the interaction between the nuclear magnetic moment and the external field. 6. the electrostatic crystal field effects of the surrounding (ligand) atoms on the unpaired electron. 7. the effect of covalent bonding between the atom on which the unpaired electron was initially present and ligand atoms. 8. exchange effects between adjacent unpaired electrons.

These effects complicate the situation not only because of the form of the Hamiltonians describing the interactions but because the relative interaction energy of each must be determined. The energies of interaction must then be ranked in order of decreasing energy and applied successively, beginning with the largest, as perturbations on the corrected wave functions (corrected for perturbations of higher energy). Each successive perturbation cannot be applied just to the unperturbed basis wave functions alone. However, it is the existence of the interactions described above which lead to the large amount of information which can be obtained from ESR absorption spectra.

The effects produced by the interactions described in 4. and 5. will not be considered in this thesis. These energies of interaction are of the order of $10^{-4}cm^{-1}$ whereas the others are usually $> 1cm^{-1}$ (12); thus, 4. and 5. will not appreciably effect the following discussion or the results.

Before considering the effects of these eight interactions on the ESR absorption curves the following general comments should be made. The greatest portion of the experimental and theoretical development of ESR has been made for single crystals. The results given in this thesis are for aqueous and frozen solutions. Generalizations from the single crystal to the aqueous and frozen solutions can be made. However, a certain amount of information is normally lost in this transformation.

Only factors effecting the overall curve shape will be considered in detail. Those factors affecting the intensity of the signal (the integrated area of the absorption curve) will not be considered in detail. The article of Beinert and Palmer (8) discusses these effects. A discussion of the factors effecting the line width is given by Bleaney and Stevens (12).

In general, the eight interactions given above will split the energy levels of higher energy states in the same way that the spin magnetic moment-magnetic field interaction splits the electronic energy levels. The spectra will then consist of more lines, corresponding to transitions between these multiple energy levels, than seen for the unpaired electron-magnetic field interaction only. These lines can then be broadened (or narrowed) by additional interactions (12).

The g value is shifted from its free electron value of 2 by interactions between the spin magnetic moment and the orbital magnetic moment. (g actually has the value 2.0023; this deviation from 2 is due to relativistic effects.) Free radicals have orbital angular momentum

very nearly equal to zero. Thus the electron spin resonance occurs at a g close to 2. This is not the case for the transition metals. The orbital angular momentum is not zero and deviations of g from 2 are almost always seen. In addition, when the environment about the unpaired electron is less than spherically symmetrical, coupling between the electron and orbital magnetic moments can occur, and, generally, this coupling will depend on the orientation of the environment about the unpaired electron with respect to the magnetic field. That is, the Lande g factor will have different values for different orientations of the crystal field. Strictly speaking the g value dependence on angle is a continuous function of the angle. Usually, however, axes can be chosen so that a maximum of three principle g values are obtained, g_x, g_y, and g_z. This results in three transitions for the interaction $g\beta H$; $g_x\beta H$, $g_y\beta H$, and $g_z\beta H$. The single line $g\beta H$ is split into three separate lines--this is shown in Fig. 1 in which the curves for spherical ($g_x=g_y=g_z$), axial ($g_x=g_y=g_\perp \neq g_z=g_\parallel$) and orthorhombic ($g_x\neq g_y\neq g_z\neq g_x$) symmetry are given.

A further interaction giving rise to a splitting of the resonance lines is the so called hyperfine interaction. This is the coupling between the spin magnetic moment and nuclear magnetic moment. The nuclear magnetic moment is characterized by a nuclear quantum number I (or I_z). The nuclear magnetic moment is quantized in a magnetic field H_z and 2I + 1 different orientations, corresponding to different energy levels, are allowed. Thus, the energy levels of the unpaired electron will be split into 2I + 1 different energy levels if there is

FIG. 1

ESR ABSORPTION CURVES FOR A PARAMAGNETIC SUBSTANCE IN A SPHERICALLY, AXIALLY, AND ORTHORHOMBICALLY SYMMETRIC ENVIRONMENT

(a) Plot of intensity of ESR absorption (ordinate) typical of free radicals ($g_x=g_y=g_z$) at constant frequency as function of d.c. magnetic field (abscissa), both in arbitrary units. Upper curve: absorption curve. Lower curve: first derivative of absorption curve, as generally used for representation of ESR spectra. (b) First derivative curve of paramagnetic substance in axially symmetric environment; $g_z(g_{\parallel})>g_x=g_y(g_{\perp})$. (c) Same as B for orthorhombic environment; $g_z>g_y>g_x$.

According to Beinert and Palmer (8)

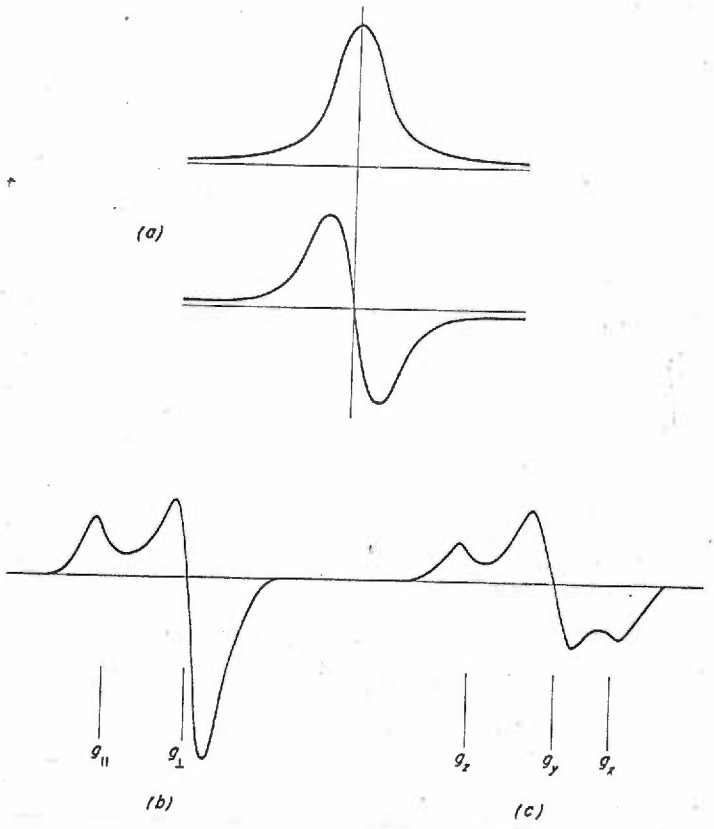
(a)
$g_{\parallel}$
$g_{\perp}$
g_z
g_y
g_x
(b)
(c)

an interaction between the spin magnetic moment and the nuclear magnetic moment. For a single g value and I = 3/2 four energy levels are obtained resulting in an absorption line with four equal components (Fig. 2).

Again, the situation has been oversimplified. As shown by perturbation theory, two quantities are needed to calculate the effect of a given interaction; the Hamiltonian describing the interaction and the wave functions of the system before the application of the perturbation. The Hamiltonians are obtained by considering the interactions as classical electro-magnetic interactions (12) and then converting these Hamiltonians to operator form (63). This leads to a "spin" Hamiltonian which will be used in discussing the results obtained. The Hamiltonians obtained from classical electro-magnetic theory for the eight interactions listed are given by Bleaney and Stevens (12).

B. ESR of Crystals

The interaction between electron spin and orbit (1.) results in an energy of interaction of 10^2-10^3 cm^{-1}. A spin-spin interaction can be eliminated by separating the unpaired electrons. The spin orbit coupling reduces to, in the spin Hamiltonian, $\mathcal{H} = \lambda \vec{L}\cdot\vec{S}$ where $\vec{L}$ is the angular momentum vector and $\vec{S}$ is the spin vector (25). λ is in units of energy and measures the extent of spin-orbit coupling. This perturbation also gives rise to relaxation effects since it is the mechanism by which the spin "feels" the effect of thermal vibrations (12). The resonance for Cu(II) compounds usually occurs at $g > 2$ indicating a large degree of spin-orbit coupling and thus the relaxation processes

FIG. 2

ENERGY LEVEL DIAGRAM FOR S = 1/2 AND I = 3/2

Energy level diagram for S = 1/2, I = 3/2 in a strong magnetic field. The allowed transitions are indicated by the arrows for a static microwave field and a varying magnetic field.

According to Bleaney and Stevens (12)

FIG. 3

THEORETICAL AND EXPERIMENTAL ABSORPTION CURVE FOR SQUARE PLANAR COPPER

Theoretical (dashed line) and experimental absorption curves for Cu(II) in a square planar environment for a single I value of the Cu nucleus.

According to Sands (98)

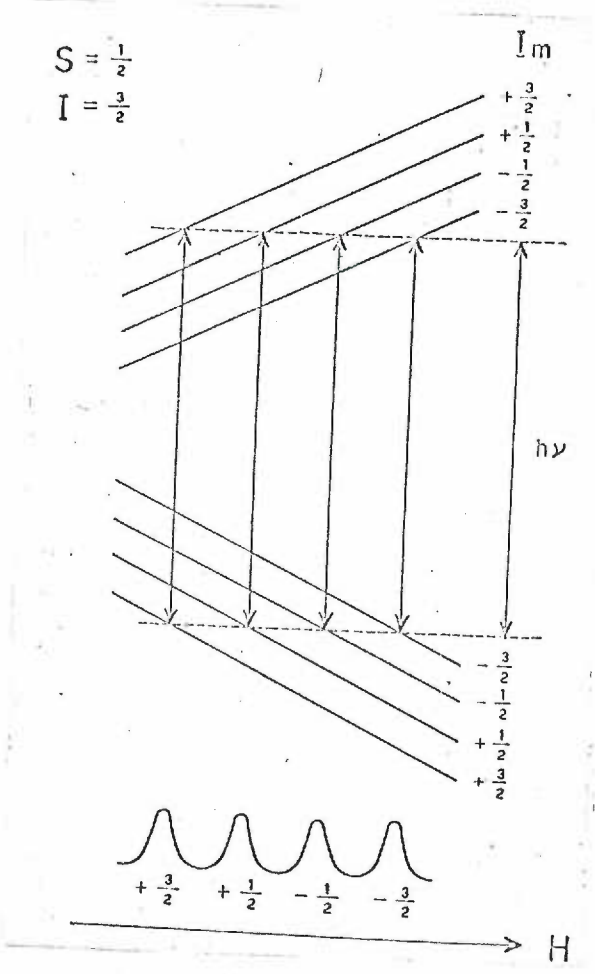
S = 1/2
I = 3/2
Im
+3/2
+1/2
−1/2
−3/2
hν
−3/2
−1/2
+1/2
+3/2
+3/2 +1/2 −1/2 −3/2
H

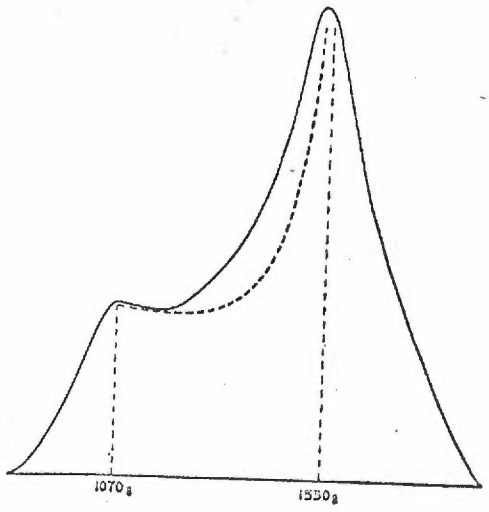
1070 g
1550 g

are relatively efficient. The ESR signals of Cu(II) are, for this reason, rarely saturated. This spin-orbit perturbation also "mixes" excited levels with the ground state giving more complex wave functions for the states in which spin-orbit coupling exists and which must be used in successive perturbation calculations (87). It is this mixing that gives a certain amount of β spin to the ground state characterized by α in the unperturbed state and a certain amount of α is mixed into the excited state β. However, since these states are distinct in a magnetic field, we assign a spin α and β to the ground and excited states respectively . Such a spin is a "fictitious" spin to which we try and attribute the magnetic properties of the sample (87).

The interaction with an external magnetic field (2.) is written as (63) $\mathcal{H} = \beta(\vec{L} + 2\vec{S})\cdot\vec{H}$ where $\vec{L}$ and $\vec{S}$ are as defined above and $\vec{H}$ is the external magnetic field. This should be contrasted with the previous case in which only the spin magnetic moment-external field interaction, $\vec{S}\cdot\vec{H}$ was considered. The coupling between the orbital magnetic moment and the external field is also included. The inclusion of this term will again mix ground and excited state wave functions (87).

If we are dealing with a singlet ground state we can ignore the spin orbit coupling and can write the interaction as $\beta\vec{H}\cdot g\cdot\vec{S}$ (12) where g is now a symmetric tensor of the second rank (87, 81) and can be represented by a 3X3 matrix. Generally the off diagonal components are very close to zero (87) and we need only the diagonal elements (the principle g values) and can write the interaction as

$$\mathcal{H} = g_x\beta H_x S_x + g_y\beta H_y S_y + g_z H_z S_z$$

This is only correct, however, when the principle axes of the g values

and those of the field $\vec{H}$ coincide. The alteration of the Hamiltonian given above when these two coordinate systems are non-coincident is derived by Pake (87) and will not be given here.

The interaction between the magnetic moment of the nucleus and the magnetic field set up by the orbital and spin moments of the electrons (3.) (energy $10^{-2}cm^{-1}$) is given by Milford (82). It contains an anisotropic part (the energy of interaction depends on orientation of the crystal field) which is described by dipole-dipole coupling (this contribution is small (55)) and an isotropic portion (no angular dependence) given by $16\pi/3\, g\mu_o\beta|\psi(0)|^2\vec{S}\cdot\vec{I}$ which is called the Fermi contact term. μ_o is the magnetic moment of the nucleus and $|\psi(0)|^2$ is the unpaired electron density at the nucleus. These interactions become, in a spin Hamiltonian, $\vec{S}\cdot A\vec{I}$ in which, like the g values, A is a tensor.

The electrostatic crystal field effects of the ligand atoms (6.) on the wave functions for the unpaired electron are complicated and are best treated by the methods of group theory. The book by Orgel (86) provides a qualitative discussion of these crystal field effects. Only the case of Cu(II), d^9, will be considered. When the crystal field about the Cu(II) possesses spherical symmetry, all five d orbitals will be of equal energy (ignoring spin-orbit coupling etc.). When a crystal field of lower symmetry is present this degeneracy will be (partially) removed; the d orbitals will now have different energies. Transitions can now occur between these separated energy levels (usually around 6,000 Å for Cu(II)--the so called d-d transitions). The dividing of the d levels into levels of different energy and the extent of this

dividing (how completely the degeneracy is removed) will be a function of the symmetry of the crystal field. As before, this crystal field perturbation will mix the original d orbitals so that the electronic orbitals are no longer described by the simple d orbitals. The wave functions describing these new orbitals will be given by perturbation theory and will be the wave functions used in further perturbation calculations. For this reason the symmetry of the field about the Cu(II) must be known before proceeding with further perturbation calculations.

The effect of covalent bonding between the ligand atoms and the paramagnetic ion (7.) is essentially an extension of the crystal field discussion. The electron now resides in orbitals on the ligand atoms as well as on the paramagnetic ion. A "smearing out" of the electron through covalent bonding will likely reduce the orbital angular momentum $\vec{L}$ and thus the neglect of the interaction $\vec{L}.\vec{H}$ is somewhat justified. Also, if the ligand atoms possess nuclear magnetic moments I, then these may have to be included in the interaction $\vec{S}\cdot A\cdot\vec{I}$. The theoretical development is given by Kivelson and Neiman (52) and will be sketched here.

Molecular orbitals, formed from linear combinations of the Cu(II) and ligand atomic orbitals, are written down. One such orbital could be (52) $(2) \propto d_{x^2-y^2} - \alpha' \left(-\sigma_x^{(1)} + \sigma_y^{(2)} + \sigma_x^{(3)} - \sigma_y^{(4)}\right)/2$ in which the $d_{x^2-y^2}$ is an atomic orbital of the Cu(II) and the σ orbitals are (sp hybrid (88)) atomic orbitals of the ligand atoms. The orbitals are classified as sigma (σ) since they have zero angular momentum about the line (bond) joining the ligand atom to the copper atom. The sigma

orbitals will be cylindrically symmetrical about this line (49). The pi (π) orbitals formed between the ligand atom and copper atom will have angular momentum about the line joining the two atoms; these orbitals will not be cylindrically symmetrical about this line.

The form of the molecular orbitals depends on the symmetry of the ligand field about the copper atom. This must be known before the molecular orbitals can be written down. In addition, the molecular orbital in which the unpaired electron is present (the ground state) must be determined as the ESR results depend on the wave function used in the calculation (the formula for the perturbation energies depends on these wave functions). Finally, these molecular orbitals may be mixed by interactions of lower energy. It may be that most of the eight interactions discussed will be of lower energy.

For Cu(II) in a square planar environment the unpaired electron is most probably in the molecular orbital given (52). Operating on this molecular orbital with the appropriate spin Hamiltonian will give the energy levels of the unpaired electron. Also, the relationships $\alpha^2 = (g_{\parallel} - 2) + 3/7 (g_{\perp} - 2) + K$ and $\alpha^2 + \alpha'^2 - 2\alpha\alpha' S = 1$, where S is the overlap integral, are obtained. The values of K and S can be estimated (52). Thus, by experimentally determining $g_{\parallel}$ and $g_{\perp}$ we can obtain α and α'. From equation (2) it can be seen that these α's weight the contributions from the copper atom atomic orbitals and the ligand atom atomic orbitals to the molecular orbital. Ignoring overlap, S(S=0.09), the electron densities (probabilities) of these atomic orbitals will be given by α^2 and α'^2. If we define a totally covalent sigma bond by $\alpha^2 = \alpha'^2$

and a totally ionic sigma bond by $\alpha^2=1$ (which gives $\alpha'^2=0$) or $\alpha'^2=1$ (which gives $\alpha^2=0$) then a totally covalent sigma bond is given by $\alpha^2=\alpha'^2=0.5$ in which the unpaired electron density is equally distributed between the copper atom and the ligand atoms and a totally ionic sigma bond is given when the unpaired electron density is totally confined to the copper or ligand atoms. Thus a determination of $g_{\parallel}$ and $g_{\perp}$ should give the degree of covalency of the copper atom-ligand atom bond. However, the conditions under which the above relationships were derived must be fulfilled for such a calculation to be made.

The exchange effects between unpaired electrons (8) can be simply thought of as magnetic dipole-dipole interactions. This interaction is proportional to $1/r^3$ where r is the distance between dipoles. Thus the interaction can be made negligible by keeping the unpaired electrons separated; i.e. by using dilute solutions of paramagnetic ions. (What has been described is essentially a spin-spin not an exchange interaction --both are, however, made negligible in the same manner-the exchange interaction is expected to fall off more rapidly with increasing distance than does the dipolar interaction (87).)

The discussion given above, for the eight interactions, assumed that the paramagnetic ion was in a crystal; known orientations of the ligand field about this paramagnetic ion with respect to the external magnetic field could be achieved. These fields about a paramagnetic ion may persist in solution. The paramagnetic ion may then be considered as residing in a microcrystal. There is, however, a fundamental differ-

ence between these microcrystals in solution and the crystalline state; the microcrystal is tumbling in a random manner. It is the effect of this tumbling on the ESR absorption spectra which will be considered next.

C. ESR of the Liquid State

The situation is best described by writing the spin Hamiltonian in two parts, one which is invariant under rotations and the other which is dependent on orientation. We begin with the axial spin Hamiltonian $(g_x = g_y = g_\perp, g_z = g_\parallel, g_\perp \neq g_\parallel)$ $\mathcal{H} = \beta[g_\parallel H_z S_z + g_\perp (H_y S_y + H_x S_x)] + A_\parallel I_z S_z + A_\perp (I_x S_x + I_y S_y)$

where the coordinates refer to the microcrystalline system not the laboratory system (the z-axis of the laboratory system taken as the magnetic field direction). This spin Hamiltonian can be transformed to laboratory coordinates (79) and written in angular independent and dependent parts. The angular independent part is $\mathcal{H} = g\beta H_0 S_z + a\,\vec{S}\cdot\vec{I}$ The portion of this spin Hamiltonian containing the angular dependent terms will average to zero if the rate of tumbling is sufficiently rapid. The rate at which tumbling must occur to average these terms to zero is given by the correlation time for rotation.

It can be shown that the mean value for the angular dependent functions is zero (87). The question then is, what amount of time is needed for the tumbling microcrystal to attain a sufficient number of different orientations for the average to be approximately zero. Since the motion is continuous, the rotation of the microcrystal will change the angle between the magnetic field and the principle axis of the micro-

crystal very little for a sufficiently short time interval; the values of the function at the beginning and end of this time interval will be very nearly equal. The values of the function are said to be correlated (87). For the average of the angular function to be zero we need a time sufficiently long that correlation will be lost. The derivation leading to the necessary time interval is given by Pake (87); if the time necessary for a loss of correlation (the correlation time) is much less than the reciprocal of the energy separation of the levels, expressed as frequency ($\tau_c << 1/\delta$), then the angular portions of the spin Hamiltonian average to zero and we have $\mathcal{H} = g\beta H_o S_z + a\vec{I}\cdot\vec{S}$. In addition, we will consider only cases in which I_z is diagonal (I_z has eigenvalues for the wave functions used). Since I_x and I_y have no diagonal matrix elements in this representation (82) we can write the spin Hamiltonian as $\mathcal{H} = g\beta H_o S_z + a S_z I_z$.

D. ESR of The Frozen State

The question now to be answered is what occurs when $1/\delta$, the reciprocal of the separation of the lines, approaches τ_c, the correlation time for molecular tumbling. As given by McConnell (79), the center of gravity of each absorption line is given by the angular independent part of the spin Hamiltonian and the angular dependent parts lead to line broadening. Generally this broadening is unsymmetrical. The problem will be discussed by first considering the result when $\tau_c = \infty$ ($\tau_c >> 1/\delta$). This situation corresponds to the frozen state; the state in which the microcrystals are not tumbling but are randomly

oriented. This was first discussed by Sands (98) and later by Kneubuhl (56), Neiman and Kivelson (85), and Gersman and Swalen (40). The abreviated discussion given here will follow that of Sands.

Sands considered the ESR absorption of Cu(II) ions in a glass. The Cu(II) is assumed to occupy a site of cubic plus tetragonal symmetry. In the glass all orientations of the crystalline field about the Cu(II) are equally probable and the absorption will be a sum over all of these orientations. The angular dependence of the g value is, as given by Pake (87), $g=(g_{\parallel}^2\cos^2\theta + g_{\perp}^2\sin^2\theta)^{1/2}$ which gives, from $h\nu = g\beta H$ (and rearrangement to $H = h\nu_0/g\beta$ since H is varied and ν fixed at ν_0 in ESR measurements) $H = (h\nu_0/\beta)(g_{\parallel}^2\cos^2\theta + g_{\perp}^2\sin^2\theta)^{-1/2}$ The absorption curve is obtained by plotting dN/dH versus H where N is the number of unpaired spins. The result is shown in Fig. 3. This absorption curve can be interpreted in terms of two overlapping curves, one centered at $g_{\parallel}$ (1070g in Fig. 3) and the other at $g_{\perp}$ (1530g in Fig.3). The $g_{\perp}$ curve is twice the area of the $g_{\parallel}$ curve since it is made up of g_x and g_y absorptions.

For Cu(II) the magnetic interaction between electron and nuclear spin must also be considered. The derivation of these curves is a more complex form of the derivation mentioned above. The result is shown in Fig. 4. It can be seen, as expected from an I = 3/2 for Cu(II), that four absorption curves result. The observed absorption curve is the sum of these four curves. Frequently, the lines centered around $g_{\perp}$ are so closely spaced that only the separation of the four lines in the $g_{\parallel}$ region is observed.

FIG. 4

DEVIVATIVE AND INTEGRATED ABSORPTION CURVE FOR COPPER IN A SQUARE PLANAR ENVIRONMENT

Derivative and integrated absorption curves for Cu(II) in a square planar environment. The dashed curves are the theoretical curves (as in Fig. 3) for the four allowed values of I. The solid curves are the experimentally obtained curves.

According to Sands (98)

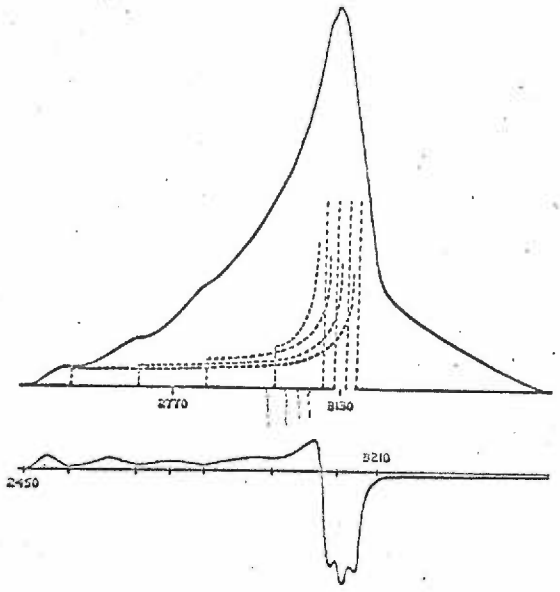
2770
3130
3210
2450

If additional interactions between spin and nuclear magnetic moments, due to unpaired electron interaction with other paramagnetic nuclei, are added to the above, each of the four curves will be split into an additional 2I + 1 curves. As is usually the case, the overlap between these curves is such that this further splitting is unresolved.

When the microcrystal begins to tumble, the center of gravity of the lines will not change (79). If we represent the curve of Fig. 3, by

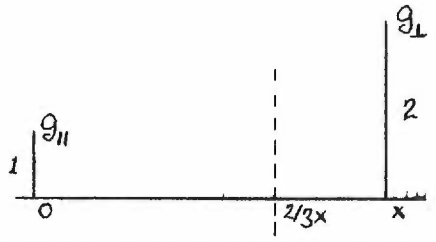

where x is the distance between the $g_\parallel$ and $g_\perp$ absorptions, then the center of gravity of the total curve is 2/3x. When the rotation of the microcrystal is sufficiently rapid so that $\tau_c \ll 1/\delta$, δ being the distance from $g_\parallel$ to $g_\perp$, each absorption of Fig. 4 will consist of a single line centered about 2/3x for that line. (Processes which broaden these single lines will give symmetrical broadening (87).) For the four lines shown in Fig. 4 a symmetric four line absorption will result (given in Fig. 2). This is what is expected since the spin Hamiltonian describing the system is $\mathcal{H} = g\beta H_0 S_z + a I_z S_z$ which gives an absorption, with a single g value, split into four equal components by I_z = 3/2, 1/2, -1/2, and -3/2 for the Cu(II) nucleus.

The intermediate case, $\tau_c \cong 1/\delta$, will only be discussed qualitatively. From the curves for $\tau_c \ll 1/\delta$, Fig. 2 (liquid state), and $\tau_c \gg 1/\delta$, Fig. 4 (frozen state), it can be seen that as τ_c increases,

(the rotational rate decreases) the symmetrical four line absorption seen for $\tau_c << 1/\delta$ will change into the curve consisting of $g_{\parallel}$ and $g_{\perp}$ absorptions. Since the rotational rate will decrease in a continuous manner, the curve for $\tau_c << 1/\delta$ will approach the curve for $\tau_c >> 1/\delta$ in a continuous manner. This is the same as saying that the symmetrical four line absorption (Fig. 2) must broaden in a continuous manner to produce the absorption pictured in Fig. 4. This broadening will not be symmetrical.

Further, since the width of the line for $\tau_c >> 1/\delta$ giving the low field line in the symmetric four line absorption ($\tau_c << 1/\delta$) is greater than that of the line producing the high field line, the low field line will broaden more rapidly than the high field line as the rotational rate of the microcrystal decreases (τ_c increases). $\tau_c \rightarrow 1/\delta$ more rapidly for the low field line than for the high field line since $1/\delta_{low\ field} < 1/\delta_{high\ field}$ Thus the lines broaden at different rates giving an asymmetric four line absorption as the rotational rate is decreased (in addition to the asymmetries produced by the anisotropic g values). This is illustrated in Fig. 5. McGarvey (81) was able to fit the experimental curve by assuming four overlapping Lorentzian curves, given by $B/[A^2+(\omega-\omega_o)^2]$, of equal area (concentration) but unequal line width A. For the curve given in Fig. 5 the A values were in the ratio, low field to high, 1.3: 1.1: .9: .7.

Additional discussion of ESR theory will be given as needed in the text.

FIG. 5

ABSORPTION CURVE OF Cu(II) ACETYLACETONATE

Plot of the absorption curve for a 0.01 molar solution of copper (II) acetylacetonate in dioxane. The sharp peak on the left is from the reference free radical and the heavy dashed line is a fitted curve constructed from four equally spaced Lorentzian curves of equal area but different widths.

According to McGarvey (81)

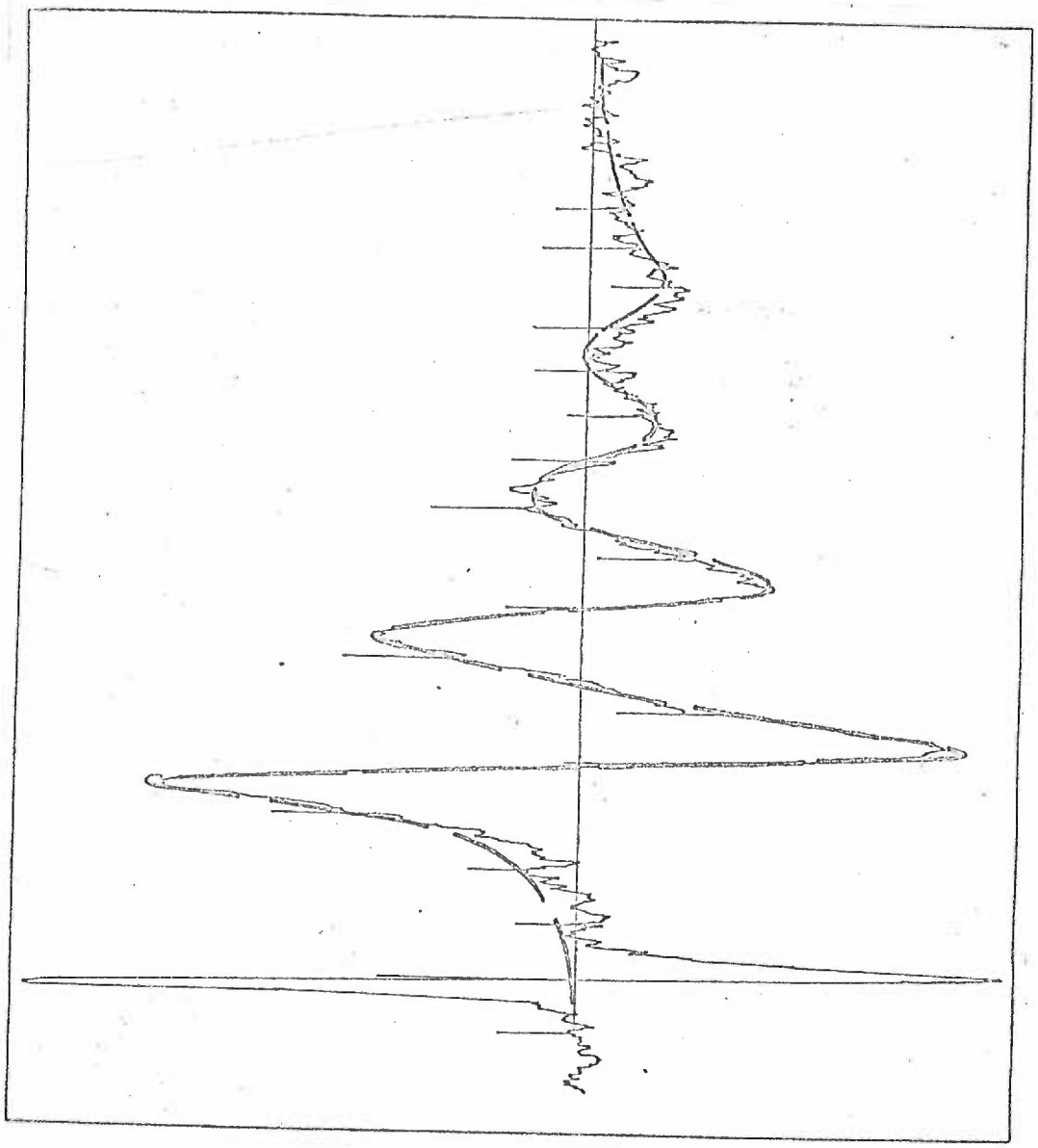

3. Peptide Cu(II) Complexes

Much of the early work on the binding of Cu(II) by peptides was part of a general study of the biuret reaction, which was first observed by Wiedemann (114), in 1847, as the color reaction shown by biuret (NH_2-CO-NH-CO-NH_2) and Cu(II) in an alkaline solution (93). The absorption spectra and criteria for the biuret color are reproduced from the article of Kober and Haw (58) in Appendix II. In 1873 Ritthausen (96) discovered that proteins undergo a similar reaction in the presence of Cu(II) and alkali. Schiff (99), who made the first extensive investigations of the biuret reaction, precipitated the salt formed from the reaction between biuret and Cu(II) and in this way established the formula for the complex as $Cu(biuret)_2^{2+}$.

Schiff also made the observation that many compounds which structurally resemble biuret show a similar color reaction with Cu(II) in the presence of alkali; he did not isolate any of the products of these reactions. He divided the compounds showing a positive biuret reaction into the following three classes (93): (1) compounds resembling biuret with the grouping

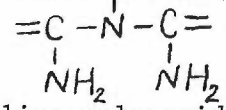

(2) compounds resembling malonamide, with the grouping

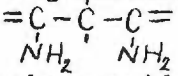

and (3) compounds of the oxamide type having the grouping

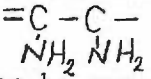

The classification can be generalized to the grouping 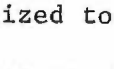 which will, steric and stoichiometric factors allowing, give a biuret type reaction with Cu(II) and alkali.

Kober and Sugiura (57), in 1912, found that all di-, tri-, and tetra-peptides which they investigated (given in Appendix I) combined in a 1:1 molar ratio with Cu(II) giving the biuret reaction. Schiff had previously found a 2:1 ratio for the biuret-Cu(II) complex. Werner (64) stated "that they had isolated the (1:1 peptide:Cu(II)) compound before the appearance of Kober and Sugiura's paper. The results however for 'external' reasons were not published till more than a year later."* The similar work of Kober et al. (57, 58) was published first and since it seems to have been largely ignored in subsequent publications, it will be described here.

"It is our belief that a quantitative study of the copper salts of proteolytic substances will throw some light on the constitution of protein, and it is therefore our intention to present from time to time our results in this field."* For the investigations which are the subject of this thesis the above need only be modified to state that it is hoped that these investigations will "throw some light" on the constitution of the copper proteins. The paper of Kober and Sugiura (57) dealt almost entirely with the solid salts of various peptides and Cu(II). The method used was as follows: $CuCl_2$ was treated with NaOH and the precipitated $Cu(OH)_2$ was collected on a filter. The collected $Cu(OH)_2$ was then stirred with the peptide of interest (an excess of $Cu(OH)_2$ was used) for 5 or 10 minutes. The solution was then filtered removing the excess $Cu(OH)_2$. The Cu(II) salt of the peptide was then precipitated,

*Kober and Suigura (57)

usually by the addition of ethanol or ether, and a chemical analysis of the salt was made. Chemical analysis of the Cu(II) salts of α-amino acids gave, without exception, the general formula CuA_2 where A equals one molecule of monobasic α-amino acid (Appendix I). For the Cu(II) salt of the dipeptide of leucyl glycine "Fischer concluded that one molecule of copper hydroxide combined with one molecule of leucyl glycin, and that two molecules of the copper leucylglycin are connected by an oxygen atom. Although we have found one molecule of copper hydroxide to one of leucylglycin, we have not been able to find that an oxygen atom connects two molecules of copper leucylglycin." * In general, it was found that " one molecule of peptide, whatever number of amino acids it may contain, combines with only one molecule of copper hydroxide,"* when the above method was used. The results obtained by Kober and Sugiura for the binding of Cu(II) by di-, tri-, and tetra-peptides are reproduced in Appendix I. To summarize, the copper salts of 33 di-peptides, 26 tri-peptides, and 4 tetra-peptides were investigated and the results were consistent with the formula (peptide) $_1Cu_1$. In addition, Kober and Sugiura proposed the structures reproduced in Fig. 6 for the peptide Cu(II) complexes. Any attempt to assign the proper authorship for these structures is, however, somewhat meaningless, as Schiff had earlier proposed a structure for the Cu(II)-biuret complex and it seems likely that other metal coordination complexes had earlier been assigned molecular structures.

* Kober and Sugiura (57)
** Kober and Haw (58)

FIG. 6

PROPOSED STRUCTURES FOR Cu(II)-PEPTIDE COMPLEXES

Structure A is alkaline Cu(II) glycylglycine, structure B is alkaline Cu(II)-glycylglycylglycine, and structure C is alkaline Cu(II)-triglycylglycine.

According to Kober and Sugiura (57)

FIG. 7

TITRATION CURVE OF EQUIMOLAR Cu(II) AND GLYCINE

Titration curve of solution containing glycine (0.005M) + $CuCl_2.2H_2O$ (0.005M).

According to Dobbie, Kermack, and Lees (31)

FIG. 8

TITRATION CURVE OF 2:1 GLYCINE: Cu(II)

Titration curve of solution containing glycine (0.01M) + $CuCl_2$ (0.005M).

According to Dobbie, Kermack, and Lees (32)

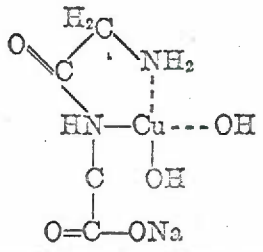

Alkaline
Cu(glycyl-glycin)

A

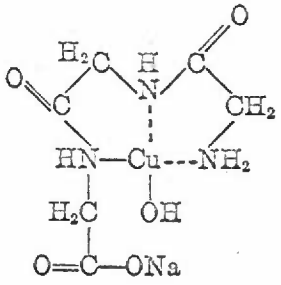

Alkaline
Cu(glycyl-glycyl-glycin)

B

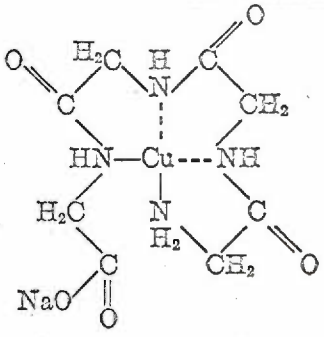

Alkaline
Cu(tri-glycyl-glycin)

C

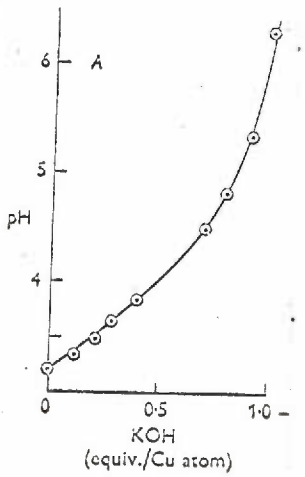

7

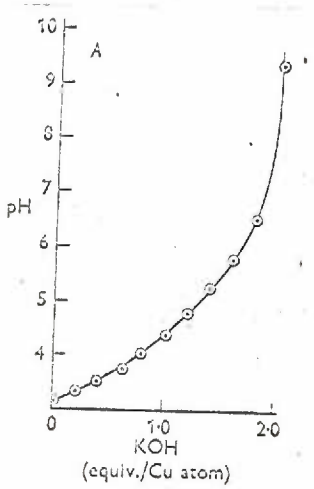

8

This study was extended by Kober and Haw (58) in 1916 to include a spectrophotometric study of the Cu(II)-peptide complexes. In the first paper of Kober (57) it was found that "the copper complexes of amino derivatives and derivatives of other similar substances could be divided, according to their color, into three classes. (1) Blue, (2) purple--called "semi-biuret"--and (3) red--called "biuret". The first class was also characterized by the fact that there were in each complex 2 nitrogen groups so placed, that by forming "stable" rings (4, 5, or 6 membered rings), they could combine with the copper. The complexes of the second class had 3 such groups and the third class had 4."** The nitrogen groups could be either amino, imino, imide, or amide as earlier observed by Schiff. The absorption spectra obtained for aqueous solutions of various Cu(II)-peptide complexes are given in Appendix II. These spectrophotometric results can be summarized as follows: three types of absorption curves are seen, (1) Blue complexes, absorption beginning around 480 mu and reaching a maximum at 630 mu. This is observed for di-peptide-Cu(II) complexes in neutral, slightly alkaline, and alkaline solution, and for tri- and tetra-peptide-Cu(II) complexes in neutral solution..(2) Purple or semi-biuret complexes: the absorption begins at about 459 mu and reaches a maximum at 540 mu. This is observed for slightly alkaline solutions of tri- and tetra-peptide-Cu(II) complexes. (3) Red or biuret complexes: the absorption begins beyond 443 mu and reaches a maximum at 505 mu. This is observed for the tetra-peptide Cu(II) complexes in alkaline solution.

** Kober and Haw (58)

In all cases "the results show three types and only three types of absorption."**

Brill et al. (19) point out that if one looks at the wavelengths of the absorption maxima for the peptide-Cu(II) complexes as a function of increasing chain length (increasing number of amino acid residues) it is seen that the absorption maximum approaches that of the Cu(II)-biuret complex (505 mu for the dibiuret Cu(II) complex), from the long wave length side, as the chain length of the peptide increases. Thus, "it is somewhat arbitrary to state that the biuret color has or has not appeared."*

The following explanation is given by Kober and Haw for this shift in the absorption maximum to shorter wave lengths (higher energy). "That the nitrogen plus copper is not a red producing chromophore and that the red colors are produced, simply by removing the blue-producing aquo groups, yielding the true color of cupric copper in a non-hydrated condition seems probable, but cannot be decided definitely yet."** The present interpretation is that the interactions between the cupric copper and the ligands provide the energy level shifts that shift the absorption maximum. This is based on crystal field and covalent bonding theory as discussed in the section on ESR theory. In the notation of ligand field theory the shift is due to the nitrogen plus copper (4).

Kober and Haw also observed that "the amount and nature of the absorption of a given complex is somewhat dependent on the concentration of the hydroxyl ions."** As will be shown later, the pH or hydroxyl

* Brill, Martin, and Williams (19)
** Kober and Haw (58)

ion concentration of the solution is decisive in determining the form of the complex.

To show that the color of these copper complexes is essentially dependent on the presence of nitrogen atoms in the complexing molecule, Kober and Haw offer the following evidence. Compounds which contain no nitrogen atoms, but do contain oxy- or hydroxy- groups, such as the hexoses, are "quantitatively from 50 to 90% decomposed in a weakly alkaline solution in which all complexes of amino acids, peptides and other protein derivatives are perfectly stable."* That is, the Cu(II) is from 50 to 90% precipitated as $Cu(OH)_2$. Also, "oxy or hydroxy complexes of copper, no matter what configuration they may possess, are all blue or green, and never red..."*

The work of Rising and co-workers was undertaken for the express purpose of understanding the biuret reaction as it occurs in protein solutions. The first of a series of papers (93) dealt with the biuret reaction of acid imides of which diethylbarbituric acid and barbituric acid were the two representatives used. The first extensive study of the biuret reaction of the acid imides was made by Tschugaeff (106) who isolated the salts formed from the reaction between succinimide and Cu(II). The analysis of these salts conformed to the empirical formula, $Cu(imide)_4^{+2}$ which should be compared to the 1:2 ratio found by Schiff for the biuret type reagents.

In addition to the difference in empirical formulas between the acid imide and biuret Cu(II) complexes, the formation of the biuret

* Kober and Haw (58)

color with Cu(II) and the acid imides requires no addition of hydroxide when Cu(II) is added as $Cu(OH)_2$. Considering the formula for the acid imides it can be seen that tautomeric forms exist.

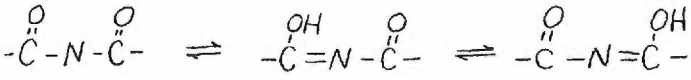

As is well known (88), two canonical* forms result in stabilization. In the presence of alkali, proton ionization can occur which leads to three canonical forms for the ionized structure,

(1) 

whereas for the biuret type grouping, only two resonance forms would be possible,

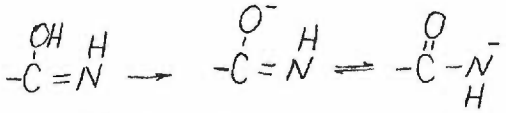

It would be expected that the presence of three ionized forms in equation (1) would stabilize the acid imide over the biuret structure (2). This is equivalent to saying that the ionization of a proton would occur at a lower pH in the acid imides than it would in the oxamide type grouping. The formation of the biuret color between the acid imides and Cu(II) in the absence of alkali can be explained in this way.

This paper of Rising et al. (93) contains, to this author's knowledge, the first proposal for proton ionization occuring in binding of Cu(II) in biuret type complexes. However, in view of the fact that resonance was a well established concept, (Kekule's paper on the resonance forms of benzene appeared in 1865) it does not seem unlikely

* Resonance forms which are linearly independent are called canonical structures (49). A canonical structure cannot be expressed as a linear combination of the other resonance structures possible.

that the idea of resonance forms lowering the pK had its origin elsewhere. A similar ionization in the case of the Cu(II)-peptide complexes has been recently proposed.

Rising et al. (93) found that N-alkylated succinimides failed to show the biuret reaction. They concluded that there are two atoms in an imide molecule which are intimately concerned in the biuret reaction: (1) a replaceable hydrogen atom attached to (2) an amine nitrogen atom with a basic character sufficiently strong to "insure its ready entrance into a copper complex."*

In a later paper (94) Rising et al. found that the amino acid amides would also undergo a positive biuret reaction with $Cu(OH)_2$ without the addition of alkali. The salts formed had the empirical formula, Cu(amino acid amide)$_2$. These complexes are of the oxamide type and have dissociated at this "neutral" pH due to displacement by Cu(II). That they are neutral salts was shown by the fact (94) that a solution containing a 1:2 molar mixture of $Cu(OH)_2$ and amino acid amide showed zero conductance. This same solution showing zero conductance does conduct an electric current upon addition of alkali and the colored complex migrates to the anode. "The effect of alkali upon copper leucinamide may be to form a soluble compound, potassium copper leucinamide hydroxide, of formula $K_2Cu[(OH)_2(\ (CH_3)_2CH\text{-}CH_2\text{-}CH(NH)_2)CO(:NH)\ ]_2$, somewhat as copper ammonium sulfate reacts with alkali to form copper ammonium hydroxide."** In all systems studied, the empirical formula

* Rising and Johnson (93)
** Rising et al. (95)

of the isolated salt of the Cu(II) and biuret reagent was such that there were always four basic nitrogen atoms available for the binding of the Cu(II).

The investigations of Rising et al. of the Cu(II) salts of triglycyl-glycine and tetraglycylglycine were undertaken to understand the biuret reaction of proteins (95, 112). The procedure employed was to add an excess of $Cu(OH)_2$ and NaOH to a solution of a peptide of interest. The excess $Cu(OH)_2$ was filtered off after five minutes, and the solution was mixed 1:20 with an ethanol-ether mixture. The complex salt which was precipitated, carefully dried and analysed for Na, Cu, C, N, and H. The analytical date indicate the empirical formula for the salt formed from Cu(II) and triglycylglycine; $Na_2(Cu(NH_2(CH_2CON)_3CH_2CO_2))\cdot 2H_2O$. If the molecular and empirical formulas are identical (no molecular weight determinations were made) the structure of the salt may be

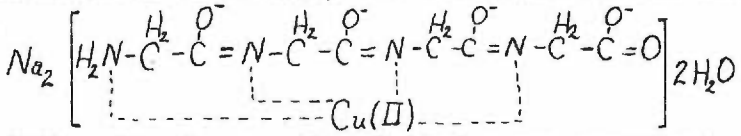

The Cu(II) salt of tetraglycylglycine was prepared and analysed (112). The results were substantially as obtained with triglycylglycine with the exception that the amount of sodium found was less than that calculated from the emperical formula

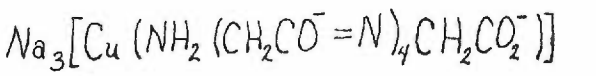

and at the same time the hydrogen found was correspondingly higher than that indicated by the above formula. It is now known that the copper combines with a maximum of four nitrogen atoms in these peptide-Cu(II) complexes (60) and that a proton is not displaced from a fourth peptide group.

These papers of Rising et al. make the first proposal for ionization of a proton from the peptide linkage and subsequent binding of Cu(II) by this linkage. The interpretation is that "the enol tautomer of tetraglycylglycine is considered to contain five ionizable hydrogen atoms. In the course of the formation of a molecule of sodium copper tetraglycylglycine three of these are considered to be neutralized by the alkali used."* The two protons not neutralized by added alkali were neutralized by the $Cu(OH)_2$ used. This interpretation is in agreement with the results for the Cu(II) binding by acid imides.

B. Potentiometric Titrations

The reactions between peptides and Cu(II) have been extensively investigated by potentiometric methods (30,31,32,33,73,84,92,60). The first of these investigations was that made by Dobbie and Kermack (31, 32). The problem can be outlined by considering the reaction of Cu(II) with glycine. It is assumed that the Cu(II) can not combine with the zwitterion form; the reaction can then be written

(1) $$\ce{NH3+CH2COO- <=> NH2CH2COO- + H+} \qquad pK$$

(2) $$\ce{NH2CH2COO- + Cu+2 <=> [NH2CH2COO-Cu]+1} \qquad pK_1$$

or, since the reactions are studied at equilibrium we can consider the reaction of interest as being the sum of the above reactions. This gives

(3) $$\ce{NH3+CH2COO- + Cu+2 <=> [NH2CH2COO-Cu] + H+}$$

*N Wenaas (112)

The pK of the reaction is an experimentally determined quantity; by obtaining the pH at which the reactants and products are in equal concentrations, a direct measurement of the pK is made. If this pK determination is made for the proton ionization occurring when glycine binds Cu(II), pK_2 is obtained, and it follows from the reactions that $pK_2 = pK + pK_1$. Thus only if pK_1 is zero will the ionization of the proton from the ammonium group occur at the same pH for the Cu(II)-glycine mixture as it does for uncomplexed glycine. This is seldom the case since, as is experimentally determined, the binding constants for Cu(II) binding by peptides are large ($\sim 10^8$) and positive, leading to a depression of the observed pK of the proton ionization. This observation seems to be easily overlooked. Using standard methods (pH and beginning concentrations) the value for pK_1, or K_1, the stability constant, can be determined. When equimolar $CuCl_2$ and glycine are titrated with NaOH the curve shown in Fig. 7 results. When a 2:1 molar mixture of glycine and $CuCl_2$ are titrated with NaOH the curve shown in Fig. 8 is obtained. The following two observations should be made. In the 1:1 mixture one equivalent of NaOH is consumed in the pH range 1 to 6 and a precipitate of $Cu(OH)_2$ begins to form above pH6. In the 2:1 mixture two equivalents of NaOH are consumed in the pH range 1 to 7 and no precipitate is formed on going to higher pH's. These results are interpreted in terms of the following reactions (G represents the glycine zwitterion),

$$Cu^{+2} + G^- \rightleftharpoons CuG^+ \qquad K_1 = [CuG^+] / [Cu^{+2}][G^-]$$

$$CuG^+ + G^- \rightleftharpoons CuG_2 \qquad K_2 = [CuG_2] / [CuG^+][G^-]$$

As before, these reactions could have been written

$$Cu^{+2} + G \rightleftharpoons CuG^{+} + H^{+} \qquad pK_1'$$

$$CuG^{+} + G \rightleftharpoons CuG_2 + H^{+} \qquad pK_2'$$

To evaluate K_1 and K_2, values of K_1 and K_2 are estimated at certain points on the titration curves (31) and are then checked by calculating the theoretical titration curve using these values of K_1 and K_2 and comparing this with the experimental curve. The values of K_1 and K_2 are then adjusted until the best fit is obtained. Values obtained (31) were $K_1=10^{8.5}$ and $K_2=10^{7.5}$. Martell has shown (74) that these values depend on the ionic strength of the medium and this must be considered when results of different investigations are compared. Values for the ionization constants of the amino and carboxyl groups of glycine at 20° C ar $10^{-9.86}$ and $10^{-2.22}$ respectively. Using these values (binding to the carboxyl group will depress its apparent pK to a value so low that it will not be observed in these experiments--IR data indicate that such binding does occur) it is seen that $pK_1'=1.36$ and $pK_2'=2.36$; as expected the apparent pK of the terminal ammonium group is considerably depressed. This clearly illustrates the difficulties in correlating observations made at various pH values with the binding of a metal ion to a specific group. The binding constant of the metal must also be known to make such a correlation. The observed precipitation of the $Cu(OH)_2$ in the equimolar glycine-$CuCl_2$ solution at pH 6 is also explained by considering the reaction $Cu(II) + OH^- = Cu(OH)_2$ and writing the reaction between glycine and Cu(II) at high pH (>6) as $Cu(II)+2G^-=CuG_2$. There is then competition between these two reactions at these pH values and due to the larger value of K (over that of K_s)

this reaction predominates. However, when the reaction mixture is equimolar in glycine and Cu(II) the reaction $Cu(II) + G^- = CuG^+$ cannot compete with the reaction $Cu(II) + OH^- = Cu(OH)_2$ above pH 6. The reaction $CuG^+ + G^- = CuG_2$ gives a more stable form of Cu(II) and leaves 1/2 of the Cu(II) uncomplexed, which will be precipitated as $Cu(OH)_2$.

The reaction of Cu(II) with glycylglycine is more complicated. When an equimolar mixture of $CuCl_2$ and glycylglycine is titrated with NaOH the curve shown in Fig. 9 results. From this curve it can be seen that in the pH region 3.4 to 7.5 a buffering effect is operative and two equivalents of NaOH are consumed. A further equivalent of hydroxide is consumed between pH 7.5 and 10. The values for the proton ionization constants for the carboxyl and terminal ammonium groups are $10^{-3.12}$ and $10^{-8.37}$ respectively (32). By analogy with the Cu(II)-glycine solutions, one equivalent of hydroxide consumed in the range pH 4 to 7 can be attributed to proton ionization from the terminal ammonium group. The reason for the uptake of the second equivalent of hydroxide in this pH region is still unsettled. Two proposals are under consideration. One is that the buffering is due to proton ionization from the peptide bond and the other is that it is due to hydroxyl ion association with the Cu(II) in the glycylglycine complex (32). The ionization of a proton from the peptide bond is considered the most likely possibility for the following reasons. The uptake of hydroxyl ion is associated with the formation of the intense absorptions seen for these complexes (the biuret reaction). If the groups around the nitrogen are modified to increase the acid strength of the nitrogen atom (lower the pK of the

FIG. 9

TITRATION CURVE OF EQUIMOLAR Cu(II) AND GLYCYLGLYCINE

Titration curve of solution containing glycylglycine (0.005M) + $CuCl_2 \cdot 2H_2O$.

According to Dobbie and Kermack (32)

FIG. 10

TITRATION CURVE OF 2:1 GLYCYLGLYCINE: Cu(II)

Titration curve of solution containing glycylglycine (0.01M) + $CuCl_2 \cdot 2H_2O$ (0.005M).

According to Dobbie and Kermack (32)

FIG. 11

TITRATION CURVE OF 3:1 GLYCYLGLYCINE:Cu(II)

Titration curve of solution containing glycylglycine (0.015M) + $CuCL_2 \cdot 2H_2O$ (0.005M).

According to Dobbie and Kermack (32)

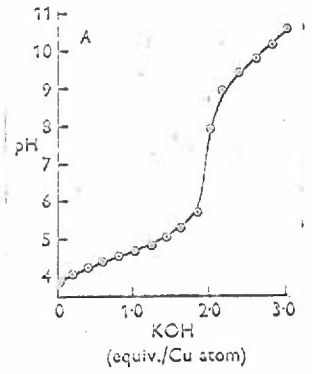
A
pH
11
10
9
8
7
6
5
4
0
1·0
2·0
3·0
KOH
(equiv./Cu atom)

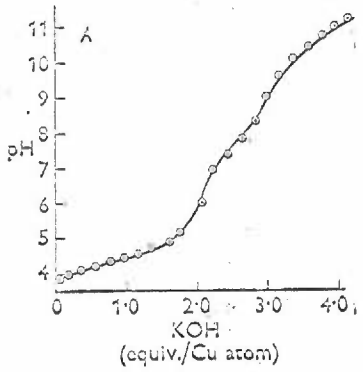
A
pH
11
10
9
8
7
6
5
4
0
1·0
2·0
3·0
4·0
KOH
(equiv./Cu atom)

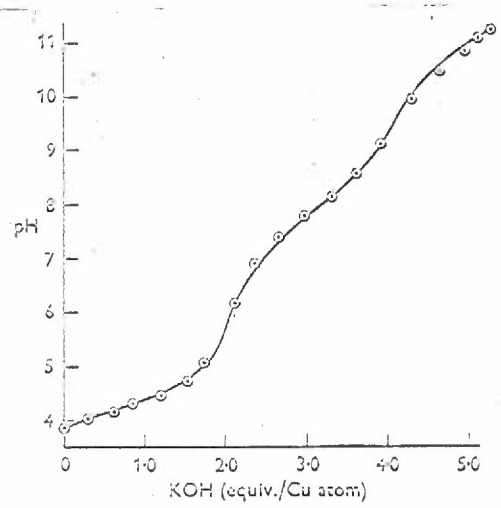
pH
11
10
9
8
7
6
5
4
0
1·0
2·0
3·0
4·0
5·0
KOH (equiv./Cu atom)

proton ionization) then the color reaction occurs at a much lower pH (93). Chemical analysis of the precipitated salts of these complexes show a decreased hydrogen content over that of the free peptides (112). The consumption of two equivalents of hydroxide in the pH range 4 to 7 is seen only for the peptides, not for the simple amino acids; it would appear that the buffering is associated with some property peculiar to peptides (32). The shift to lower wave lengths upon the addition of the second equivalent of hydroxide is associated with the formation of nitrogen atom-Cu(II) atom bonds not oxygen atom-Cu(II) atom bonds (58). Data and Rabin (30) have shown that replacement of the proton on the peptide nitrogen by a methyl group (glycylsarcosine) results in a behaviour similar to that seen for equimolar Cu(II)-glycine mixtures; only one equivalent of hydroxyl ion is consumed in the pH range 4 to 7 and $Cu(OH)_2$ is precipitated beginning at pH6. IR and ESR evidence indicate that a proton on the peptide nitogen atom is necessary for binding of the copper atom to the peptide bond. Crystallographic studies of the glycylglycine and triglycylglycine-Cu(II) complexes indicate that a proton has been dissociated from the peptide nitrogen atom (39). Thus, all the evidence indicates that the proton ionizations in the pH range 4 to 7 are due to terminal ammonium and peptide nitrogen atoms dissociating a proton. It is likely that the buffering in the region pH 7 to 10 (one equivalent of hydroxide consumed) is due to hydroxyl ion association with the Cu(II) atom or, to the ionization of a proton from one of the water molecules in the hydration sphere of the Cu(II).

The equilibria used to describe the Cu(II)-glycine reactions cannot be employed to describe the reactions occurring in the Cu(II) glycylglycine solutions. There is an additional proton ionization in the pH region 4 to 7 to account for, and the buffering in the pH 7 to 10 region must also be described by the equations used. "Before it is possible to set up relationships for equilibrium constants, it is first necessary to decide what reactions probably occur under the experimental conditions."* Generally, the reaction between Cu(II) and glycylglycine (GG) in the pH region 4 to 7 can be represented as (84), $Cu(II)+H_2GG+2OH^- = CuGG+2H_2O$ which accounts for the two equivalents of hydroxide consumed. Dobbie and Kermack (32) consider the possibility that a reaction analogous to that observed for the glycine Cu(II) solutions will occur and write the above reaction in two parts,

(1) $Cu(II) + GG \overset{K_1}{=} CuGG^+$

(2) $CuGG^+ \overset{K_c}{=} CuGG + H^+$

in which they consider the reaction for the displacement of the terminal ammonium proton as a separate reaction. The overlapping of reactions (1) and (2) prevents the occurrence of an inflection at one equivalent of NaOH added which would be expected if the reactions were taking place in two separate steps.

The reaction occurring above pH 7 is written (32)

$$CuGG + H_2O \overset{K_c'}{=} CuGG(OH)^- + H^+ .$$

Using methods first set forth by Bjerrum (10) and fully developed

* Murphy and Martell (84)

by Albert (1) equations can be derived for making successive approximations to the equilibrium constants for the above reactions and in this way values for the equilibrium constants can be obtained. The method used is much the same as that described for the Cu(II)-glycine mixtures. Martell (74) has reviewed the experimental methods used (potentiometric, utilizing various electrodes, polarographic, and spectrophotometric) for the determination of these stability constants.

Dobbie and Kermack also postulate the following reactions as occurring in glycylglycine-Cu(II) solutions,

$$CuGG + GG^- \overset{K_2}{=} CuGG_2^-$$

$$CuGG_2^- \overset{K_c''}{=} CuGG_2^{2-} + H^+$$

The fitting of experimental data (the titration curves) to the proposed reaction schemes is a necessary but not sufficient condition that these reactions represent those that actually occur. Also, the calculation of the equilibrium constants by first assuming values is subject to some error. The values obtained by Dobbie and Kermack are $K_1 = 10^{5.88}$, $K_2 = 10^{3.26}$, $K_c = 10^{-4.25}$, $K_{c'} = 10^{-9.65}$, and $K_{c''} = 10^{-10.20}$. Using these values Dobbie and Kermack have calculated various pH values and glycylglycine to Cu(II) ratios in which the complex forms Cu(II), CuGG, $CuGG(OH)^-$, $CuGG_2^-$, and $CuGG_2^{2-}$ separately account for at least 90% of the complexed Cu(II). The complex $CuGG^+$ cannot be obtained in high concentration ($>10\%$). The tables are reproduced in Appendix III.

The titration curves for 2:1 and 3:1 glycylglycine to Cu(II) ratios are given in Fig.'s 10 and 11. The existance of the 2 to 1 glycylgly-

cine to Cu(II) complex is in doubt (34,84). "It is apparent that the 2:1 titration curves can be interpreted in a number of alternative ways. Therefore in the absence of additional evidence, it is not justifiable to assume more than the formation of structures (which represent only 1:1 complexes)."* Therefore, writing equations describing the formation of such complexes is also not justified. The titration curves for the 2:1 molar mixtures of glycylglycine and Cu(II) can be explained assuming the formation of the 2:1 complexes as given by Dobbie and Kermack or by assuming that the titration curves actually represent the overlapping of two titration curves; that of the Cu(II)-glycylglycine 1:1 complex and that of the neutralization of excess uncomplexed glycylglycine (84). The latter interpretation is favored by Doran et al. (34). Kim and Martell (51) assumed the following two reactions as occurring in 2:1 glycylglycine Cu(II) solutions

(1) $CuGG + GG^{-} = Cu(GG)_2^{-}$

(2) $Cu(GG)_2^{-} = Cu(GG)_2^{2-} + H^{+}$

analogous to the reactions proposed by Dobbie and Kermack. The equilibrium constant for reaction (2) could not be obtained from the potentiometric data. Consistent values for equilibrium constants could be obtained assuming that only reaction (1) occurred. This is consistent with the findings of Koltun et al. (60) rather than with the assumption of Dobbie and Kermack (32) and Datta and Rabin (30) that reaction (2)

* Murphy and Martell (84)

also occurs. Kim and Martell state that the value of the equilibrium constant for reaction (1) indicates that $Cu(GG)_2^-$ is the predominant species in 2:1 molar mixtures of GG and Cu(II) at pH 9. This is not consistent with ESR results given in the Results section. Structures for the complex species proposed by Kim and Martell are given in Fig. 12.

Dobbie and Kermack found that, as judged from potentiometric data, the complexes formed between glycylleucine and glycyltyrosine are essentially the same as those formed between glycylglycine and Cu(II). The phenolic hydroxyl group of glycyltyrosine does not appear to take part in the reaction between this peptide and cupric ions. The peptide carnosine (β-alanylhistidine)-shows a consumption of two equivalents of hydroxide in the pH range 5 to 7 when in equimolar to 4:1 molar ratio with Cu(II). It would appear, if the situation is analogous to the glycylglycine-Cu(II) complexes, that the imidazole group (pK 6.90) is associated with the Cu(II) below pH 5. The evidence for the binding of Cu(II) to the imidazole group is that there is no buffering seen in the region pH 5 to 7 that cannot be accounted for by the terminal ammonium and peptide nitrogen atoms ionizing protons. The binding of Cu(II) to the imidazole group would be expected to lower the apparent pK of the imidazole group to a value such that it would have no buffering capacity in the pH region 5 to 7. ESR data to be given agrees with this interpretation.

Koltun, Roth, and Gurd (60) consider the following three reactions to be responsible for the uptake of three equivalents of hydroxide in the pH range 4 to 10 for an equimolar Cu(II)-glycylglycine mixture,

FIG. 12

PROPOSED STRUCTURES FOR Cu(II)-GLYCYLGLYCINE COMPLEXES

Proposed structures for the complexes formed between Cu(II) and glycylglycine. Structure I corresponds to the complex $CuGG^{+}$, structure II corresponds to the complex CuGG, structure III corresponds to the complex $CuGG(OH)^{-}$, and structure IV corresponds to the complex $(CuGG)_2(OH)^{-}$.

According to Kim and Martell (51)

FIG. 13

TITRATION CURVE FOR EQUIMOLAR DIGLYCYLGLYCINE AND Cu(II)

Titration curve of solution containing diglycylglycine (0.005M) + $CuCl_2 \cdot 2H_2O$(0.005M).

According to Dobbie and Kermack (33)

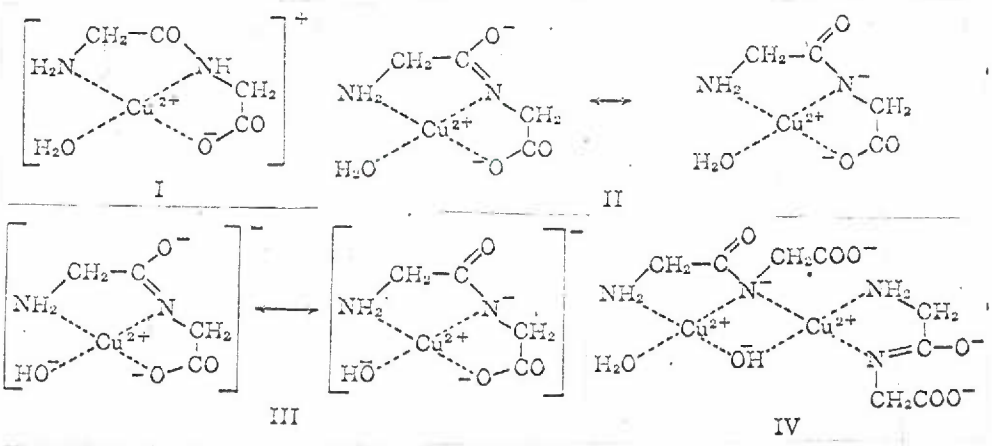
I
II
III
IV

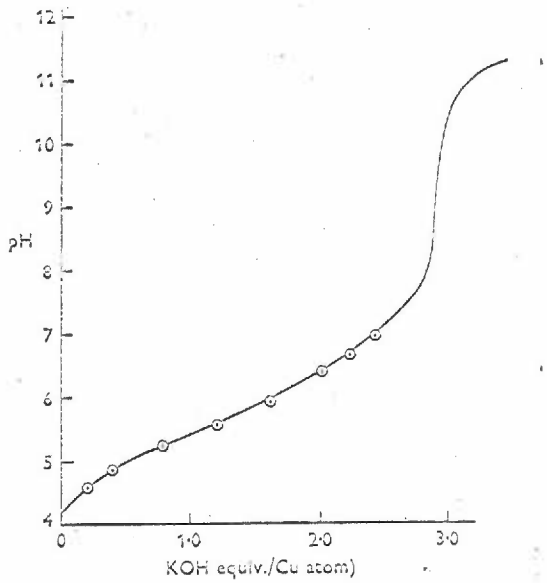
pH
12
11
10
9
8
7
6
5
4
0
1·0
2·0
3·0
KOH equiv./Cu atom)

$$CU(II) + GG^{-} + CuGG^{+}$$

$$CuGG^{+} \rightleftharpoons CuGG + H^{+}$$

$$CuGG = CuGGOH^{-} + H^{+}$$

Which are the same as those first postulated by Dobbie and Kermack. In addition they consider the following reaction as occurring in the pH range 10 to 12

$$CuGGOH^{-} = CuGG\ (OH)_2^{2-} + H^{+}$$

with a pK of 12.2. They also found it necessary to include the following reaction to fit their postulated reactions to the experimental curves,

$$CuGG \pm CuGGOH^{-} = (CuGG)_2OH^{-}$$

with an equilibrium constant of $10^{2.30}$. The results of Koltun, Roth, and Gurd are in general agreement with the results of Dobbie and Kermack.

The earlier investigation of Murphy and Martell (84) supports the findings presented above. In addition, they found that the equilibrium constants for the reactions between glycylglycine and Cu(II) show very little variation over the temperature range 0.35°C to 48.80°C (Table 1). It is to be expected that the forms of the complex ions in solution over this temperature range will be essentially the same.

The potentiometric results obtained for the diglycylglycine-Cu(II) solutions will not be considered in detail as the experiments reported in this thesis have not been sufficiently complete to make a detailed comparison. When an equimolar mixture of diglycylglycine and Cu(II) is titrated with NaOH the titration curve shown in Fig. 13 results. It can be seen from this curve that three equivalents of hydroxide are

TABLE 1

EQUILIBRIUM CONSTANTS FOR THE REACTIONS BETWEEN Cu(II) GLYCINE, GLYCYLGLYCINE, AND DIGLYCYLGLYCINE AS A FUNCTION OF TEMPERATURE

Acid dissociation and chelate formation constants for the reactions between Cu(II) and glycine, glycylglycine, and diglycylglycine. The equilibrium constants are

$$K_2 = [H^+][G^-] / [HG^\pm]$$

$$K_1 = [MG^+] / [M^{+2}][G^-]$$

$$K_2 = [MG_2] / [MG^+][G^-] .$$

According to Murphy and Martell (84)

Ligand	Temperature	pk_2	Log, chelate formation constants						
			Ratio	K_1^{Mn}	K_1^{Mn}	K_1^{Cu}	K_2^{Cu}	K_{1a}	K_{2a}
	°C.								
G	0.35	10.25	1:1	2.12	3.21	8.08			
	0.35		2:1		3.42	8.01	7.34		
	30.00	9.44	1:1	2.23	3.12	8.13			
	30.00		2:1		3.19	8.04	6.39		
	48.80	9.00	1:1	x*	3.01†	7.85			
	48.80		2:1		3.14	7.73	6.49		
GG	0.35	8.71	1:1	x	2.21	6.58		−5.35	
	0.35		2:1		1.87	6.40			
	30.00	8.01	1:1	x	3.33	7.17		−5.38	
	30.00		2:1		3.00	6.94			
	48.80	7.50	1:1	x	3.80	5.78		x	
	48.80		2:1		4.06	5.75			
GGG	0.35	8.57	1:1	1.60	1.85	5.74		−7.32	−6.02
	0.35		2:1			5.68			
	30.00	7.74	1:1	1.95	2.08	5.51		−6.04	−5.52
	30.00		2:1			5.28			
	48.80	7.51	1:1	2.08	2.38†	5.51		x	−4.83
	48.80		2:1		2.51†	5.38			

consumed in the pH range 4 to 8. Dobbie and Kermack found (33) that the potentiometric-titration data alone did not permit calculation of all the relevant equilibrium constants due to the greater variety of distinct molecular species. These were calculated from consideration of both potentiometric and spectrophotometric data. One additional reaction must be inserted to account for the uptake of a third equivalent of hydroxyl in the region pH 4 to 8. By the same arguments given for the glycylglycine-Cu(II) complex, this is assumed to be due to the ionization of a proton from the second peptide nitrogen. Recent work (60) has shown that if the proton on the peptide nitrogen atom nearest the terminal carboxyl is replaced with a methyl group, the complex glycylglycylsarcosine-Cu(II) resembles, potentiometrically, that of glycylglycine. The assumption that this proton ionization does come from the peptide nitrogen thus seems justified. The potentiometric titration curve for glycylsarcosylglycine-Cu(II) mixtures is virtually identical with that of glycine-Cu(II) mixtures shown in Fig.'s 7 and 8 (60). Thus the Cu(II) must first bind to the peptide nitrogen atom nearest the terminal amino group before it can bind to the next peptide nitrogen, or the methyl group sterically hinders such a binding.

C. Spectrophotometric Results

The spectra of the peptide-Cu(II) complexes are best understood using the treatment of crystal-field theory (4, 11) discussed in the section on ESR theory. Such analyses have not been made for the results reported in this thesis and the interpretations based on crystal-field theory will not be considered; the absorption spectra will only be used

to estimate the multiplicity of complex species in solution. A general discussion of the spectra of Cu(II) coordination complexes was given in the first part of this section.

Changes in the absorption spectrum during titration with alkali may be attributable to the formation of successive complexes having different absorption spectra. If these spectra and the relative amount of a given species present under certain specified pH and concentration conditions were known, then a composite absorption curve could be calculated assuming the spectral contributions of the different complexes are additive. Thus, the absorption at any wave length, pH, and Cu(II)-glycine ratio will be given by $E_o = \alpha_1 E_1 + \alpha_2 E_2 + \alpha_3 E_3$ where the E's are the extinction coefficients at that wave length and α_1 is the mole fraction of Cu(II) present, α_2 the mole fraction of CuG^+ present, and α_3 the mole fraction of CuG_2 present. The α's can be calculated from the potentiometrically determined equilibrium constants. E_o, E_2, and E_3 can be determined experimentally since Cu(II) and CuG_2 can be obtained in high concentrations. Thus E_1 can be calculated. This process can also be used to provide an additional equation for the calculation of the equilibrium constants; that is, one less equilibrium constant need be estimated. The observed and calculated E's at various wave lengths and the calculated absorption spectra for Cu(II)-glycine are given in Appendix III and Fig. 14 respectively.

Due to the greater number of (postulated) complex species in the glycylglycine-Cu(II) mixtures the derivation of the absorption curve for each complex species is less straightforward than for glycine and

FIG. 14

ABSORPTION CURVES FOR THE Cu(II)-GLYCINE COMPLEXES

Computed absorption curves of free cupric ions and copper-glycine complexes. Curve A, Cu^{2+}; curve B, CuG^{+} and curve C, CuG_2. (G^{-} represents the glycine anion.)

According to Dobbie, Kermack, and Lees (31)

FIG. 15

ABSORPTION CURVES FOR THE Cu(II)-GLYCYLGLYCINE COMPLEXES

Absorption curves of copper-glycylglycine complexes. Curve A, $CuGG^{+}$; curve B, CuGG; curve C, $CuGG(OH)^{-}$; curve D, $CuGG_2^{-}$; and curve E, $CuGG_2^{2-}$. (GG^{-} represents the glycylglycine anion.)

According to Dobbie and Kermack (32)

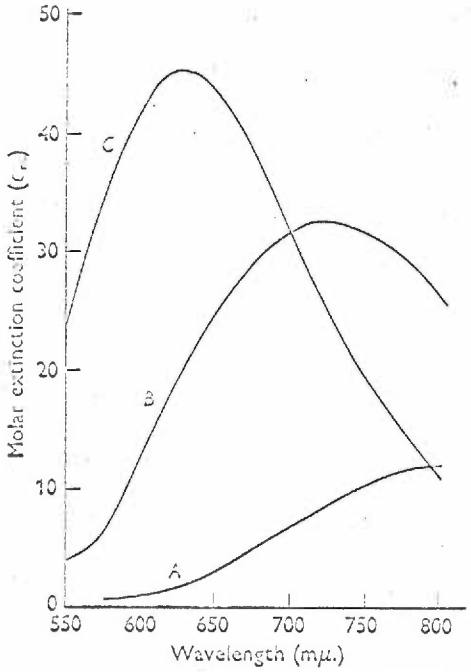
Molar extinction coefficient (ϵ_m)
50
40
30
20
10
0
C
B
A
550
600
650
700
750
800
Wavelength (mμ.)

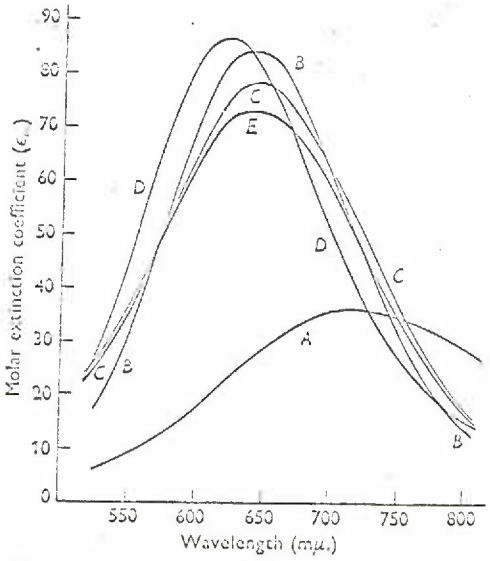
Molar extinction coefficient (ϵ_m)
90
80
70
60
50
40
30
20
10
0
B
C
E
D
D
C
A
C
B
B
550
600
650
700
750
800
Wavelength (mμ.)

Cu(II). The method used is the same as described for the glycine-Cu(II) mixtures but more "adjustment" of parameters is necessary for obtaining a satisfactory fit. The absorption curves so calculated are shown in Fig. 15. The values for the E's are given in Appendix III.

What is observed experimentally is that as the glycylglycine-Cu(II) ratio is increased (at pH >7) a shift to shorter wave lengths occurs (Fig. 15). This can be explained by assuming the formation of complexes with absorption maxima at shorter wave lengths or by assuming that a shorter wave length absorption (300 mu) is overlapping the 600 mu absorption more strongly as the glycylglycine:Cu(II) ratio is increased. Assuming a Lorentzian or a Gauusian shape for the absorption curves, it can be shown that if two such curves are overlapping then the absorption maxima (where the first derivative is zero) are not the same for the overlapping curves as they are for the separated curves. This overlapping will move the absorption maxima together. The absorption spectra for glycylglycine-Cu(II) obtained by Kim and Martell (51) are presented in Fig. 16. These were obtained by varying the pH of an equimolar glycylglycine-Cu(II) mixture. No shift in the absorption maximum at 640 mu is seen, only an increase, or decrease, in the absorbancy. It can also be seen that the absorbancy at 480 is increasing. This could be due to the increased overlap of a higher wave length absorption. Experimental verification of one explanation or the other has not been obtained.

The absorption specta and calculated E values for the Cu(II) diglycylglycine complexes are shown in Fig. 17 and Appendix III respectively. The shift in the wave length from 600 mu to 550 mu when the solu-

FIG. 16

ABSORPTION CURVES FOR EQUIMOLAR Cu(II) AND GLYCYLGLYCINE AT VARIOUS pH VALUES

Visible spectra of Cu(II)-glycylglycine complexes in aqueous solution: (a) pH = 3.75; (b) pH = 4.07; (c) pH = 4.52; (d) pH = 4.75; (e) pH = 5.00; (f) pH = 7.76; (g) pH = 9.83.

According to Kim and Martell (51)

FIG. 17

ABSORPTION CURVES FOR EQUIMOLAR Cu(II) AND DIGLYCYLGLYCINE

Computed absorption curves of copper-diglycylglycine complexes. Curve A, $CuGGG^{+}$; curve B, CuGGG; curve C, $CuGGG^{-}$; curve D, $Cu(GGG)_2^{-}$ and curve E, $Cu(GGG)_2^{-}$. (GGG^{-} represents the diglycylglycine anion.)

According to Dobbie and Kermack (33)

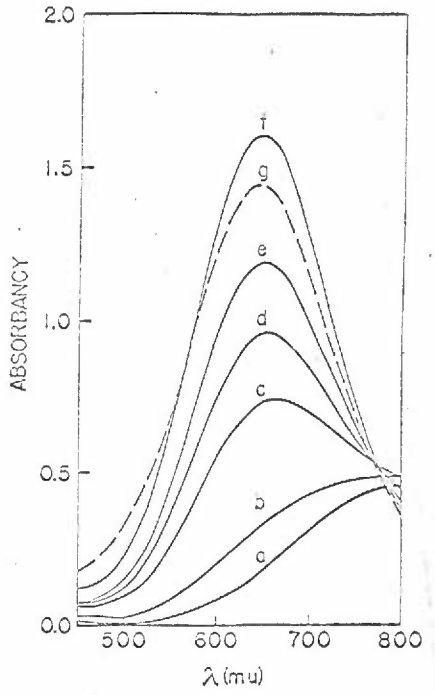
2.0
1.5
1.0
0.5
0.0
ABSORBANCY
f
g
e
d
c
b
a
500
600
700
800
λ (mμ)

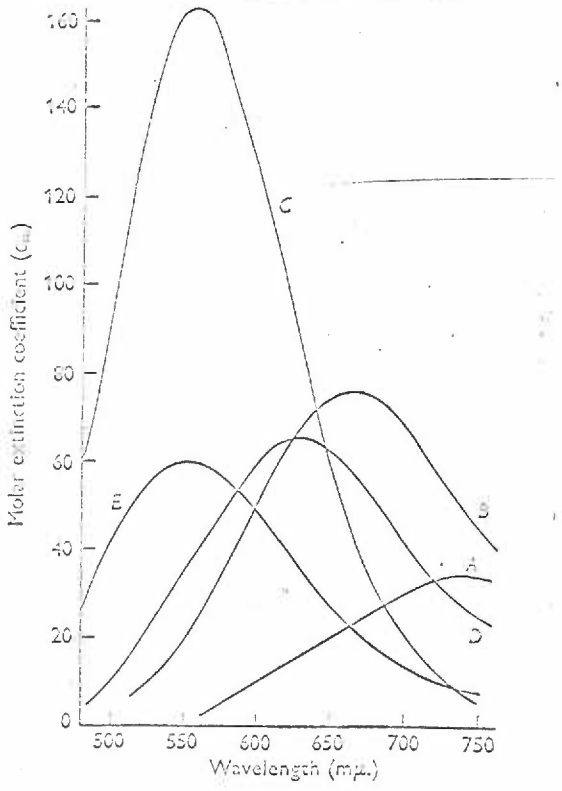
160
140
120
100
80
60
40
20
0
Molar extinction coefficient (εM)
C
B
A
D
500
550
600
650
700
750
Wavelength (mμ.)

tion is made strongly alkaline is the blue to purple (biuret) shift discussed earlier.

The absorption maxima and extinction coefficients for the various forms of the Cu(II) complexes with glycylglycine, diglycylglycine, triglycylglycine, diglycylsarcosine, glycylsarcosine, and glycylsarcosylglycine are given in Table 2. The conclusions that can be drawn from these results are the same as those given by Kober and Haw (58). The binding of Cu(II) by oxygen atoms produces blue or green solutions with $\lambda_{max} \cong 650$ mu. The binding of the Cu(II) by nitrogen atoms shifts the absorption maximum to lower wave lengths; the greater the number of nitrogen atoms involved in the binding, the greater the blue shift of the absorption maximum. Possible explanations for this will be considered in the Discussion.

D. Infrared Results

Lenormant and Chouteau examined the IR spectral modifications of peptides and proteins accompanying the binding of Cu(II). They attributed the binding of the Cu(II) to the peptide linkage since the perturbed IR band was characteristic of this linkage. To make this assignment unambigious, they examined the IR spectrum of acetylglycylglycyl-N-ethylamine (CH_3-CONH-CH_2-CONH-CH_2-COHN-C_2H_5), which contains only the peptide linkage as a functional group, and its complex with Cu(II) (23, 24). The complex was formed at pH 12 to 13 and the solution was evaporated to dryness; the IR spectrum of the residue was determined. The results are shown in Fig. 18 and are the same as previously observed for the peptide-and protein-Cu(II) complexes. The

TABLE 2

ABSORPTION MAXIMA AND EXTINCTION COEFFICIENTS FOR Cu(II)-PEPTIDE COMPLEXES

According to Koltun, Roth, and Gurd (60)

Absorption characteristics in visible region of individual Cu(II)-peptide complexes

Peptide	CuP^+		CuP		CuP^- or $CuPOH^-$		CuP_2^-	
	λ_{max}	ϵ_{max}	λ_{max}	ϵ_{max}	λ_{max}	ϵ_{max}	λ_{max}	ϵ_{max}
	$m\mu$	$M^{-1}\ cm^{-1}$	$m\mu$	$M^{-1}\ cm^{-1}$	$m\mu$	$M^{-1}\ cm^{-1}$	$m\mu$	$M^{-1}\ cm^{-1}$
Glycylglycine[a]	735	65	635	84	650	75	625	82
	(720)[b]	(38)	(640)	(84)	(645)	(77)	(625)	(85)
Diglycylglycine	730	37	660	75	555	149	600	68
	(735)[c]	(35)	(660)	(76)	(555)	(162)	(620)	(66)
Triglycylglycine	730	39	660	72	590	101	600	71
Diglycylsarcosine	725	37	640	67	630	65	620	83
							CuP_2	
Glycylsarcosine[a]	720	32	[d]	[d]	[d]	[d]	675	45
Glycylsarcosylglycine	720	40	[d]	[d]	[d]	[d]	670	44

FIG. 18

IR SPECTRA OF THE Cu(II)-ACETYLGLYCYLGLYCYL-N-ETHYL AMIDE COMPLEX

IR spectra of solid samples of acetylglycylglycyl-N-ethylamide at neutral pH, at pH 12-13, and at pH 12-13 in the presence of $Cu(OH)_2$.

According to Chouteau (24)

FIG. 19

IR SPECTRA OF EQUIMOLAR Cu(II) AND GLYCYLGLYCINE

Infrared spectra of Cu(II)-glycylglycine complexes in aqueous (D_2O) solutions (1:1). $T_{Cu}=T_{GG}=0.2333$ M, and ionic strength 1.0, adjusted with KCl: — — —, pD 3.58; ----, pD 4.24; — · · — · —, pD 5.18; ———, pD 10.65.

FIG. 20

IR SPECTRA OF 2:1 GLYCYLGLYCINE:Cu(II)

Infrared spectra of Cu(II)-glycylglycine complexes in aqueous (D_2O) solutions (1:2). $2T_{Cu}=T_{GG}=0.2333$M, and ionic strength 1.0, adjusted with KCl: — — —, pD 3.85; ----, pK 5.35; — · — · —, pD 9.14; ———, pD 11.82.

According to Kim and Martell (51) Fig. 19, 20

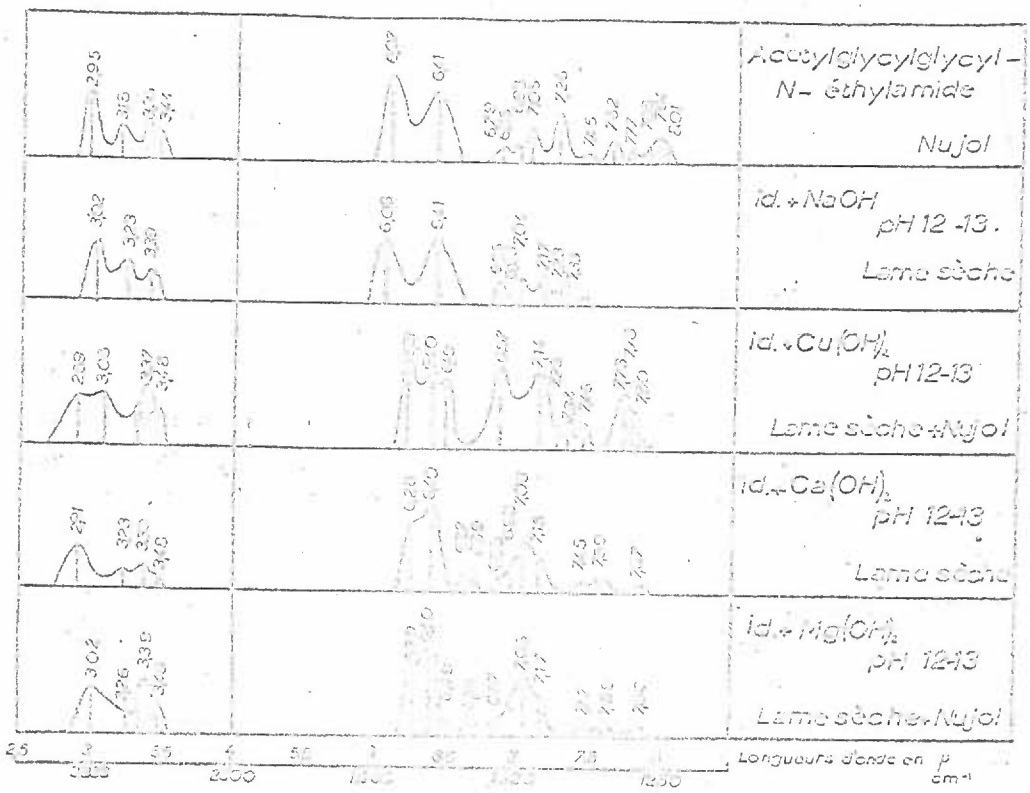
Acetylglycylglycyl-
N- éthylamide
Nujol
id. + NaOH
pH 12 -13.
Lame sèche
id. + Cu(OH)2
pH 12-13
Lame sèche + Nujol
id. + Ca(OH)2
pH 12-13
Lame sèche
id. + Mg(OH)2
pH 12-13
Lame sèche + Nujol
Longueurs d'onde en μ
cm-1

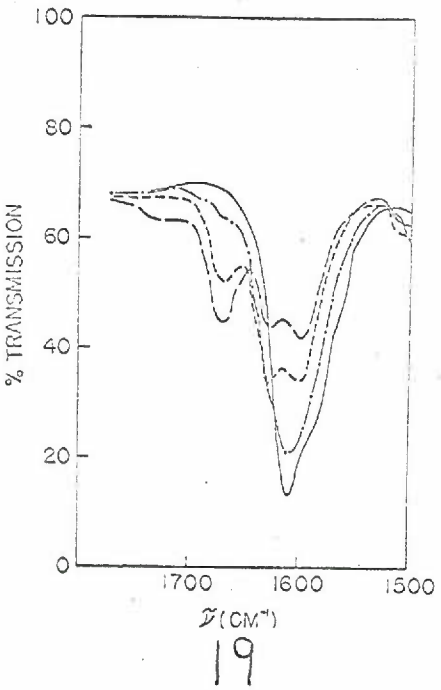
100
80
60
40
20
0
% TRANSMISSION
1700
1600
1500
ν̄ (CM⁻¹)

19

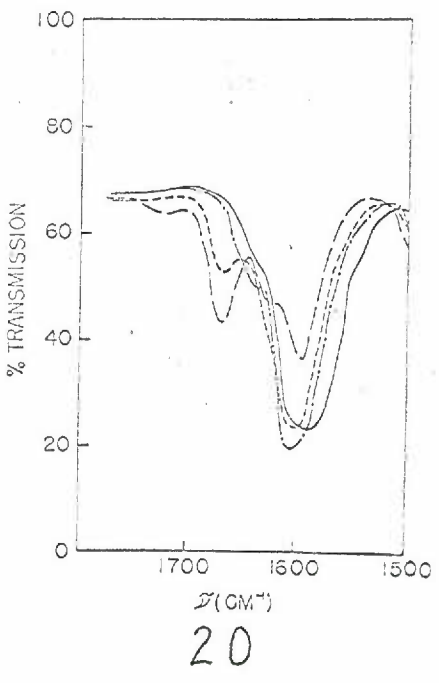
100
80
60
40
20
0
% TRANSMISSION
1700
1600
1500
ν̄ (CM⁻¹)

20

disappearance of the 6 μ band is taken as evidence for the binding of the Cu(II) to the peptide bond.

Kim and Martell (51) determined the IR spectral modifications in D_2O solution when glycylglycine binds Cu(II). The IR specta obtained are shown in Fig.'s 19 and 20. The four absorption bands that appear in the carbonyl region at low pD (3.6) are unionized carboxyl (1720 cm^{-1}), peptide carbonyl with an adjacent positive amonium group (1670 cm^{-1}), peptide carbonyl with an adjacent neutral α-nitrogen atom (1625 cm^{-1}), and unionized carboxyl (1598 cm^{-1}). At the corresponding pD only the first two bands are observed with free glycylglycine. Thus at this pD some Cu(II) has combined with the glycylglycine with displacement of protons from carboxyl and terminal amino groups analogous to the binding of Cu(II) by glycine.

As the pD is raised, the unionized carboxyl band disappears as do the other three bands and a new band at 1610 cm^{-1} appears. If the displacement of a proton from the peptide linkage occurs, the following resonance structures are possible

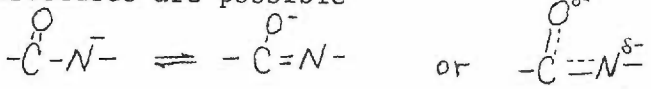

The stretching vibration $\overleftrightarrow{C=O}$ is that giving rise to the 1600 cm^{-1} absorptions. If the double bond character is reduced, as above, then this stretching vibration would shift to lower frequencies (lower energy). That such a shift does occur provides indirect evidence for the ionization of a proton from the peptide bond in the presence of Cu(II). Whether the Cu(II) is bound to the oxygen or the nigrogen atom of this linkage cannot be determined from this data. The direct confirmation of the

loss of a proton from the peptide nitrogen, the loss of the peptide $\backslash N\text{-}H$ absorption, cannot be made since the frequency of this absorption is masked by strong O--D absorptions.

E. Crystallographic Results

The crystal structures of copper (II) monoglycylglycine trihydrate (102, diglycylglycine copper (II) (26), and triglycylglycine copper (II) decahydrate (39) have been determined and the crystal structures are shown in Fig.'s 21, 22, and 23.

The crystal copper (II) monoglycylglycine trihydrate contains two non-equivalent copper complexes in the unit cell. The differences are found in the hydrogen bonding of the complexes. These differences are subtle and reference should be made to the article of Strandberg et al. for a complete exposition. The arrangement of the other atoms about the Cu(II) is consistent throughout the crystal. This is shown in Fig. 21. The arrangement of the atoms about the Cu(II) places the Cu(II) in an approximately square planar environment. This involves a water molecule and the terminal amino, peptide nitrogen, and oxygen of the terminal carboxyl of a single glycylglycine molecule. This involves a distortion of the C-N-C' bond angle from a normal value of ~110° (88) to 122°. The Cu(II) atom is moved slightly out of the N, O_1, O'', N plane towards a loosely coordinated water molecule. No drastic change is observed at the peptide nitrogen atom arising from replacement of the hydrogen ion by a copper (II) ion. The bond length of the Cu--N (amino) bond is 2.02 Å and that for the Cu--N (peptide) is 1.88 Å. Possible implications of these results are to be discussed

FIG. 21

CRYSTAL STRUCTURE OF Cu(II)-GLYCYLGLYCINE

(A) shows a general view of the packing of the molecules. The dashed lines are hydrogen bonds. (B) shows the coordination around the Cu(II) ions. Inathe upper and lower limits of the bond distances and in b the bond angles are given.

According to Strandberg, Lindqvist and Rosenstein (102)

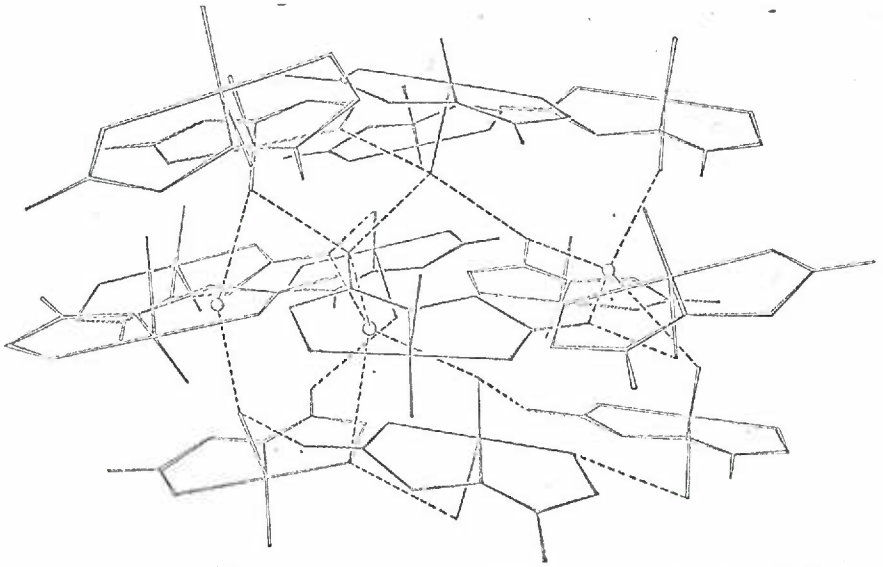

A

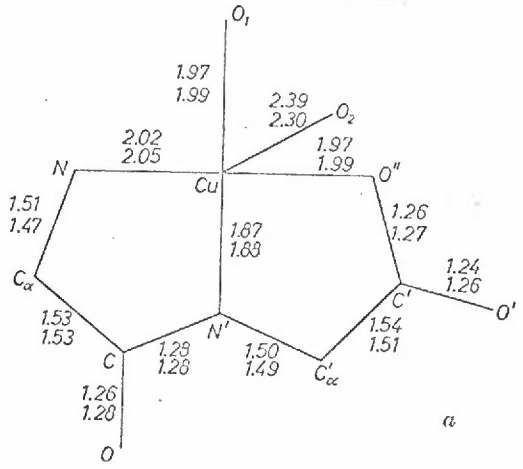
O1
1.97
1.99
2.39
2.30
O2
2.02
2.05
N
1.97
1.99
O''
Cu
1.51
1.47
1.87
1.88
1.26
1.27
1.24
1.26
Cα
C'
O'
1.53
1.53
N'
1.54
1.51
C
1.28
1.28
1.50
1.49
C'α
1.26
1.28
O

a

B

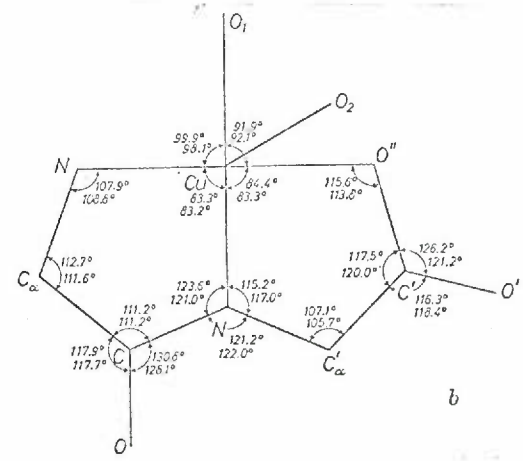
O1
O2
99.9°
98.1°
91.9°
92.1°
N
O''
107.9°
108.6°
Cu
83.3°
83.2°
84.4°
83.3°
115.6°
113.8°
112.7°
111.6°
Cα
117.5°
120.0°
126.2°
121.2°
C'
O'
123.6°
121.0°
115.2°
117.0°
116.3°
118.4°
111.2°
111.2°
107.1°
105.7°
N
121.2°
122.0°
117.9°
117.7°
C
130.6°
126.1°
C'α
O

b

later.

The crystal structures of two complexes of glycylglycylglycine-Cu(II) have been determined. A blue green crystal was obtained by partial evaporation of an equimolar $CuCl_2$-diglycylglycine solution. The pH of such a solution is ~4 and it would be expected that only the terminal carboxyl group and terminal amino have dissociated a proton at this pH. The structure is shown in Fig. 22. The Cu(II) is five-coordinate, the terminal amino and adjacent carbonyl oxygen of one diglycylglycine molecule providing two ligands, the terminal carboxyl of another diglycylglycine molecule providing a third, and the remaining two coming from a water molecule and a chloride ion. Thus, while the peptide bond is involved in the binding it is involved through the oxygen atom and only one peptide bond per diglycylglycine is involved in Cu(II) binding. Each peptide chain is bound to two Cu(II) atoms; to one through the terminal carboxyl and to the other through the terminal amino. The Cu(II) site approximates square planar symmetry with the Cu(II) displaced from the amino, carbonyl, carboxyl, chloride plane towards the water molecule.

Another crystalline form of glycylglycylglycine-Cu(II) analysed was the same as that obtained by Rising et al. (95). As previously described, the crystals were formed from a strongly alkaline solution of glycylglycylglycine and Cu(II) and were purple in color. The pH of the solution was ~10 and at this pH the peptide nitrogens are thought to ionize protons upon binding Cu(II). The crystal structure is shown in Fig. 22. The Cu(II) is again five coordinate and approxi-

FIG. 22

CRYSTAL STRUCTURE OF THE pH 4 AND pH 10 COMPLEXES OF Cu(II) AND DIGLYCYLGLYCINE

(A) is the crystal structure of the pH 4 Cu(II) diglycylglycine complex and (B) is the crystal structure of the pH 10 Cu(II) diglycylglycine complex.

According to Cooper, Freeman, Robinson, and Schoone (26)

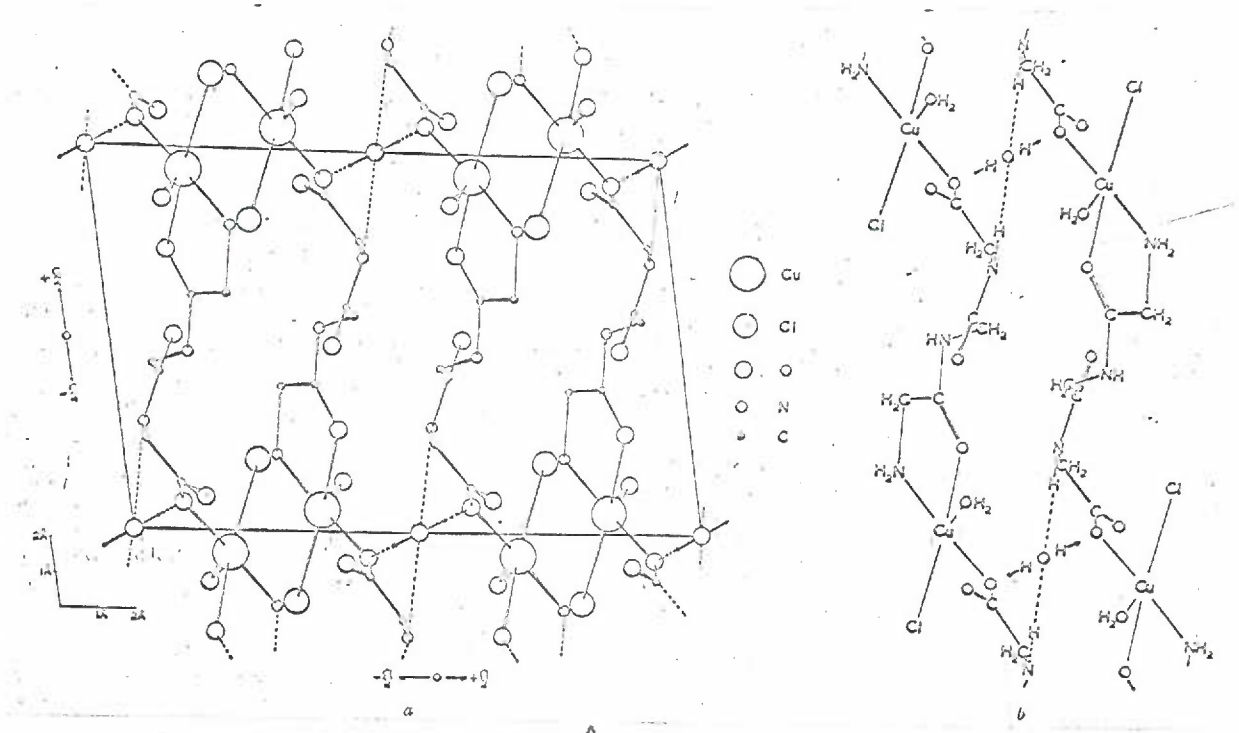

A

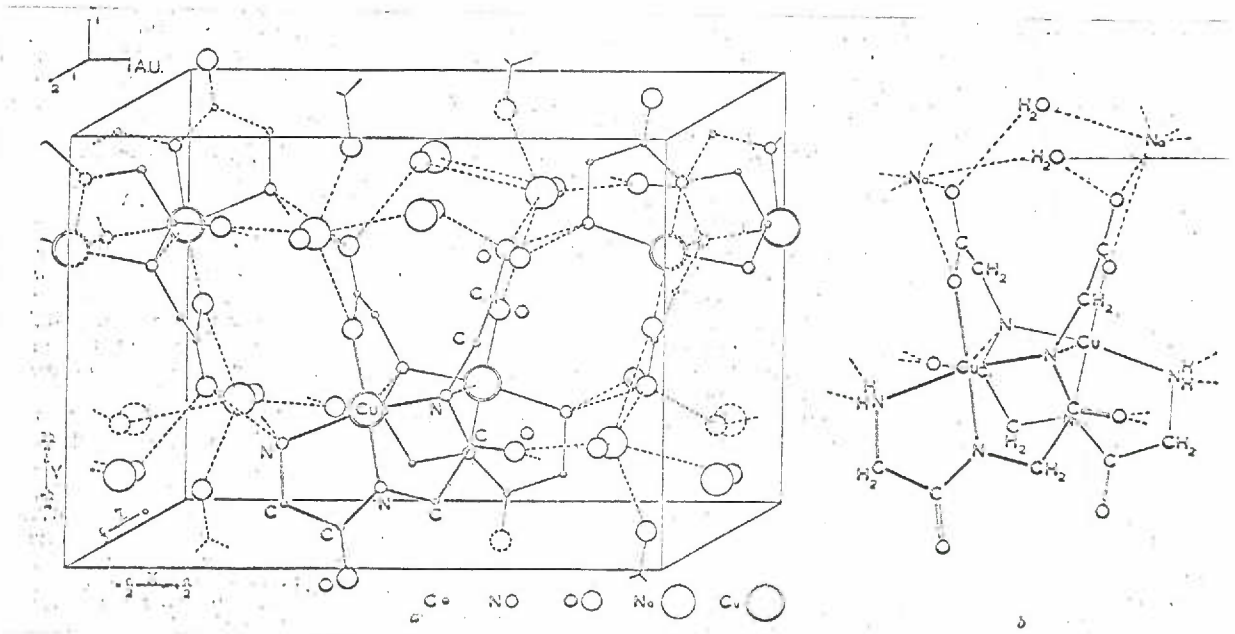

B

mates square planar symmetry. The atoms providing the square planar arrangement of ligand atoms are the terminal amino nitrogen atom and the two peptide nitrogen atoms of the same diglycylglycine molecule and the carboxyl oxygen of another diglycylglycine molecule. In addition, the peptide nitrogen atom nearest the carboxyl group of the diglycylglycine molecule providing the carboxyl oxygen ligand atom is bound, at right angles to the plane, to the same Cu(II) atom as is the terminal carboxyl oxygen atom. Each Cu(II) atom is bound by two peptide molecules and each peptide molecule is binding two Cu(II) atoms; the unit cell is a dimer of the form $Cu_2(peptide)_2$.

The complex disodium glycylglycylglycylglycino cuprate(II) decahydrate was crystallized as red needles from an alkaline solution containing equimolar quantities of cupric hydroxide and triglycylglycine. The crystal consists of layers of triglycylglycine cuprate (II) anions shown in Fig. 23. The Cu(II) is four coordinate with the terminal amino nitrogen atom and the three peptide nitrogen atoms providing the ligands. The Cu(II) site is distorted square planar, the distortion being attributable to the strain of forming three 5-membered rings. The protons formally attached to the peptide nitrogen atoms of the free peptide are ionized. On the basis of bond lengths, the Cu(II) bonding to the four nitrogen atoms is not, for any of the four bonds, equivalent.

It would seem that on this basis the structure of the Cu(II) peptide complexes has been determined. Two general comments can be made. A crystal structure analysis does not provide proof that a complex

FIG. 23

CRYSTAL STRUCTURE OF THE pH 10 COMPLEX OF
Cu(II) AND TRIGLYCYLGLYCINE

The configuration and interatomic distances of the glycylglycylglycylglycinocuprate (II) anion. (Distances are in Å.)

According to Freeman and Taylor (39)

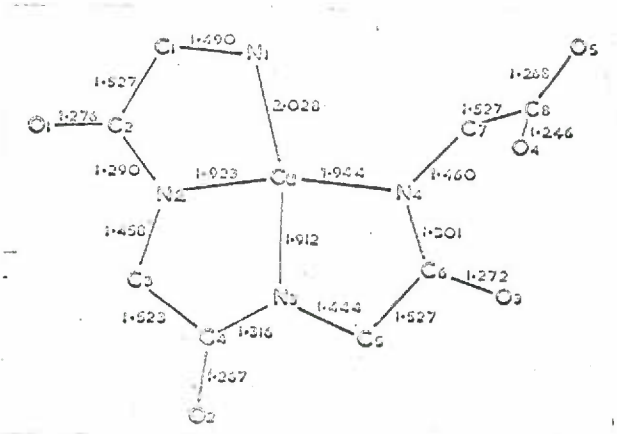
C1
1·490
N1
1·527
2·028
O1
1·276
C2
1·290
N2
1·923
Cu
1·944
N4
1·460
C7
1·527
C8
1·268
O5
1·246
O4
1·458
1·912
1·301
C3
C6
1·272
O3
1·523
N3
1·444
1·527
C5
1·316
1·267
O2

has a particular structure in solution. The determination of crystal structures does not provide electron probability distributions. Specifically, in the complexes glycylglycine-Cu(II), diglycylglycine-Cu(II), and tri-glycylglycine-Cu(II) the Cu(II) is bonded to two peptide molecules. This is in conflict with the potentiometric data in which only 1:1 complexes are seen to be present in solution. Finally, the crystal lattice may impose stereochemical restrictions on the symmetry of the complex which would not be present in solution. Direct experimental evidence relating the crystal structure and the structure of the complex in solution must be given for every case.

4. Model Copper Proteins

The copper-containing proteins in which the protein combines reversibly* with copper ions have been less extensively investigated than the copper proteins to be discussed in the following section. They are characterized by the following properties; the metal is loosely bound to the protein and dissociates readily; the stoichiometry between the metal and protein is less rigid than for the copper proteins; and the binding is non-specific in that, generally, several different metal ions are bound by the same protein.

A. The "Biuret" Complex of Proteins

The best known Cu(II)-protein complex is that formed in the biuret reaction. Ritthausen discovered (96), in 1873, that proteins undergo, under alkaline conditions and in the presence of Cu(II), a color reaction that has come to be known as the biuret reaction. This discovery led to the practical application of the biuret reaction for the qualitative and quantitative determination of proteins. The elucidation of the nature of the protein-Cu(II) complex formed in the biuret reaction has been under investigation ever since. Kober and Haw (58) studied, spectrophotometrically, the reaction between casein, egg al-

* The term "reversible" cannot be used without qualification. The possibility exists that the proper conditions have not been obtained which will lead to reversible removal of the metal from the protein. Thus, the terms "reversible removal" must be further qualified by conditions as "under mild alkaline or acid conditions". Curzon (29) demonstrated that for ceruloplasmin the color and oxidase activity towards paraphenylene can be reversibly abolished, accompanied by the removal of Cu(II), by treatment with acetic acid and a pH of 3.5. In the presence of Cu(II), when the pH is returned to 7, the color and oxidase activity is 90% restored accompanied by the rebinding of the Cu(II).

bumin, erestine, and peptone and $Cu(OH)_2$ under strongly alkaline conditions. Their findings are reproduced in Appendix II. The protein-Cu(II) complexes have an absorption maximum at 540 mu which is the same as that shown by many tripeptide Cu(II) complexes under slightly alkaline conditions. Kober and Haw conclude that, "These results support, if they do not prove two points: (1) that the so called 'biuret reaction,' a test used for the past half century for detecting proteins qualitatively, is no other than a complex formation with copper and, therefore, as far as color formation is concerned, no decomposition of the protein is involved. (2) That the protein configurations are such that permit only 3 nitrogen groups to form rings with copper; and, therefore, the protein molecule must be aggregated, and is not in the form of long free chains or branches of peptides or conjugated amino acids."* Strickland et al. (103) estimated that between 5 and 6 peptide nitrogen atoms were involved in the binding of the Cu(II), but this estimate was based on estimated total peptide bonds in the proteins studied and the total number of Cu(II) atoms bound. Koltun, Roth, and Gurd (60) found that a maximum of 4 nitrogen atoms (terminal amino plus peptide) are directly involved in the binding of Cu(II).

B. Serum Albumin

Klotz et al. (53) found that the binding of Cu(II) by bovine serum albumin produced an absorption band at 375 mu (Fig. 24). The dependence of the height of the peak on pH is shown in Fig. 25. A copper sulfhy-

* Kober and Haw (58)

FIG. 24

ABSORPTION SPECTRUM OF Cu(II)-BOVINE ALBUMIN

Change in the absorption band of copper-bovine albumin with time. Cu(II) 0.0033M; bovine albumin, 0.0003M; pH 6.

According to Klotz, Urquhart, Klotz, and Ayers (53)

FIG. 25

EFFECT OF pH ON THE ABSORPTION MAXIMUM OF Cu(II)-BOVINE ALBUMIN

Effect of pH on the initial height of the 375 mu band in Cu(II) (0.0033M) and bovine albumin (0.0003M).

According to Klotz, Urquhart, Klotz, and Ayers (53)

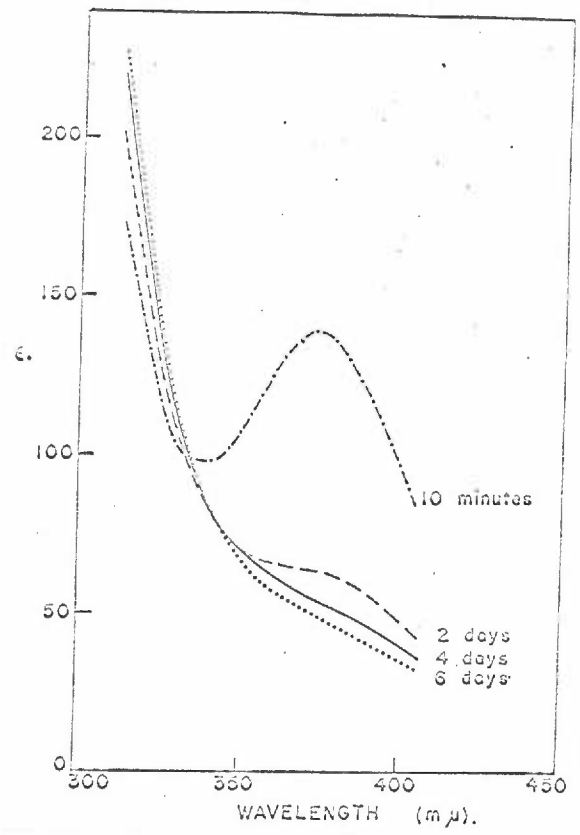
200
150
ε.
100
50
0
10 minutes
2 days
4 days
6 days
300
350
400
450
WAVELENGTH (mμ).

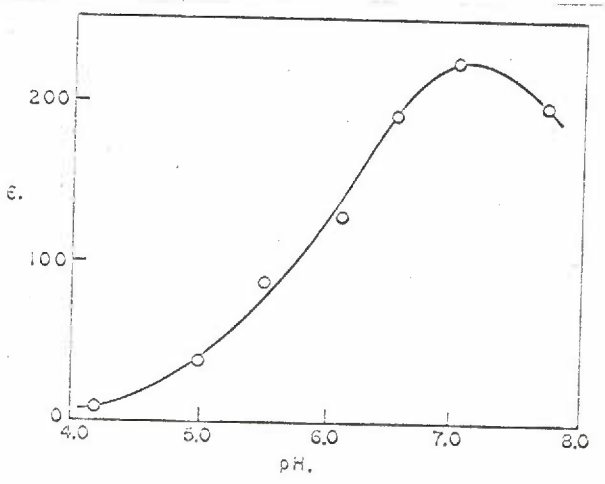
200
ε.
100
0
4.0
5.0
6.0
7.0
8.0
pH.

dryl bond was implicated by experiments in which reagents which block sulfhydryl groups were used. In bovine serum albumin treated with a sulfhydryl reagent the addition of Cu(II) gave no indication of an absorption peak at 375 mu. However, this should be considered in terms of the work of Fraenkel-Conrat (111) discussed below. The binding of Cu(II) by sulfhydryl groups is different from its binding by simple peptides. This will be discussed in the section on preliminary results.

The use of potentiometric data for the identification of binding groups in metal protein complexes is, in general, ambiguous. Tanford (104) studied the effect of the binding of various metal ions by serum albumin, as a function of pH, on the limiting polarographic current. The formation of metal complexes considerably reduces the limiting polarographic current (diffusion current) over that seen for the free (hyrated) metal ion. This is due to a lowered diffusion rate in solution for the metal complex (59). Tanford et al. found that the polarographic current was considerably reduced in the pH range 5 to 7 for serum albumin-metal ion solutions whereas below pH 5 the limiting polarographic current is much the same as that seen for the free metal ion. It was concluded that, since this is in the region of the pK of the imidazole ionization, the Cu(II) must bind to imidazole groups. These results were compared with those obtained using pepsin, which contains only two imidazoles per molecule, in which no significant drop in the polarographic current is seen until pH 10 (one wonders why all metal ions had not precipitated as the hydroxide at a pH much lower than this).

It was concluded that, for metal binding by pepsin, the primary binding comes from amino, tyrosyl or sulfhydryl groups which have pK's in this range. As discussed in the Cu(II) peptide section, it is virtually certain that the pK of any group binding a metal ion will be considerably depressed and unless the new pK can be determined no assignment of binding groups can be made on this basis alone. Evidence of this sort essentially implicates every group dissociating a proton which has a pK above that of the measured pH at which Cu(II) binding occurs.

C. Conalbumin and Transferrin

Conalbumin, a protein from egg white, combines stoichiometrically with ferric or cupric ions (111). When the metal-protein complex is formed, hydrogen ions are displaced from the conalbumin. It was found that 2.9 equivalents of protons were displaced in ferric ion binding and 1.9 were displaced in cupric ion binding. This displacement of protons was constant over the pH range 4 to 9.5. As no proton dissociations occur in conalbumin up to pH 9,5, the pK of the group ionizing a proton in the presence of Cu(II) must be greater than 10 in its absence. In an effort to identify the groups responsible for the binding, chemical modifications of specific groups have been made. It was found that the metal binding capacity was reduced by every type of modification employed. The electrophoretic mobility of conalbumin at pH 11.2 was essentially the same as that of the ferric-conalbumin complex, while at pH 8.6 the mobility of the conalbumin was appreciably less than that of the complex. This means that some groups on the conalbumin which have not ionized at pH 8.6 have at least partially ionized

at pH 11.2. If it is assumed that these groups which are ionizing are the same as those binding the metal ions (which perhaps is not justified a priori) then the binding groups will have pK's in the range pH 11.2. The phenolic hydroxyl group is deemed the most logical choice (111). However, Dobbie and Kermack found no evidence for Cu(II) binding by the phenolic hydroxyl in glycyl tyrosine (32).

The binding of Cu(II) by human plasma transferrin parallels that of the Cu(II) binding by conalbumin (116). The ESR spectra of lyophilized and aqueous Cu(II) conalbumin at liquid nitrogen temperatures are shown in Fig. 26. The ESR spectra of chicken, turkey, and Japanese quail conalbumin and human transferrin and lactotransferrin were all essentially the same (116). The ESR spectra are the same as those seen and calculated (98) for Cu(II) in an axially symmetric site (square planar). Additional hyperfine structure is evident on the $g_{\perp}$ absorption. It is better resolved for the frozen acqueous sample; six hyperfine lines can be seen. The existence of six lines is not consistent with unpaired electron interaction with magnetically equivalent nitrogen atoms (I=1). If one hyperfine line is ignored the resulting five line hyperfine is consistent with an interaction of the unpaired electron with two equivalent nitrogen atoms. The observed number of hyperfine lines in the $g_{\perp}$ region for the tris complex of Cu(II) and 1, 10 phenanthroline was found to be reduced when only ^{63}Cu was used (2) in place of the naturally occurring ^{63}Cu-^{65}Cu mixture (70% and 30% respectively). This is due to the slight difference in Fermi contact terms for the two isotopes. While the spectra are the same (both isotopes

FIG. 26

THE ESR SPECTRUM OF Cu(II)-CONALBUMIN

(A) is the ESR spectrum at liquid nitrogen temperature for a lyophilized sample of chicken conalbumin saturated with copper. (B) is the ESR spectrum at liquid nitrogen temperature for an aqueous solution of copper-conalbumin.

According to Windle, Wiersema, Clark, and Feeney (116)

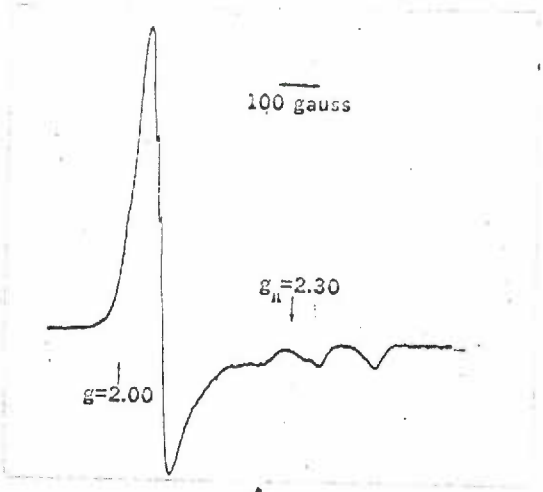

A

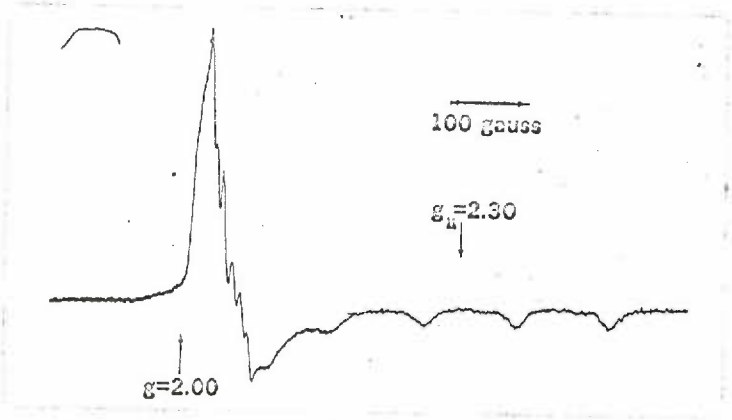

B

have I = 3/2) this difference in the Fermi contact term, due to a difference in magnetic moments, produces two spectra which are slightly out of phase. This in turn gives rise to anomalous hyperfine structure. Experiments utilizing ^{63}Cu only were not conducted with conalbumin and transferrin. Until the number of hyperfine lines present in the ESR spectra is accurately determined, no conclusions as to possible binding groups can be made.

D. Metmyoglobin

The binding of Cu(II) by sperm whale metmyoglobin has been studied by Breslow and Gurd(17). This protein was used since its crystal structure is known (50) and there is good reason to believe that its conformation in solution is the same as it is in the crystalline state (9). It had previously been found that of the twelve imidazoles present per metmyoglobin molecule, six were available for reaction with protons and for the hydrolysis of p-nitrophenyl acetate (44).

The methods used for the study of the binding of Cu(II) by metMb were the hydrolysis of p-nitophenyl acetate and potentiometric titrations. The results obtained are ambiguous. The binding of Cu(II) is non-specific; that is, the number of moles of Cu(II) bound per mole of metMb is a function of the Cu(II) concentration. Native metMb contains six imidazole groups which can catalyze the hydrolysis of p-nitrophenyl acetate. At an ionic strength of 0.06 and pH 6.4 the binding of Cu(II) does not alter the hydrolysis rate of p-nitrophenyl acetate. Thus it would seem that the imidazoles are not involved in the binding of the Cu(II). However, results at an ionic strength of 0.16, at which the

metMb precipitates upon addition of Cu(II), indicate that a conformational change occurs when the metMb binds the Cu(II) and, at an ionic strength of 0.06, the same conformational change occurs but the copper protein complex remains in solution. The lack of increased or decreased reactivity towards p-nitrophenyl acetate could be attributed to the binding of Cu(II) to the imidazoles and the subsequent unmasking of the normally unreactive imidazoles. The converse could also be true in that the Cu(II) could bind to the normally masked imidazoles after the conformational change. The binding of Cu(II) is accompanied by the dissociation of protons with the attendant lowering of pH. The number of protons dissociated is a function of the pH of the solution (Fig.27). This aspect of Cu(II) binding was considered in the section on Cu(II) peptide complexes. Gurd et al. (17) consider the proton ionizations in the pH range 5 to 7 to be due to proton displacement from the imidazoles by the Cu(II). It was found by Dobbie and Kermack (32) that, in the system carnosine (β-alanylhistidine) Cu(II), there is no evidence of buffering by the imidazole group in the pH region 5 to 7, indicating that, if a proton is displaced and Cu(II) subsequently bound to the imidazole group, the proton displacement upon Cu(II) binding occurs below pH5. These results obtained from potentiometric data for the Cu(II) metMb complex are subject to a wide variety of interpretation and until further experimental data is obtained any conclusions made from the potentiometric data alone would be mostly speculation.

E. Carbonic Anhydrase

Apo-bovine carbonic anhydrase can bind Cu(II) (65), but the Cu(II)

FIG. 27

TITRATION OF METMYOGLOBIN IN THE PRESENCE OF Cu(II)

Titration of metMb in presence of $CuCl_2$, $\Gamma/2$ 0.06. For each value of $\bar{\nu}_M$, the solid curve applies to the protein before exposure to pH 3 and the dashed curve after such exposure. Experimental points for $\bar{\nu}_M$ of 2.3 apply to the following ranges of titration: ●, from pH 5.73 to pH 7.18; ○, from pH 7.18 to pH 2.47; ◒, from pH 2.47 to pH 6.88. Corresponding codings (■,□,◪) largely superimposed for $\bar{\nu}_M$ of 4.2, are for the ranges of pH 5.18 to 7.09, 7.09 to 2.53, and 2.53 to 6.70, respectively. $\bar{\nu}_H$ is the average number of protons bound per molecure of metmyoglobin.

According to Breslow and Gurd (17)

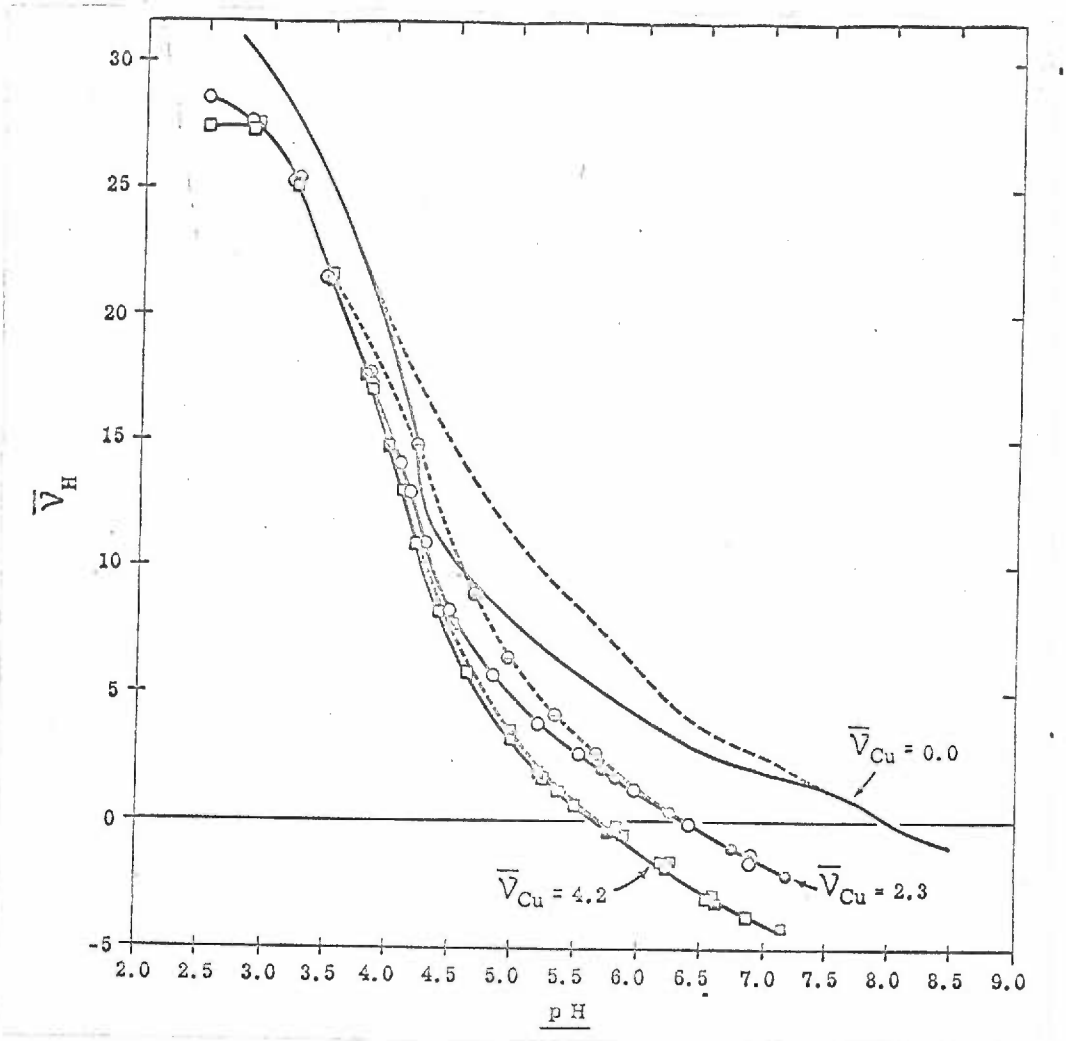
30
25
20
15
10
5
0
-5
$\overline{V}_H$
2.0 2.5 3.0 3.5 4.0 4.5 5.0 5.5 6.0 6.5 7.0 7.5 8.0 8.5 9.0
pH
$\overline{V}_{Cu}$ = 0.0
$\overline{V}_{Cu}$ = 2.3
$\overline{V}_{Cu}$ = 4.2

form of the enzyme is inactive. Replacement of the Cu(II) by Zn(II), which can only be accomplished by prior removal of the Cu(II), restores the enzymic activity. It appears that the Cu(II) is bound to the same site as is the Zn or at least blocks the Zn binding site. The ESR spectrum obtained for the Cu(II)-apocarbonic anhydrase was of the type seen for most Cu(II) chelates (71). Thus on this basis alone, very little can be said about the site of Cu(II) binding and thus, perhaps, the binding site of Zn(II) in carbonic anhydrase.

It must be concluded that ESR investigations of the model protein complexes disscussed above have given little information about the binding groups of the Cu(II). Other experimental methods have not provided unequivocal identification of any of these binding groups either.

E. Insulin

The investigations of Brill and Venable (18) on the ESR spectra of crystalline Cu(II) insulin are of interest in that they constitute the most unequivocal effort in this field. The binding of divalent metal ions by insulin has been investigated by both chemical and physical methods. The physical investigation of importance is that of Schlichtkrull (100) in which a structure determination of a Cu(II) insulin crystal was made. Knowing the crystal structure, the Cu(II) could be placed in the magnetic field in known orientations and the ESR absorption curve obtained. The interpretation is then made on the basis of the ESR theory for single crystals given earlier. This interpretation is not simple and for a complete analysis of the ESR results a

computer analysis was made (109). The analysis was not unequivocal. It was found that the symmetry of the ligands about the Cu(II), as judged from the ESR spectra, is consistent with that obtained from the crystal structure analysis. The Cu(II) occupies a site of trigonal symmetry (distortion of an octahedron along the trigonal axis). (Fig.28). For a specified crystal orientation the high field absorption line is modified by the appearance of five sub-peaks. The most likely coordinating groups responsible for these splittings are two magnetically equivalent nitrogen atoms (18). These results are consistent with the conclusions of Tanford and Epstein (105). They showed, by potentiometric titrations, that for zinc free insulin two groups are titrated in the range pH 6.5 to 7, which would be consistent with the pK of imidazole groups. However, in the presence of Zn(II) the pK of the proton ionization is shifted to approximately 4. This is the expected result if the binding of the Zn(II) ions is to the imidazole groups. Dobbie and Kermack found that in the binding of Cu(II) to histidyl peptides this pK was shifted to even lower values (2.5) but it is also seen (74) that the affinity of Cu(II) for the imidazole is greater than that of the Zn(II). The observed pK is consistent with the binding of Zn(II) to imidazoles; a separate determination of the pK for the Cu(II) binding has not been made. The groups responsible for appearance of the five hyperfine lines remain to be identified. The appearance of five lines which can be attributed to two magnetically equivalent nitrogen atoms does not imply that the splitting is caused by two <u>structurally equivalent</u> nitrogen atoms as will be shown in the Results section of this thesis.

FIG. 28

POSSIBLE SYMMETRIES IN Cu(II) COMPLEXES

The positions labelled 1 - 4 represent the square planar, 1 - 5 the square pyramid, and 1 - 6 the octahedral arrangement of ligands about the Cu(II) situated at the origin. A compression or extension of 5 and 6 along the z-axis gives the distorted octahedral configuration (axial symmetry); a distortion along the x-and z-axis (unequal distortions) would give an orthorhombic configuration; an extension or compression of the 1-2-5 and 3-4-6 planes along the line passing through the origin and the center of the faces of these planes gives a trigonal configuration.

According to Bjerrum, Ballhausen, and Jorgensen (11)

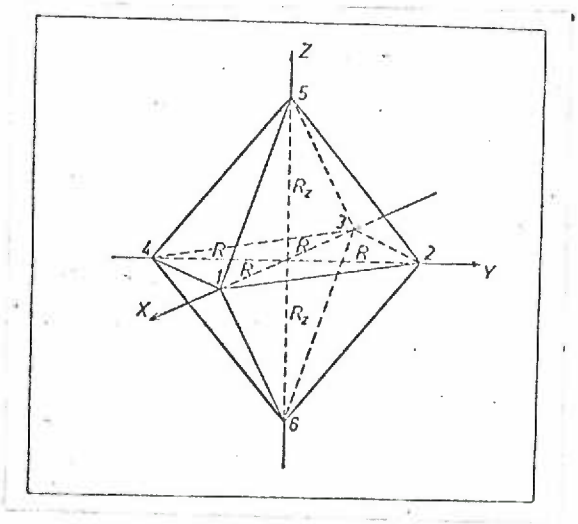
Z
5
R_z
4
R
3
R
2
Y
1
R
X
R_z
6

5. Naturally-Occurring Copper Proteins and Their ESR Spectra

This section will be limited to the following copper-proteins: laccase and ceruloplasmin (20), azurin (20), Pseudomonas aeruginosa blue copper protein (75), Pseudomonas denitrificans blue copper protein (75), two copper proteins from Rhus vernicifera latex (14), and cytochrome oxidase (5). Limiting this review to these seven copper proteins is not as severe a restriction as it might at first appear. With the exception of hemocyanin and tyrosinase these are the only copper proteins which have been studied in detail by ESR (72). ESR investigations of ascorbate oxidase (117) have been directed toward detection of monodehydroascorbate, and not the spectrum of the enzyme.

The investigations can be placed in two categories; those concerned with the determination of structure, the placement and nature of the groups binding the copper, and those concerned with the mechanism of action of the copper proteins. Regarding the latter, "The copper is presumably necessary in the mechanisms of action of the cuproproteins but in not all cases has even the biochemical function of the cuproprotein been established."*

A. Laccase and Ceruloplasmin

The copper proteins laccase and ceruloplasmin were first studied with ESR by Malmstrom et al. (20, 70, 71). Their initial study was a structural investigation (70) of the proteins laccase, ceruloplasmin, erythrocuprein, and Cu(II)-carboxypeptidase. The latter two are, in the terminology of this paper, the model copper proteins. They are included

*Brill, Martin, and Williams (19)

here for comparison purposes. The ESR absorption spectra are shown in Fig.'s 29 and 30. Three features of these ESR spectra are of importance; the general shape of the absorption curve; the g values; and the hyperfine splitting distances A. The overall curve shape is much the same as that derived by Sands for Cu(II) in a soda-lime-silica base glass as discussed in the section on ESR theory. The basic assumption in Sands' derivation is that the Cu(II) occupies a site of 4/mmm symmetry. From the equivalence of the experimental and derived curves the copper in the proteins laccase, ceruloplasmin, erythrocuprein, and Cu(II) carboxypeptidase is assumed to occupy a site of square planar or distorted octahedral symmetry. These symmetries are illustrated in Fig. 28.

The g values for these proteins as well as those for various copper complexes are reproduced in Table 3 from the article of Malmstrom et al. (71).

The value of A, the hyperfine splitting constant, is the distance between the four absorption curves in the $g_{\parallel}$ region resulting from the unpaired electron interacting with the Cu(II) nucleus with I=3/2. As discussed in the section on ESR theory, the degree (distance) of separation is described by the Fermi contact term. This in turn is related to the unpaired electron density at the nucleus. The greater this density the greater the separation of the four lines in the $g_{\parallel}$ region. Laccase and ceruloplasmin have A values of approximately .008 cm^{-1}, erythrocuprein and Cu(II)-carboxypeptidase have values of approximately .020 cm^{-1}, and Cu(II) complexes have A values of approximately .017 cm^{-1} (Table 3).

FIG. 29

ESR SPECTRUM OF FROZEN SOLUTIONS OF Cu(II) COMPLEXES

The idealized ESR spectrum of frozen solutions of Cu(II) complexes, showing the method used in measuring the g- and A-values.

According to Malmstrom and Vanngard (71)

FIG. 30

ESR SPECTRUM OF CERULOPLASMIN

The ESR spectrum of a frozen solution of ceruloplasmin. The arrow indicates the resonance field for free electrons (g = 2).

According to Malmstrom and Vanngard (71)

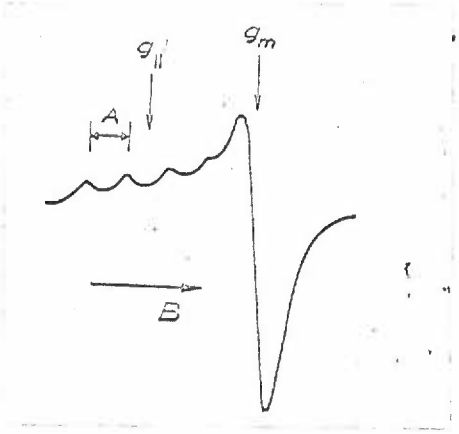
$g_{\parallel}'$
g_m
A
B

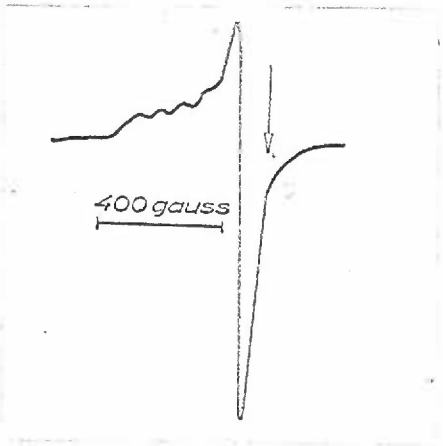
400 gauss

TABLE 3

MAGNETIC PARAMETERS OF COPPER PROTEINS AND Cu(II) COMPLEXES

Magnetic parameters which characterize the ESR and visible spectra of some copper proteins and Cu(II) complexes. The validity of the quantities α^2 and $4/7\,\alpha'^2 + \chi$, which indicate the covalent character of the copper ligand bonds, can be questioned, as was discussed in the text.

According to Malmstrom and Vanngard (71)

Parameters characterizing the ESR and visible spectra of some copper proteins and model complexes

Ligand	Co-ordinating atoms	g_m	$g_\parallel$	$\lvert A \rvert$ (cm^{-1})	Abs. max. (cm^{-1})	a^2	$\frac{4}{3}a^2 + \kappa$
Dithiocarbamate†	4 S	< 2·047	< 2·137	—	23000	< 0·48	—
Phthalocyanine‡	4 N	2·045 ($g_\perp$)	2·165	0·022	—	—	0·81
Laccase	—	2·048	2·197	0·009	16400	0·49	0·48
Ceruloplasmin	—	2·056	2·209	0·008	16500	0·52	0·45
Denatured laccase	—	2·055	2·23	0·020	—	—	0·83
Denatured ceruloplasmin	—	2·056	2·257	0·018	—	—	0·81
Cu^{2+}-carboxypeptidase	—	2·060	2·24	0·019	—	—	0·81
Erythrocuprein	—	2·063	2·265	0·016	15200	0·61	0·75
Bis-salicylaldehyde-imine‡	2 O, 2 N	2·045 ($g_\perp$)	2·200	0·0185	16300	0·49	0·75
Bis-acetylacetonate‡	4 O	2·053 ($g_\perp$)	2·266	0·0160	15000	0·60	0·75
Histidine	4 N	2·063	2·230	0·018	15600	0·54	0·78
Imidazole	4 N	2·063	2·267	0·018	16800	0·68	0·81
2,2′-Dipyridyl	4 N	2·082	2·27	0·017	14900	0·61	0·79
1,10-Phenanthroline	4 N	2·088	2·28	0·015	15200	0·64	0·74
Oxalate	4 O	2·078	2·316	0·017	15400	0·73	0·84
EDTA	4 O, 2 N	2·090	2·337	0·015	13900	0·71	0·80
Citrate	2 O	2·074	2·349	0·015	13700	0·72	0·82
1 N-$NaNO_3$	—	2·083	2·397	0·015	—	—	0·86

The conclusion is that the unpaired electron density at the copper nucleus is less for laccase and ceruloplasmin than it is for erythrocuprein, Cu(II)-carboxypeptidase, and Cu(II) complexes. This is the problem of central importance in the ESR investigations of the copper proteins; what is the arrangement of ligands or what is the nature of the ligands that decreases the density of the unpaired electron at the copper nucleus?

Laccase and ceruloplasmin have absorption maxima at approximately 620 mu (16500 cm^{-1}) with extinction coefficients of 10^3/mole Cu. Using this value as the energy at which the electron transition occurs and the g and A values obtained experimentally, and using the equations given in the section on ESR theory-covalent bonding, the parameters α^2 and β^2 were calculated. The value of α^2=1 indicates completely ionic sigma bonds; for α^2=.5 a completely covalent sigma bond is indicated. β^2 similarly indicates the covalent character of the pi bonds. Malmstrom et al. (71) obtained α^2=0.5 and β^2=1.0 for laccase and ceruloplasmin. This would indicate that the sigma bonding is 100% covalent while the pi bonding is totally ionic (19). Such an interpretation is unreasonable. The sigma and pi bonding involves virtually the same type of atomic orbitals on the ligand and Cu(II) atoms. That one combination of these into a molecular orbital involves sharing of the unpaired electron and a slightly different combination results in complete non-sharing of the same unpaired electron is difficult to reconcile. It is more reasonable to assume that the calculation is incorrect. Recalling the assumptions used in making such a calculation indicates that

there is a strong possibility that it is wrong. Firstly, the symmetry of the ligand atom placement about the Cu(II) atom must be known. It is not for these copper-containing proteins. Secondly, the atomic orbitals of the ligand atoms available for formation of molecular orbitals must be known. This means that the ligand atoms must be known. No ligand atom in any copper containing protein has been identified.

A copper-copper interaction was advanced to explain the decreased A values seen for laccase and ceruloplasmin. The lowered electron density at the copper nucleus could be due to a high degree of delocalization of the unpaired electron decreasing the unpaired electron density at the nucleus, perhaps through some type of copper-copper interaction (20). Laccase contains four copper atoms per molecule (19) and ceruloplasmin 8 (19) so that such a mechanism might exist. In addition, double integration of the ESR absorption curve and magnetic susceptibility measurements indicate that only 50% of the copper in laccase and ceruloplasmin is present as Cu(II). Thus 50% may be present as Cu(I) and a Cu(II)-Cu(I) exchange could be operative.

The first study of mechanism of action of a copper enzyme using ESR in which changes is the copper protein detectable by ESR were followed was that of Malmstrom et al. on Laccase (70). Since the work of Kubowitz on tyrosinase (62) there has been a general assumption that the catalytic action of the copper proteins is associated with a change of valency of the copper (cupric to cuprous) but no direct evidence for such a valency change had been obtained up to this time. Malmstrom has reviewed the procedure used to determine the valency of copper in copper

* Brill, Martin, and Williams (19)

proteins and has discussed the limitations of each (68). These methods are; valence specific reagents, reagents which specifically bind Cu(II) or Cu(II); exchange with radioactive copper, in which exchange between only Cu(I) and labelled Cu(I) or Cu(II) and labelled Cu(II) is assumed to occur; visible and UV spectra, in which UV and visible spectral characteristics of known Cu(I) and CU(II) complexes are correlated with those observed for the copper proteins; ESR; and magnetic susceptibility which measures the unpaired electron concentration. Malmstrom reached the same conclusion as did Brill; "No method for determining the valency of copper in a protein is beyond question."* The reason is that all methods mentioned fulfill necessary but not sufficient conditions that the copper be present as Cu(I) or Cu(II). "The best evidence for the cupric state is a well-resolved paramagnetic resonance spectrum showing the four hyperfine lines characteristic of the nuclear spin of 3/2 of copper."* That is, the number of alternative explanations for such an ESR spectrum is less than for the other experimental methods given.

Laccase shows a four line spectrum (71) (Fig. 31) so that some of the copper in laccase is in the cupric state. Cupric copper contains an unpaired electron; any one electron reduction or oxidation will make the sample diamagnetic (the ESR signal will be reduced). When catechol is added to a laccase solution, the intensity of the ESR signal is reduced (70) (Fig. 31). Since the catechol is oxidized the decrease of the signal results from cupric copper reduction to Cu(I). When the substrate has been exhausted (aerobically) or oxygen is added to the solution (anaerobically) the original signal reappears, indicat-

*Brill, Martin, & Williams (19)

FIG. 31

ESR SPECTRUM OF LACCASE

The ESR absorption curves (derivatives) recorded at -180°C. (A) is the ESR spectrum of a 2% laccase solution and (B) is the ESR spectrum of a 2% laccase solution plus excess catechol.

According to Malmstrom, Mosbach, and Vanngard (70)

FIG. 32

ESR SPECTRUM OF COPPER PROTEIN FROM PSEUDOMONAS AERUGINOSA

The ESR signal (derivative) of 1mM copper-protein from Pseudomonas aeruginosa in 0.05 M ammonium acetate, pH 6.5, temp. = -165°C.

According to Mason (75)

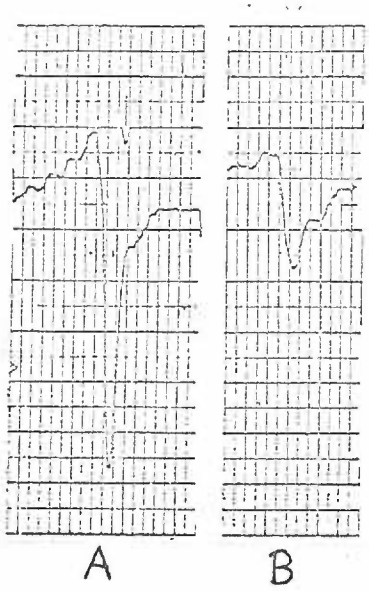
A
B

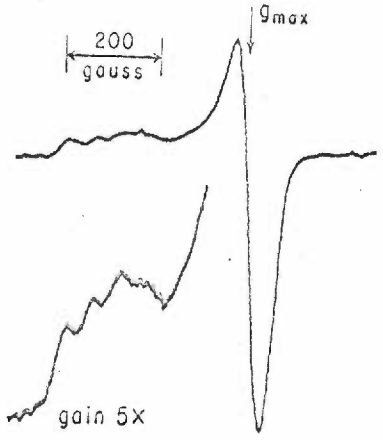
200
gauss
gmax
gain 5x

ing the reoxidation of Cu(I) to Cu(II).

Laccase and ceruloplasmin contain copper bound in almost identical manners (as judged from their ESR spectra) (71). They show similar enzyme specificity but the specific activity of ceruloplasmin is approximately 1000 times lower than that of laccase.

A correlation between the kinetics of copper oxidation and reduction and the rate of the overall reaction would be a necessary condition for the metal ion to participate in the mechanism of enzyme catalysis. The rate of reoxidation of reduced laccase and ceruloplasmin was too rapid to allow measurement in the apparatus used (20), and the rate of reduction of laccase was too fast to be measured. Thus only the kinetics of the ceruloplasmin reduction were studied.

It was shown that the catalytic mechanism of ceruloplasmin involves reduction of the Cu(II) by the substrate (ascorbate) followed by reoxidation of the Cu(I) to Cu(II) by O_2. The reduction step can be written

$$ECu^{+2} + AH_2 = ECu^{+1}\ (AH_2)^{+1}. \qquad (1)$$

Any structure-function correlations must be tentative because little is known about either the structure or catalytic mechanism of these copper proteins. For the electron transfer to occur as rapidly as possible, the overlap of the copper orbital which is to gain an electron (reaction (1) above) and the ascorbate orbital which is to lose an electron should be a maximum (37). Such an overlap would be facilitated if the unpaired electron orbital of Cu(II) was highly (spacially) delocalized. Delocalization of the unpaired electron has been invoked to

explain the reduced hyperfine splitting distance A observed in the ESR spectra of ceruloplasmin (20). This increased delocalization could lead to a large overlap of donor and acceptor orbitals and to rapid electron transport, and would thus be consistent with the functioning of the enzyme. This interpretation makes the assumption that the electron distribution about the copper atom is the same in the "resting" copper protein as it is in the complex $ECu^{+1}(AH_2)^{+1}$ or $ECu^{+2}(AH_2)$. Such an assumption does not seem justified. As stated by Mason (76) the effect of the protein on the electron distributions of the substrate must be determined; direct evidence will have to be given for every case. The opposite is also true--the effect of the substrate on the electron distributions in the protein must also be determined. An attempt to detect, with ESR, such an enzyme-substrate complex was made with enolase and phosphoglyceric acid. It was hoped that the ternary complex enzyme-metal-substrate could be measured in this way. No resonance for such a complex was detected (69). The decreased hyperfine splitting A due to a decreased electron density at the copper nucleus could be explained by a decreased s character of the unpaired electron orbital as well as by an increased delocalization. It must be concluded that the evidence available does not allow any definite structure-function correlations to be made for these copper proteins. The state of oxidation of copper in these enzymes remains uncertain.

B. Pseudomonas Copper Proteins and Azurin

Mason determined the ESR spectra of two copper proteins from Pseudomonas aeruginosa and Pseudomonas denitrificans (75) (Fig. 32).

The ESR spectrum of azurin has been determined by Malmstrom et al. (20) (Fig. 33). All three show ESR absorption curves and hyperfine splitting constants A virtually identical with those of laccase and ceruloplasmin; all three have extinction coefficients for the 16500 cm^{-1} absorption of 10^3/mole copper; and all three have only one copper atom per molecule. Thus, "The explanation for small hyperfine splittings in the g-parallel region of the ESR spectrum, and for exhaltation of absorption in the 610 mu region, must be sought in a configuration which involves one copper atom only."* Blumberg has shown (13) that by suitable choice of ligands and symmetry of the ligands about the Cu(II) the decreased hyperfine splitting in the ESR spectrum and the exhaltation of absorption in the 610 mu region can be explained. As stated by Blumberg, all that can be said is that if these copper proteins did have the proposed "structure" (about the Cu(II)) then the ESR and optical absorption data could be explained.

C. Copper Proteins From Rhus Vernicifera Latex

The ESR spectra from the two copper proteins from Rhus vernicifera are shown in Fig. 34 (14). The copper protein of spectrum A is a laccase and contains more than one copper atom per molecule. The copper protein giving spectrum B contains one atom of copper per molecule. Both ESR specta show unresolved hyperfine structure in the g parallel region and the copper protein containing one copper atom per molecule shows a well resolved g perpendicular absorption. The magnetic constants for both copper proteins are reproduced in Table 4. The copper in the

*Mason (75), 1965.

FIG. 33

ESR SPECTRUM OF AZURIN

The experimental ESR spectrum at 77°K of an approx. $5X10^{-4}$ M aqueous solution of azurin (solid line) and spectrum calculated with Gaussian shape (dashed line) with g = 2.273, g = 2.049, A = 55 gauss = $0.006cm^{-1}$, B = 0 (splittings in the g region) and line-widths A = 49, 56, 63, and 70 gauss for the four hyperfine lines in order with increasing magnetic field. Microwave frequency, 9166 Mcycles/sec.

According to Broman, Malmstrom, Aasa, and Vanngard (20)

FIG. 34

ESR SPECTRA OF TWO PROTEINS FROM RHUS VERNICIFERA LATEX

(A) is the ESR spectrum of Rhus vernicifera laccase taken at 77°K. The sample contains 78 ug of Copper. (B) is the ESR spectrum of Rhus vernicifera blue protein taken at 77°K. The sample contains 72 ug/ml of copper.

According to Blumberg, Levine, Margolis, and Peisach (14)

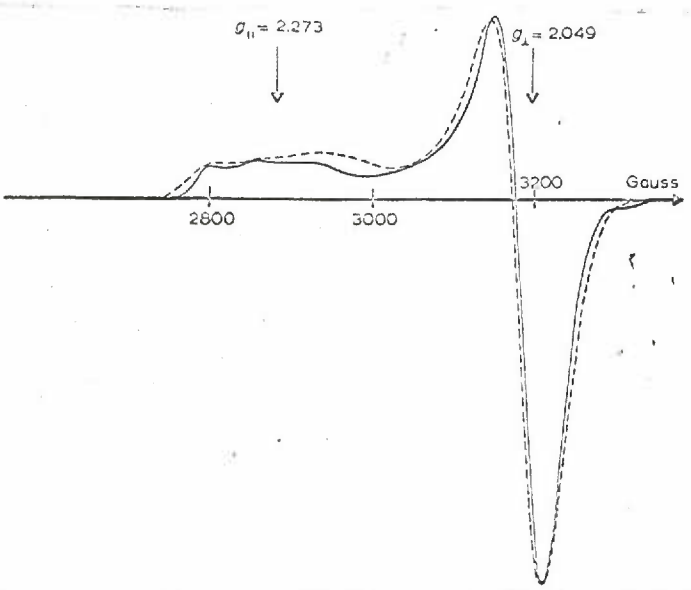
$g_{\parallel}$ = 2.273
$g_{\perp}$ = 2.049
2800
3000
3200
Gauss

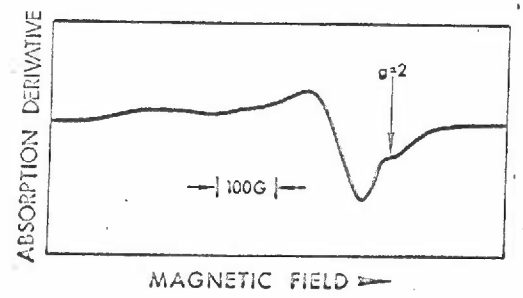
ABSORPTION DERIVATIVE
g=2
100G
MAGNETIC FIELD

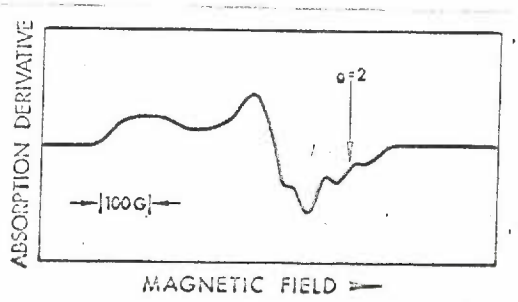
ABSORPTION DERIVATIVE
g=2
100G
MAGNETIC FIELD

TABLE 4

MAGNETIC CONSTANTS FOR RHUS VERNICIFERA COPPER PROTEINS

The magnetic constants for the copper proteins from Rhus vernicifera. The laccase is assumed to reside in a site of orthorhombic symmetry giving three A values. These A values cannot be measured accurately due to limitations of the instrument used.

According to Blumberg, Levine, Margolis, and Peisach (14)

FIG. 35

ESR SPECTRA OF CYTOCHROME OXIDASE

ESR spectra of submitochondrial particles and cytochrome oxidase. A, 10 mg of particles were suspended in 0.10 ml of 0.25 M sucrose, pH 7,5, containing 0.015 M $MgCl_2$ and 0.001 ATP (X2). B, 5.5 mg of cytochrome oxidase were dissolved in 0.10 ml of 0.25 M sucrose, pH 7.4. C, To B were added 2 ul of 1 M phosphate of pH 7.3 and 2 ul of 0.5 M cyanide of pH 11.5. Phosphate by itself does not change the spectrum. D, The sample of C after dialysis against 0.01 M Trisacetate and 0.01 M cyanide, pH 8.0, followed by removal of cyanide by dialysis against Tris-acetate only. E, 5.5 mg of cytochrome oxidase dissolved in sucrose, incubated in 0.1 M neutralized NH_2OH for 1 hour at $0^{\circ}C$ (XO.5).

From Beinert, Griffiths, Wharton, and Sands (5)

MAGNETIC CONSTANTS FOR RHUS VERNICIFERA COPPER PROTEINS

Laccase		Blue Protein	
g_x=2.00	A_x=<0.0007 cm^{-1}	$g_{\|\|}$ =2.30	$A_{\|\|}$ =0.0040 cm^{-1}
g_y=2.09	A_y=<0.0007 cm^{-1}	$g_\perp$ =2.04	$A_\perp$ =0.0058 cm^{-1}
g_z=2.27	A_z= 0.0040 cm^{-1}		

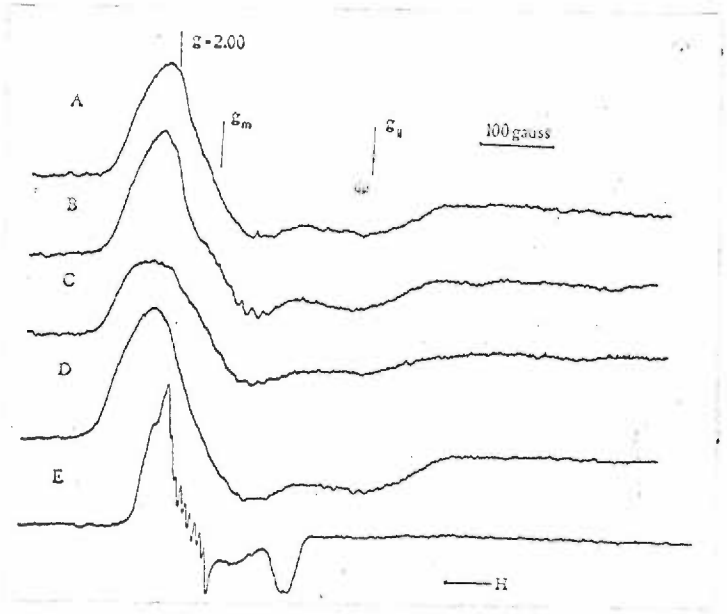

laccase studied was not all present as Cu(II) as determined by integration of the ESR absorption spectrum.

D. Cytochrome Oxidase

The ESR signal shown by cytochrome oxidase (Fig. 35) (5) is probably due to Cu(II). Comparison with the ESR curve for laccase and ceruloplasmin (Fig.'s 30 and 31) shows a difference in the shape of the curves. It is stated, "The EPR spectrum of cytochrome oxidase is similar to that of other known copper proteins, such as laccase or ceruloplasmin, in which copper is present in the cupric form. ...the lack of nuclear hyperfine structure in the spectrum of the enzyme indicates that at least two copper ions are in close proximity in the enzyme and undergo an exchange interaction."* Only part (40%) of the chemically determinable Cu(II) is detectable by ESR. No evidence exists to show that this is due to a copper-copper exchange. The ESR absorption curve is not the same as that of laccase and ceruloplasmin and the hyperfine splitting distances A cannot be measured since they are not seen. The latter could be due to the splittings A being very small ($\lesssim .004 cm^{-1}$(8)) or to the absence of hyperfine structure. If the two copper atoms are in close proximity and undergo an exchange reaction then on this basis cytochrome oxidase is different from laccase and ceruloplasmin as an exchange interaction does not occur in these copper proteins. Exchange interaction in cytochrome oxidase is a hypothesis that awaits verification. ESR studies with varying microwave power and at liquid helium temperature ($4^{o}K$) may provide evidence for the copper-copper interaction concept (7) in that at very low temperatures the exchange reaction

* Beinert et al. (5)

may be eliminated so that an ESR spectrum due to Cu(II) alone would be seen. The results from such experiments on cytochrome oxidase have been inconclusive (7) since the ESR spectrum does not alter at liquid helium temperatures.

Beinert and Palmer (7) have shown that the ESR signal in "damaged" cytochrome oxidase (cytochrome oxidase with added $CuCl_2$ or treated with urea or acetone) contains two ESR detectable components which saturate at different microwave powers. The easily saturating component arises from extraneous copper while the signal which does not saturate at 270 mw of klystron power is attributed to the copper in its native state. (Fig. 36). The easily saturating component was not reduced by cytochrome c.

These results agree with those of Morrison et al. (83) who found that an ESR signal similar to that of "damaged" cytochrome oxidase could be converted to a signal typical of the native cytochrome oxidase by; chelation of the extraneous Cu(II) by bathocuproine disulfonate and separation of this complexed Cu(II) from the cytochrome oxidase in a sephadex column; reduction of the extraneous Cu(II) by KBH_4 which does not reduce the "native" Cu(II) (5,83). The Cu(II) signal which can not be reduced by KBH_4 can be reduced by ascorbate or cytochrome c.

The role of copper in cytochrome oxidase action is still under debate (5, 36). Beinert and co-workers (5) have shown that the copper in cytochrome oxidase undergoes an oxidation reduction commensurate with the turnover of the heme a in the oxidase. The rate of reduction of heme a in cytochrome oxidase was followed by low temperature spectro-

FIG. 36

POWER SATURATION BEHAVIOUR OF THE ESR SIGNALS OF CYTOCHROME OXIDASE

Difference in power saturation of the EPR signals obtained from a mixture of cytochrome oxidase and copper sulfate before and after addition of reduced cytochrome c. A mixture of 0.35m*M* cytochrome oxidase and 0.18m*M* $CuSO_4$, 0.1 ml., in 0.1*M* Tris-chloride of pH 8.3 was placed in an EPR tube for anaerobic work. The tube was repeatedly evacuated and flushed with purged nitrogen. 0.1 ml. of 9m*M* cytochrome c (horse heart monomer reduced with ascorbate) in Tris buffer as above was added immediately to the oxidase and mixed with it in the anaerobic tube under a stream of nitrogen. The sample was frozen after 1 min. at room temperature. In control experiments, 0.1 ml. of Tris buffer without cytochrome c was added to the oxidase–copper mixture and to an oxidase sample without added copper. The conditions of EPR spectroscopy were: power, 0.25, 25, and 250 mw., as indicated in the figure; modulation amplitude, 6 gauss; scanning rate, 60 gauss/min.; temperature, −170°. The *first, third,* and *fifth* lines, marked *reduced,* show the spectra of the sample to which reduced cytochrome c was added. The *second, fourth,* and *sixth* lines, marked *oxidized,* show the spectra of the control sample without cytochrome c at the three power levels. To obtain spectra of sufficient size, the amplification at 0.25 mw. was adjusted to 12.5 times and that at 25 mw. to twice the value used at 250 mw.

According to Beinert and Palmer (7)

FIG. 37

ESR ABSORPTION FROM COPPER IN CYTOCHROME OXIDASE

The ESR absorption (derivative) curve from copper in cytochrome oxidase (1.025 mM in Cu) at 77°K. Field modulation 100 kc, 12 and 3 gauss peak to peak for A and B, respectively. Magnetic field increases from left to right. Microwave power approx. 0.25mW.

According to Ehrenberg and Yonetani (36)

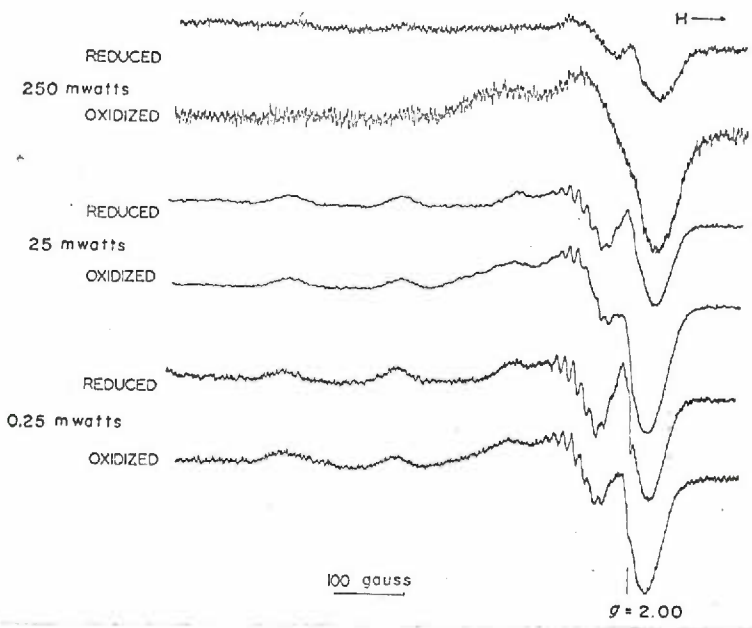
H
REDUCED
250 mwatts
OXIDIZED
REDUCED
25 mwatts
OXIDIZED
REDUCED
0.25 mwatts
OXIDIZED
100 gauss
g = 2.00

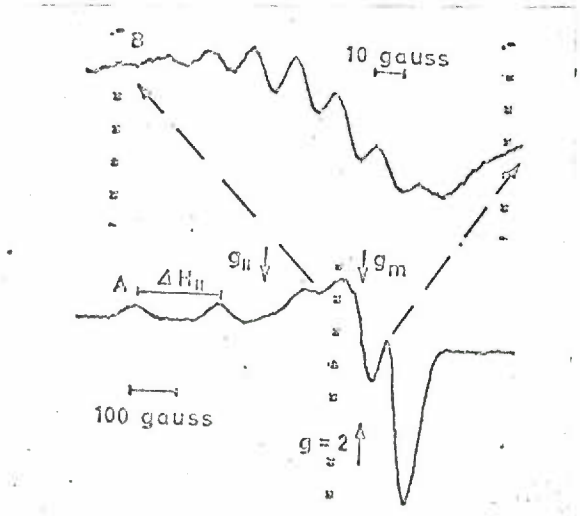
B
10 gauss
A
ΔH∥
g∥
gm
100 gauss
g = 2

photometric methods and the rate of reduction of Cu(II) was followed using the rapid mixing and freezing methods of Bray and low temperature ESR. It was found that with the substrates ascorbate and cytochrome c the heme a reduction and reoxidation was closely followed by the reduction and reoxidation of the copper. However, the time resolution in these experiments was too long (10 msec) to prove that the copper is a necessary intermediate in the electron transport path terminating with O_2. Beinert et al. conclude that the idea of the copper in cytochrome oxidase being a component of the oxidation-reduction function of the oxidase should not be discarded yet on the basis of rather limited evidence. This limited evidence also limits any conclusions that can be made about the role of copper in cytochrome oxidase.

Ehrenberg and Yonetani found (36) that in their cytochrome oxidase preparation the Cu(II) ESR signal could not be abolished by cytochrome c while spectrophotometric observations indicated that the heme components had been reduced. On the basis of these results the copper does not play a role in the functioning of cytochrome oxidase. Beinert et al. (5) have observed the following about the ESR signal of Yonetani's cytochrome oxidase preparation; the signal resembles that which Beinert et al. attribute to Cu(II) in "damaged" enzyme; the signal observed by Beinert et al. (5), which is also the signal present in intact mitochondria is not the major component of the ESR signal of Yonetani's preparation (Fig. 37). If these conclusions are correct the discrepancy between the results of Ehrenberg and Yonetani, and Beinert et al. is due to the copper in Yonetani's cytochrome oxidase not being in its native state.

Chance has recently reported (22) that in intact mitochondria the reduction of the Cu(II) is slower than that of the heme components. These results are based on the assignment of an 800 mu absorption band in mitochondria to Cu(II) (43). The assignment of this band to a Cu(II) absorption is tentative.

In summary, the copper proteins ceruloplasmin, laccase, azurin, and those from Pseudomonas seem to have the copper atoms bound in much the same way. The symmetry of the ligand field about the copper atom is probably 4/mmm(tetragonal). The observed low hyperfine splitting value, A, which indicates a lowered unpaired electron density at the copper nucleus, can not be accounted for through copper-copper interaction. No definite statement can be made about the ligand atoms which give rise to the above mentioned properties (19).

The binding of the copper in cytochrome oxidase seems to be fundamentally different from that in the other copper proteins discussed.

The change in the valence state of the copper atom, when the copper protein catalyzes an oxidation or reduction reaction, has been established for the oxidase enzymes laccase, ceruloplasmin, and cytochrome oxidase. Whether this change in valence is obligatory for the functioning of the enzyme or not has not been rigorously established. This is due to the lack of sufficiently short time resolution in the kinetic experiments and, in addition, a Kubowitz type experiment* has not been accomplished with these copper proteins.

* To demonstrate that the enzymic activity is lost upon removal of the Cu(II) and is regained upon rebinding of the Cu(II) by the copper protein.

II EXPERIMENTAL

1. Materials

All water used was distilled and deionized by passage through a Barnstead standard mixed-bed ion exchange column. Determination of possible transition metal ion contamination was made using ESR.

Buffers used were prepared according to the procedures described in Methods in Enzymology, volume I (41).

The peptides used were obtained from Nutritional Biochemicals Corporation and from Cyclo Chemical Corporation; they were used without further purification. Homogeneity was checked using chromatography with butanol-acetic acid-water and phenol-water solvents.

Cu(II) was used as $CuCl_2$ and $CuSO_4$. Contamination with other transition metal ions was determined with ESR.

^{63}Cu, as CuO, was supplied by Oak Ridge National Laboratory in 99.9% purity.

D_2O was supplied by Volk Radiochemical Company and was of 99.64% purity.

NaOD was prepared by dissolving Na metal in D_2O. Standardization was with potassium acid phthalate.

Glycine ^{15}N was supplied by Bio-Rad Laboratories and was of 96% purity. It was recrystallized once from an ethanol-ether-water mixture.

All liquid reagents used in the glycylglycine ethyl ester synthesis were carefully dried, according to the procedures given in Vogel, Practical Organic Chemistry (110), where needed.

The ethylchloroformate used was supplied by Cal Biochem. The carbobenzoxychloride was supplied by Sigma Chemical Company. Both were used without further purification.

The Cu(II) bis-imidazole complex was supplied by Professor J.. Fruton of Yale University, to whom I am grateful.

The blue copper protein from Pseudomonas aeruginosa was given by Dr. P. Ambler, Molecular Biology Institute, Cambridge.

2. Equipment

Determinations of pH were made with a Radiometer TTT1-a pH meter.

Visible spectrophotometric measurements were made with a model 14 Cary recording spectrophotometer and with a Zeiss M4QIII spectrophotometer.

Spectrophotometric flow measurements were made using a syringe drive (15) and a 2 mm path length flow cell. All flow measurements were made on the Cary spectrophotometer.

Electron spin resonance spectroscopy was performed using a Varian model V4500 EPR spectrometer with 100 kc field modulation and equipped with a fieldial VFR2200 magnetic field regulator. A Hewlett Packard klystron frequency meter was used to determine the klystron frequency. The magnetic field strength was determined using a proton resonance probe connected to a Varian F8 nuclear fluxmeter which in turn was connected to a Hewlett Packard 524 C electronic frequency counter. Control of incident microwave power was achieved using a circulator of the design of R. Sands and R. Hansen (6). Power was measured at

the entrance of the cavity by a Hewlett Packard 431B power meter.

A Varian F-80 X-Y recorder was used to record all ESR spectra obtained.

Temperature control for the ESR experiments was achieved using the Varian liquid nitrogen accessory and a Varian EPR heater control unit. Temperature control was accurate to $\pm 1^{\circ}C$.

Five types of sample cells were used for the ESR experiments. For the aqueous samples the Varian supplied quartz flat cell gave best sensitivity. This could not be used with the variable temperature attachment. Two types of cells were employed for these measurements; utilized to the greatest extent was a cell constructed by sealing the end of a pyrex tube, .8mm id-1.2mm od, into which the sample was placed. This in turn was placed inside a standard quartz ESR tube, 3mm id-4mm od, which contained either benzene or hexane as a heat transferring agent. The capillary tube projected above the outside quartz tube and could be centered in the quartz tube by wrapping with Parafilm. Measurements made in these sample tubes were checked using a quartz cell of 4mm od and containing two side by side holes of 1 mm diameter. Anaerobic room temperature measurements were made using a cell designed by Dr. T. Shiga utilizing a quartz flat cell and two sample chambers arranged so that two reagents could be mixed and placed in the flat cell after the cell was evacuated and flushed with nitrogen. Liquid nitrogen temperature measurements were made using quartz tubes 3mm id by 4mm od. A syringe drive and a pneumatic flow device (15) were used for the ESR flow experiments.

Chromatography of the peptides utilized was performed in large glass battery jars. Chromatograms were run at ambient temperatures.

Optical rotatory dispersion measurements were made with a Rudolph spectropolarimeter in the laboratory of Dr. J. Schellman at the University of Oregon.

Nuclear magnetic resonance measurements were made on a Varian A-60 spectrometer in the laboratory of Dr. E. Marvel at Oregon State University.

Glassware used in the peptide synthesis was designed in such a way that the reaction mixtures would be exposed to a minimum of atmospheric moisture. Standard design was used throughout.

Conductivity measurements were made with a Radiometer conductivity meter.

3. Procedure

pH titrations were carried out using a Radiometer pH meter. Addition of NaOH was made with an Agla, Burroughs-Wellcome, .5 ml microburet. Samples of .5 ml volume could be easily titrated in this manner. Samples titrated were generally of 5 ml volume.

Using the tables given by Dobbie and Kermack (Appendix III), pH and peptide to Cu(II) ratios were used which would give the maximum concentration of one form of a postulated Cu(II)-peptide complex. The ESR spectra of these mixtures were then determined at liquid nitrogen temperatures and at temperatures at which the solutions were in the liquid state. The effect of ionic strength on these ESR spectra was determined by using different NaCl concentrations in the Cu(II)-peptide solutions.

The effect of the natural mixture of ^{63}Cu and ^{65}Cu isotopes on the ESR spectra of the Cu(II) complexes was determined by using a sample consisting of $^{63}Cu(II)$ only. The ^{63}CuO was first dissolved in 1N HCl and then converted to $CuCl_2$ before use by the addition of NaOH.

The effect of temperature on the ESR spectra was determined utilizing the variable temperature attachment described previously and determining the ESR spectra over the temperature range -180° C to 90° C.

The effect of molecular tumbling on the ESR spectra was determined not only by utilizing the temperature variation procedure but also by increasing the size of the complex by the use of non-functional groups attached to the peptide of interest and also by using solvents of various viscosities.

Possible effects on the ESR spectra by protons of either the water molecules or those on the peptides which are exchangable with H_2O protons was determined by using D_2O as the solvent.

The effect of the nitrogen atoms in the peptides on the ESR spectra was determined by synthesizing the glycylglycine ethyl ester peptide utilizing ^{15}N atoms instead of the naturally occurring ^{14}N atoms. The procedure employed in the synthesis was that of mixed anhydrides as suggested by Dr. M. Cronyn at Reed College. The procedure is given in Greenstien and Winitz (42). Slight modifications were made due to the small amount of starting material (40 mg). It was found that the reactions involved were very sensitive to moisture and modifications were made so that the reactions were run without ex-

posure to the atomosphere. Reactions run at -18°C were run in a freeze room for the same reasons. The synthesis was terminated at the ethyl ester form of the peptide since it had been previously determined that the ester behaved identical to the free peptide in its binding of Cu(II). Glycylglycine ethyl ester containing only ^{14}N, containing ^{14}N in the peptide position and ^{15}N in the amino position, containing ^{15}N in the peptide position and ^{14}N in the amino position, and containing only ^{15}N were synthesized in this way. Since 96% ^{15}N glycine was used the positions containing ^{15}N should be labelled to this extent. The products of the synthesis were checked chromatographically with butanol-acetic acid-water and phenol-water buffers by comparison to commercially supplied glycylglycine ethyl ester and by comparison with measured Rf values. The peptides synthesized were homogeneous by this procedure.

The Pseudomonas aeruginosa blue copper protein supplied by Dr. P. Ambler was concentrated by lyophilization after first removing excess $(NH_4)_2SO_4$ by passage through a G-25 sephadex column. The salt elution was followed using a flow conductivity cell connected to a Radiometer conductivity meter.

Flow experiments were conducted as described by Bond (15).

III RESULTS

1. Cu(II)-Glycylglycine Complexes

The ESR spectra of equimolar Cu(II)-GG solutions at pH values specified in the Fig. and at liquid nitrogen temperatures are shown in Fig. 38. The ESR spectra of equimolar Cu(II)-GG solutions, at liquid nitrogen temperatures, and at pH values and NaCl concentrations given in the Fig. are shown in Fig. 39. The ESR spectra at room ($20^{o}C$) temperatures of the $CuCl_2$ solutions are shown in Fig. 40. The ESR spectra at $-5^{o}C$ of Cu(II)-GG solutions with no added NaCl are unaltered upon addition of NaCl over the range .1M to 2.5M added NaCl. For reasons to be discussed, it appears that, from the ESR spectra, the form of the Cu(II)-GG complex and the $CuCl_2$ complex at liquid nitrogen temperatures is dependent on the NaCl concentration whereas the form of the complexes at room temperatures is not dependent on NaCl concentration. For this reason the data were obtained at temperatures above the freezing point of the solutions.

The ESR spectra for various Cu(II)-GG ratios and the pH values are shown in Fig. 41. The spectra were obtained at $-5^{o}C$. The freezing point of these solutions is $-15^{o}C$.

Possible saturation effects were determined by obtaining ESR spectra of the different solutions of Cu(II)-GG complexes from .2 to 270 mwatts of incident microwave power. The signals followed, generally, the relationship (integrated area of absorption curve) $\sim\sqrt{\text{microwave power}}$ as expected (12) if no saturation effects are seen.

FIG. 38

-180°C ESR SPECTRA OF Cu(II)-GLYCYLGLYCINE

ESR spectra of 10 mM glycylglycine with 10 mM $CuCl_2$. Temperature, -180°C; ionic strength, 0.16. Curve A, 4 equivalents of NaOH and pH 11.5; Curve B, 3 equivalents of NaOH and pH 10.7; Curve C, 2 equivalents of NaOH and pH 6.9; Curve D, 0 equivalents of NaOH and pH 3.7

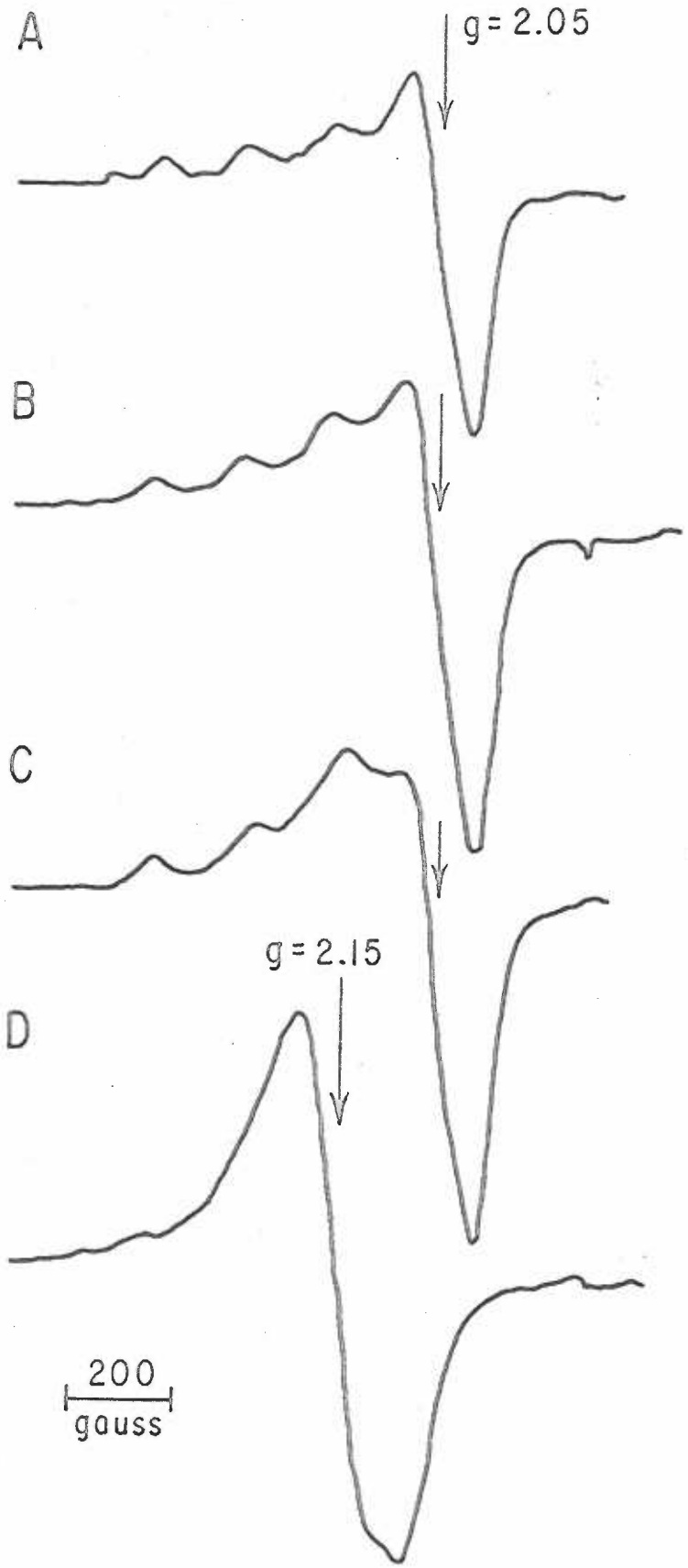
A
g = 2.05
B
C
g = 2.15
D
200
gauss

FIG. 39

-180°C ESR SPECTRA OF Cu(II)-GLYCYLGLYCINE PLUS NaCl

ESR spectra of 10 mM glycylglycine and 10 mM CuCl with 3 equivalents NaOH, pH 10.4. Temperature -180°C. Curve A, 2.5 M in NaCl; Curve B, 1 M in NaCl; Curve C, .5 M in NaCl; Curve D, .2 M in NaCl; Curve E, 0 M in NaCl.

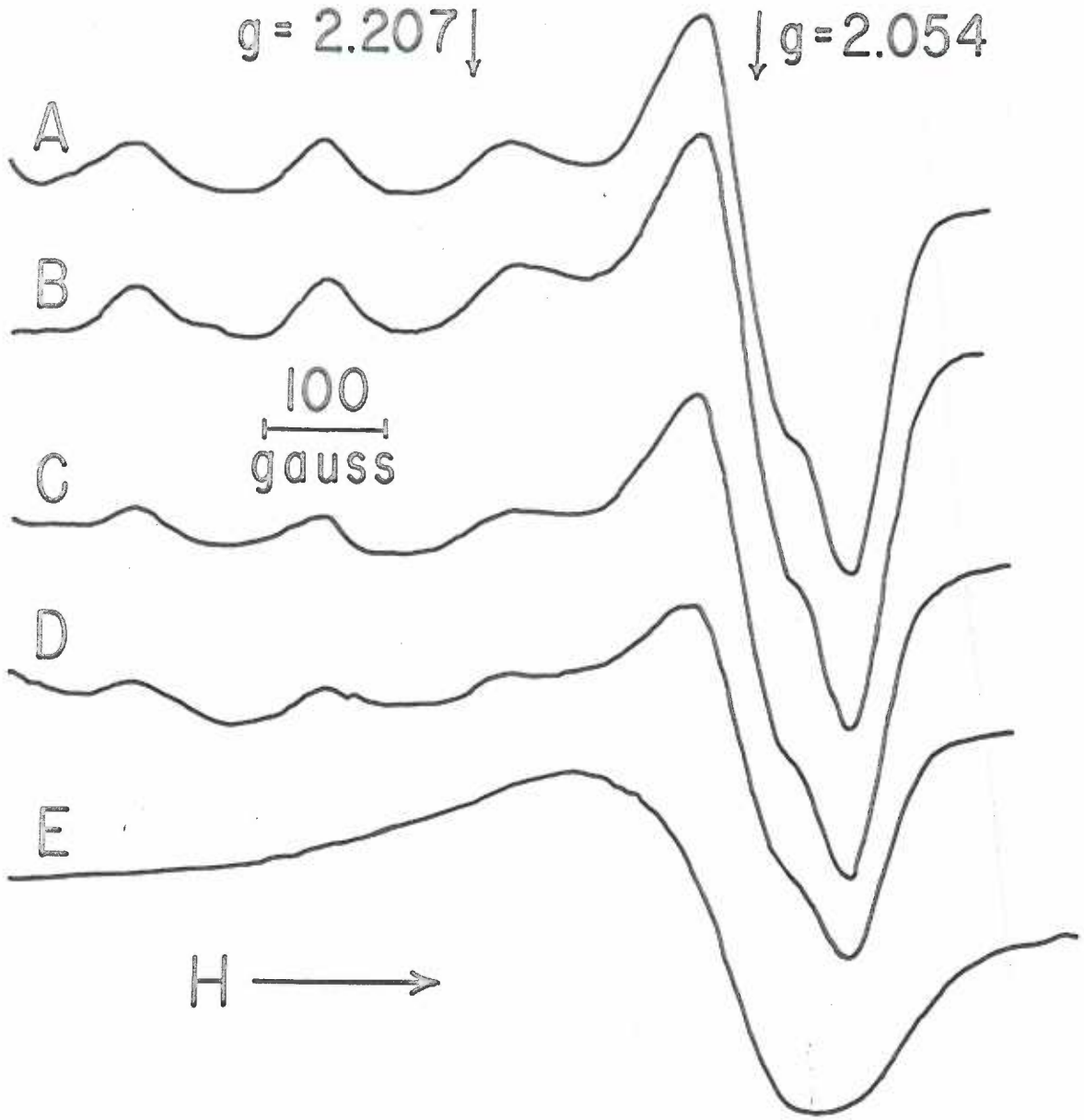
g = 2.207
g = 2.054
A
B
100
gauss
C
D
E
H

FIG. 40

ROOM TEMPERATURE ESR SPECTRA OF $CuCl_2$ WITH NaCl

ESR spectra at 20°C of 10 mM $CuCl_2$. Curve A, 2.5 M NaCl; curve B, 1 M NaCl; curve C, .5 M NaCl; curve D, .2 M Nacl.

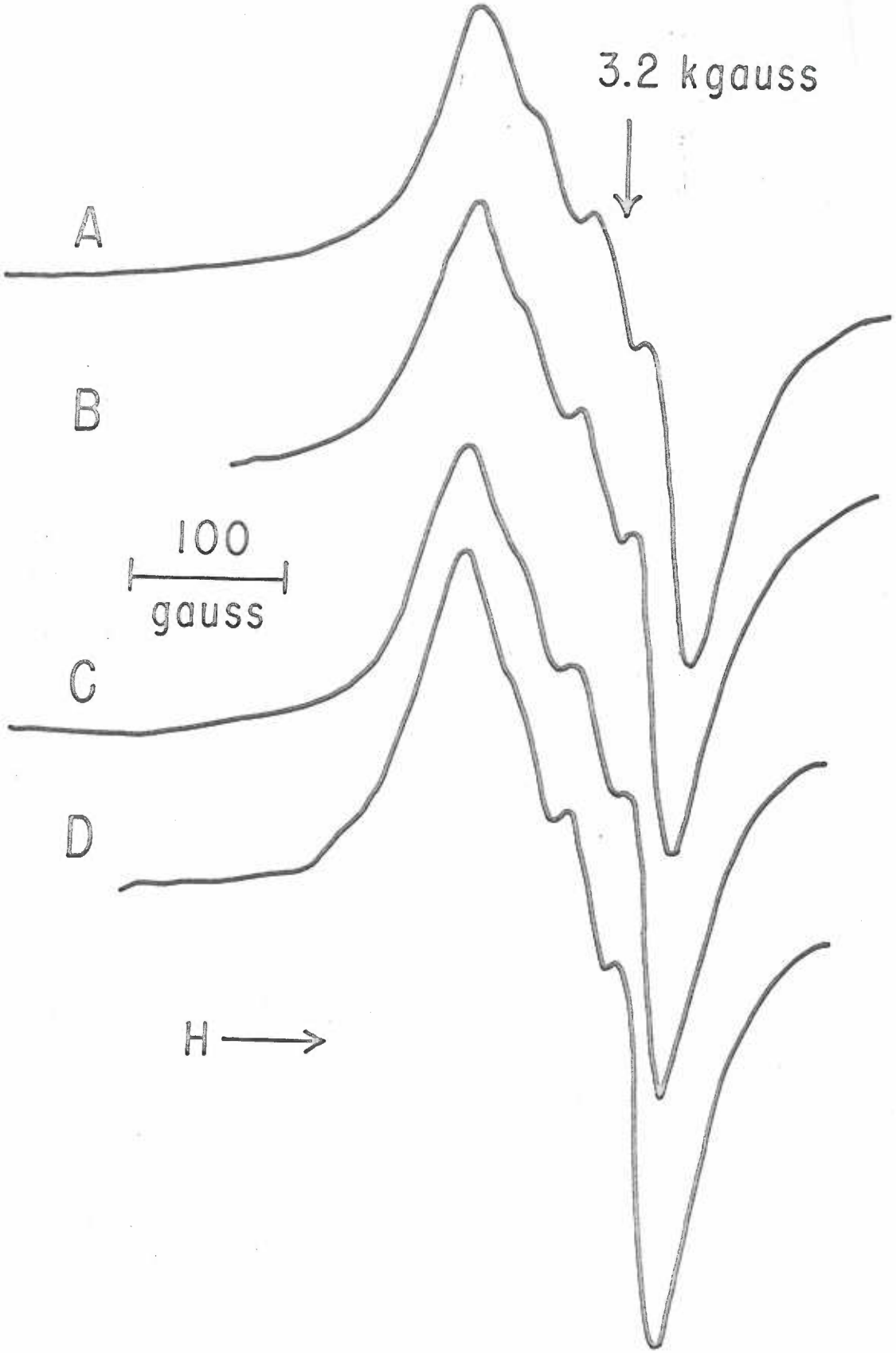
3.2 kgauss
A
B
100
gauss
C
D
H ⟶

FIG. 41

-5° C ESR SPECTRA OF Cu(II)-GLYCYLGLYCINE

ESR spectra of mixtures of glycylglycine and 10 mM $CuCl_2$. Temperature -5° C. Curve A, 20 mM GG, 4 equivalents NaOH, pH 10.7; curve B, 20 mM GG, 3 equivalents NaOH, pH 8.8; curve C, 10 mM GG, 4 equivalents NaOH, pH 11.8; curve D, 10 mM GG, 3 equivalents NaOH, pH 10; curve E, 10 mM GG, 2 equivalents NaOH, pH 7; curve F, 10 mM GG, 1 equivalent NaOH, pH 4.7; curve G, 10 mM GG, 0 equivalents NaOH, pH 3.8.

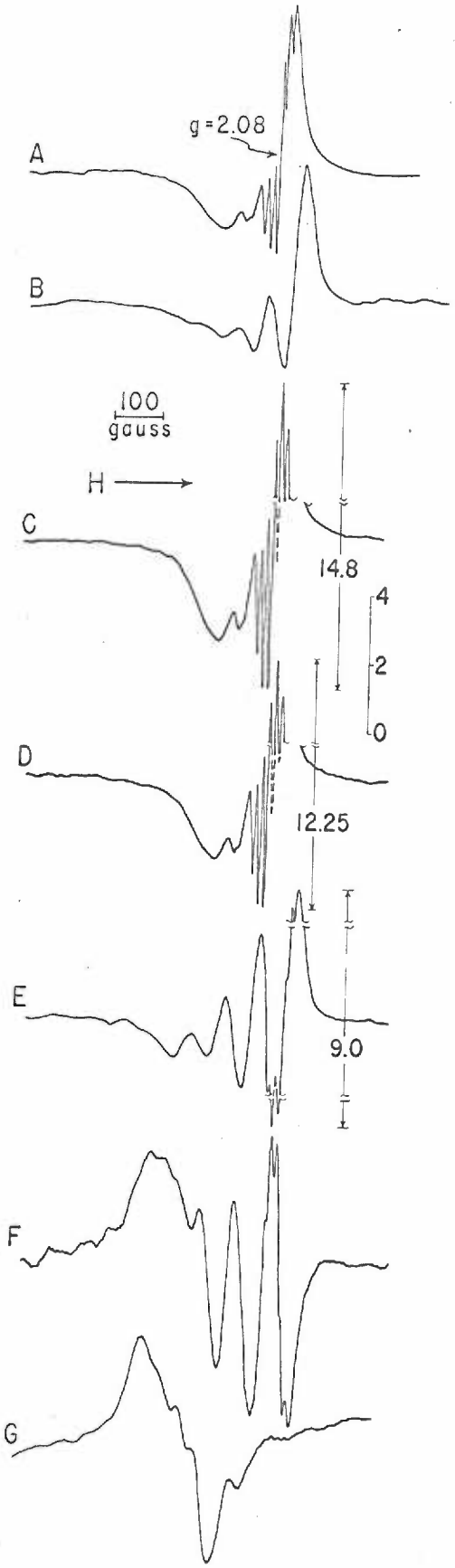
g = 2.08
A
B
100
gauss
H
C
14.8
4
2
0
D
12.25
E
9.0
F
G

Direct comparisons between samples of the unpaired spin concentrations were not possible since the cells utilized for the room temperature measurements were not of uniform size and could not be reproducibly placed in the cavity.

Modulation broadening was not a factor. All experiments were run with a modulation amplitude of 1.6 gauss. The use of modulation amplitudes <.16 gauss produced no significant narrowing of the lines.

The effect of temperature on the ESR spectra of equimolar Cu(II)-GG solutions at 2 equivalents NaOH added (pH 7) is shown in Fig. 42 for the temperature range 0°C to 60°C . The temperature effect on the ESR spectra of equimolar Cu(II)-GG solution at 3 equivalents NaOH added (pH 10) is shown in Fig. 43 for the temperature range-7°C to 85°C.

The ESR spectra of of equimolar Cu(II)-GG and Cu(II)-glycyl-tryptophane at pH 7 and temperatures from 10°C to 60°C are shown in Fig. 44.

The ESR spectra of the Cu(II) pH 7 and pH 10 complexes with GG obtained with $^{63}Cu(II)$ only in place of the naturally occurring ^{63}Cu-^{65}Cu mixture were identical to those obtained with the ^{63}Cu-^{65}Cu mixture.

The ESR spectra of equmolar Cu(II)-GG in D_2O with 2 and 3 equivalents of NaOD added (pD 7 and 10) were identical with those for the corresponding solutions obtained using H_2O and NaOH.

The ESR spectra of Cu(II)-GG ethyl ester solutions utilizing the ^{14}N-^{15}N peptides are shown in Fig.'s 45 and 46. The spectra are

FIG. 42

ESR OF pH 7 Cu(II)-GLYCYLGLYCINE COMPLEX

ESR spectra of 10 mM glycylglycine ethyl ester and 10 mM $CuCl_2$ with equivalents NaOH, pH 7. Curve A, 60°C; curve B, 20°C; curve C, 0°C.

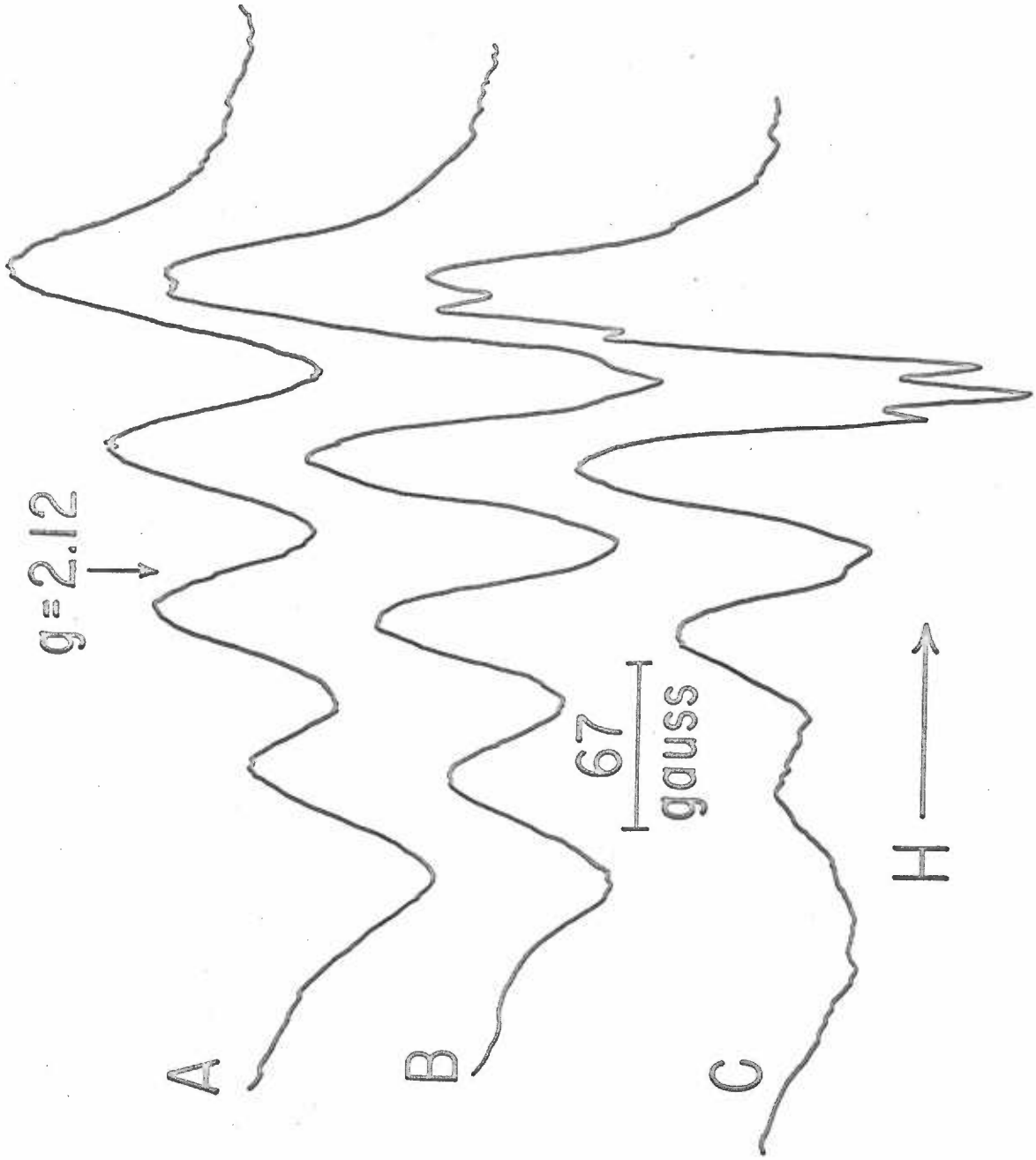
g = 2.12
A
B
C
67
gauss
H

FIG. 43

ESR OF pH 10 Cu(II)-GLYCYLGLYCINE COMPLEX

ESR spectra of 10 mM glycylglycine and 10 mM $CuCl_2$ with 3 equivalents NaOH added, pH 10. Curve A, 85° C; curve B, 60° C; curve C, 30° C; curve D, 18° C; curve E, -7° C.

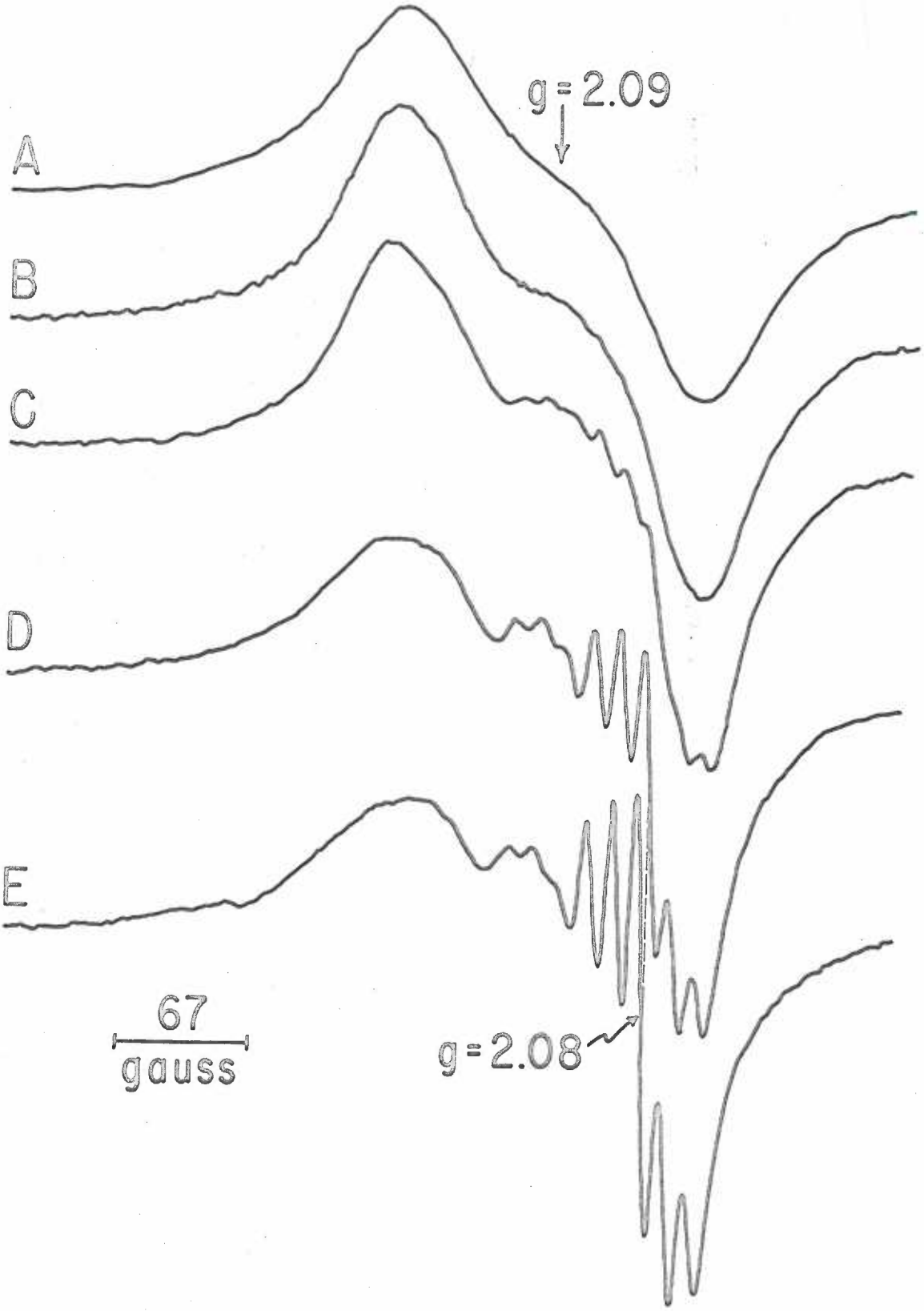
g = 2.09
A
B
C
D
E
67
gauss
g = 2.08

FIG. 44

TEMPERATURE DEPENDENCE OF pH 7 Cu(II)-GLYCYLGLYCINE COMPLEX

ESR spectra of 10 mM $CuCl_2$ with 10 mM glycylglycine (GG) and 10 mM glycyltryptophane (GT) with 2 equivalents NaOH added, pH 7. Curve A, Cu(II)-GT, 60° C; curve B, Cu(II)-GG, 60° C; curve C, Cu(II)-GT, 30° C; curve D, Cu(II)-GG, 30° C; curve E, Cu(II)-GT, 20° C; curve F, Cu(II)-GG, 20° C; curve G, Cu(II)-GT, 10° C; curve H, Cu(II)-GG, 10° C.

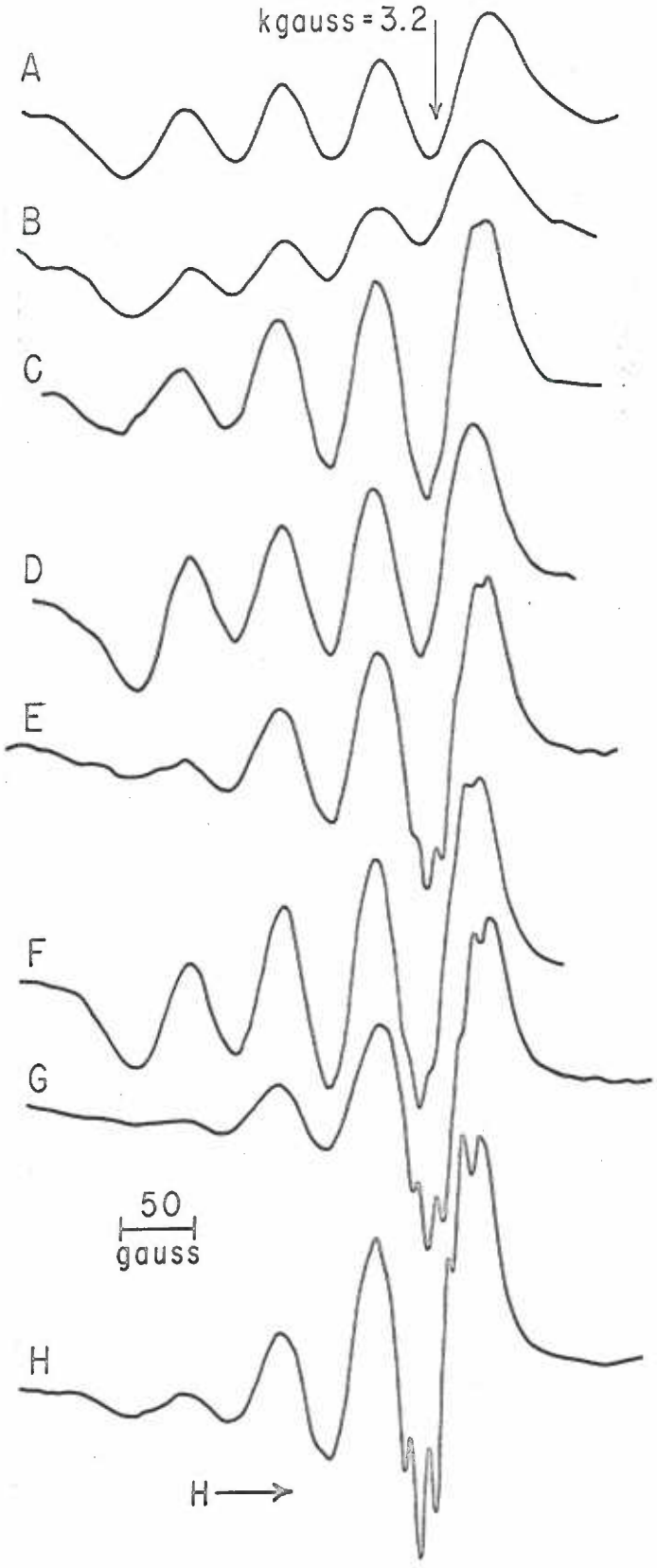
kgauss = 3.2
A
B
C
D
E
F
G
50
gauss
H
H

FIG. 45

ESR SPECTRA OF pH 7 Cu(II)-^{14}N-^{15}N-GLYCYLGLYCINE COMPLEX

ESR spectra at 10° C of 10 mM $CuCl_2$ with 10 mM glycylglycine ethyl ester. 2 equivalents NaOH, pH 7. Curve A, u^{15}N glycylglycine ethyl ester; curve B, ^{15}N(terminal amino), ^{14}N(peptide) glycylglycine ethyl ester; curve C, ^{14}N(terminal amino)-^{15}N(peptide) glycylglycine ethyl ester; curve D, u^{14}N glycylglycine ethyl ester.

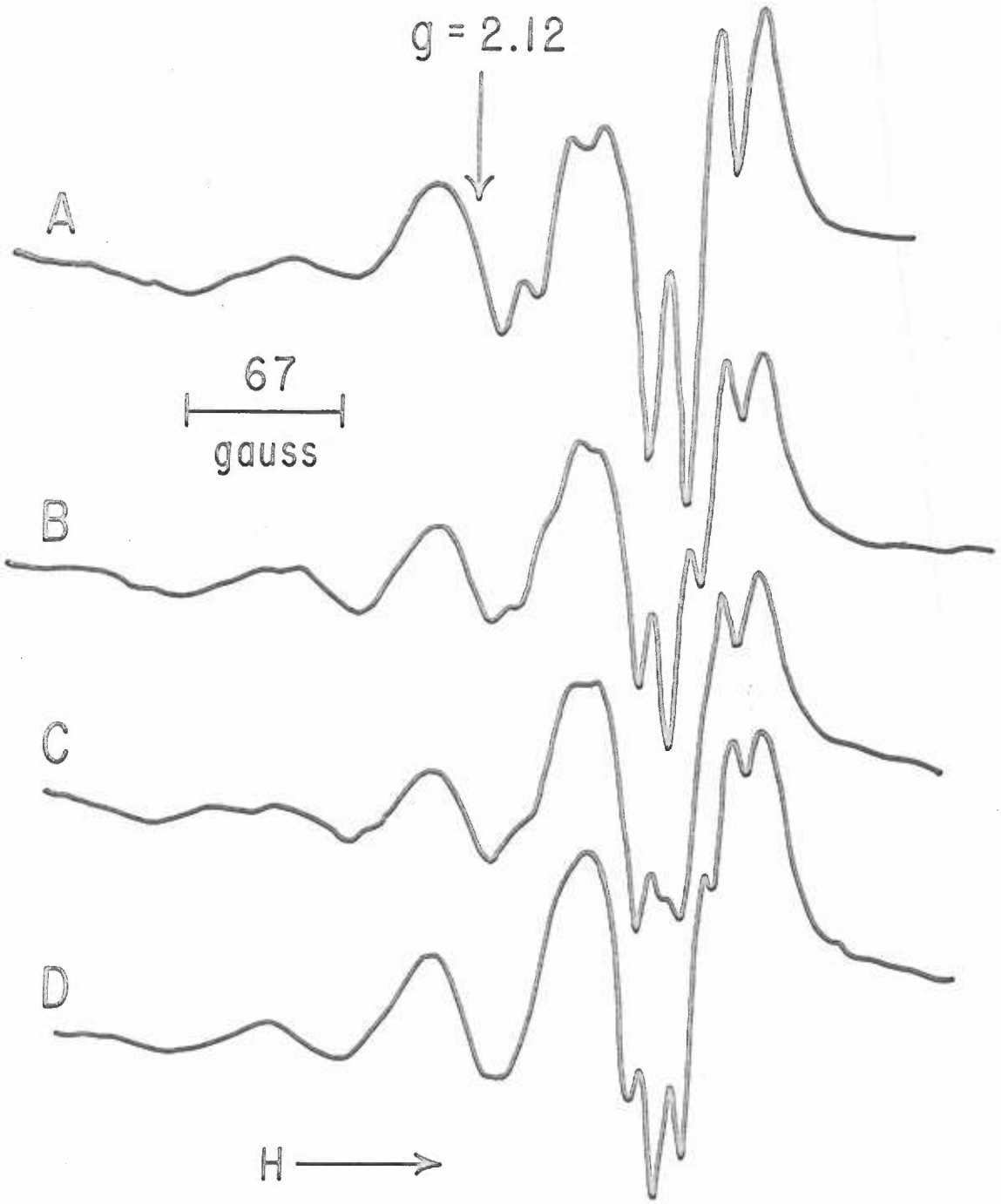
g = 2.12
A
67
gauss
B
C
D
H

FIG. 46

ESR SPECTRA OF pH 10 Cu(II)-^{14}N-^{15}N GLYCYLGLYCINE

ESR spectra at 10° C of 10 mM $CuCl_2$ with 10 mM glycylglycine ethyl ester. 3 equivalents NaOH, pH 10. Curve A, u^{15}N glycylglycine ethyl ester; curve B, ^{15}N(terminal amino)-^{14}N(peptide) glycylglycine ethyl ester; curve C, ^{14}N(terminal amino)-^{15}N(peptide) glycylglycine ethyl ester; curve D, u^{14}N glycylglycine ethyl ester.

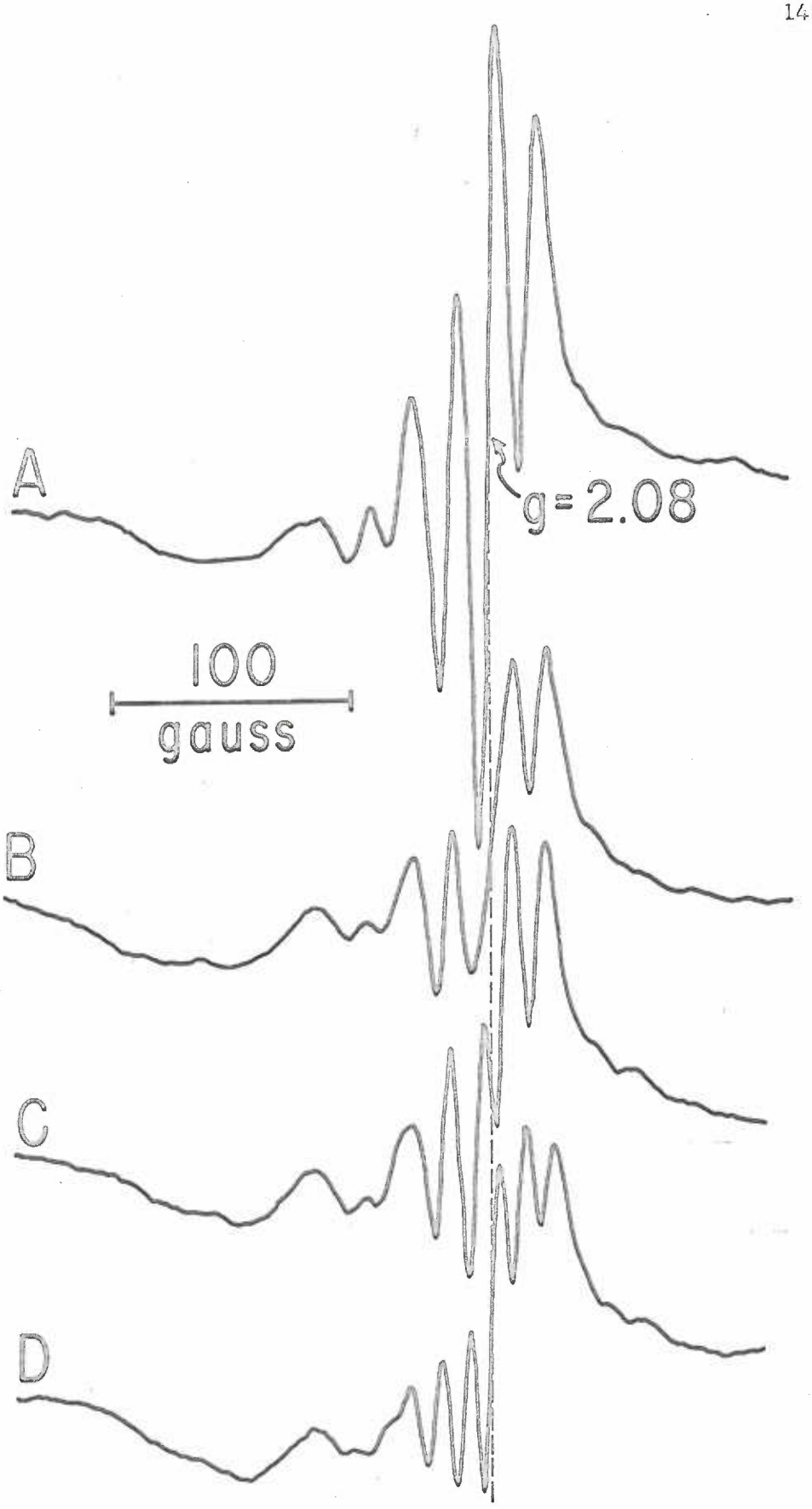
A
g = 2.08
100
gauss
B
C
D

for equimolar Cu(II)-GG solutions at pH 7 and pH 10 respectively. The ESR spectra of Cu(II)-GG and Cu(II)-GG ethyl ester were identical.

The titration curves of the equimolar Cu(II)-GG solutions for the ^{15}N-^{14}N peptides were the same as those obtained with u^{14}N GG as were the optical absorption spectra.

It was found that, in equimolar mixtures of Cu(II) and GG at pH's 7 and 10, for Cu(II) concentrations above .1M, the ESR signal was broadened as the Cu(II) concentration was increased. At high (.5M) Cu(II) concentrations the broadening had increased to the point where an absorption line with no apparent hyperfine structure was obtained. It was found that below .03M no further narrowing was observed; the ESR spectra reported here were obtained at Cu(II) concentrations below .02M.

The optical rotatory dispersion curves for glycyl-l-leucine, glycylglycine and l-leucylglycine equimolar and 3:1 with Cu(II) and at pH 10 are shown in Fig. 47.

Nuclear magnetic resonance experiments gave little information. Proton resonance absorptions were seen in a D_2O solution of glycylglycine but upon addition of Cu(II) to make the solution equimolar in Cu(II) and GG, a single, broad, proton resonance absorption curve was obtained. This can be attributed to the enhancement of the relaxation rates of the protons by the presence of a paramagnetic ion (Cu(II)).

An experiment designed to directly confirm the ionization of a proton from the peptide bond when Cu(II) is bound to the peptide bond was unsuccessful. The H-N(peptide) stretching frequency is detectable

FIG. 47

ORD CURVES FOR Cu(II)-GLYCYLLEUCINE SOLUTIONS

ORD curves for the pH 10 complexes of glycylglycine, glycyl-l-leucine, and l-leucyl-glycine-Cu(II). The conditions under which the experiments were run are specified in the Fig. Temperature 20° C.

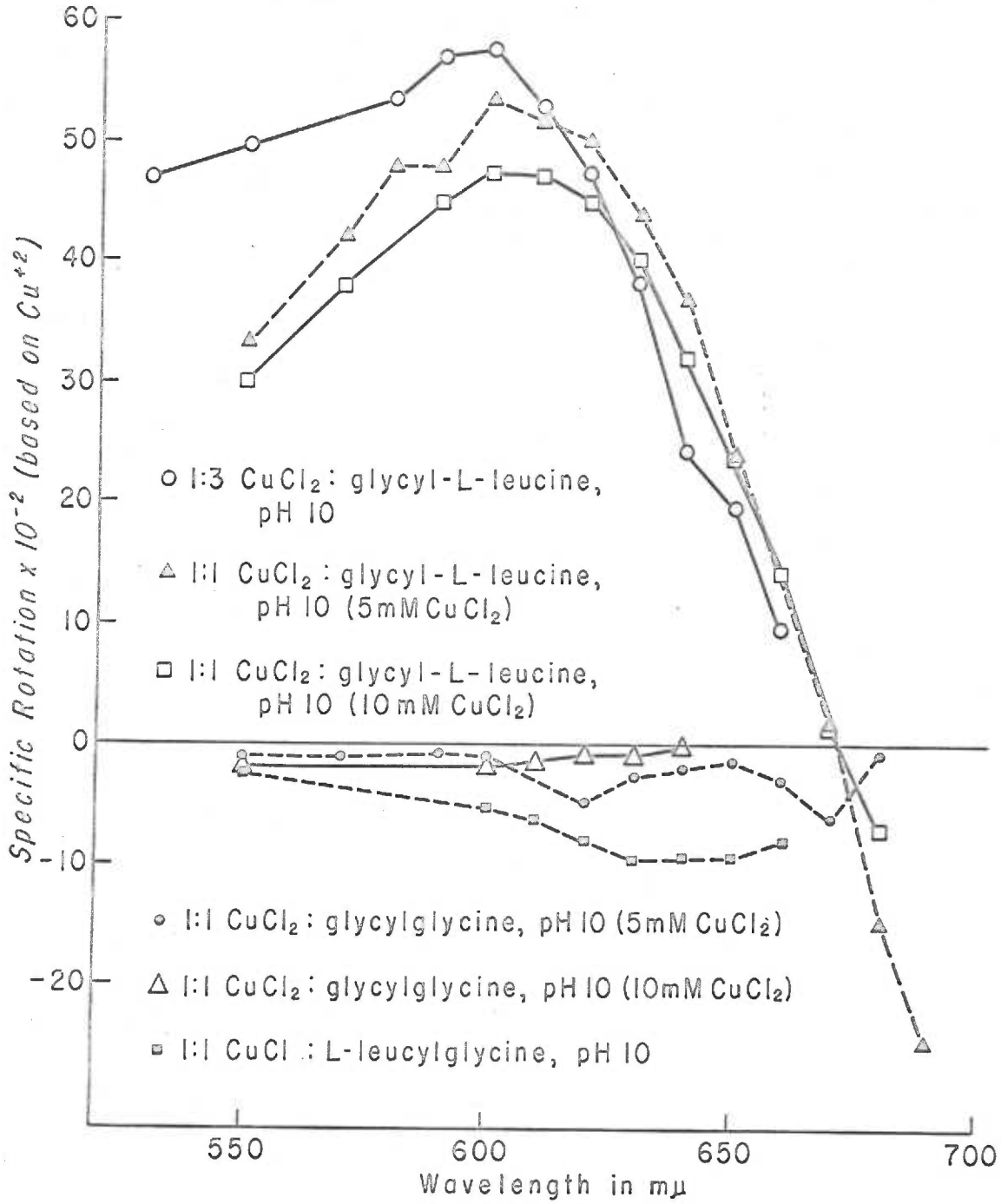
60
50
40
30
20
10
0
-10
-20
Specific Rotation x 10⁻² (based on Cu⁺²)
○ 1:3 CuCl₂ : glycyl-L-leucine, pH 10
△ 1:1 CuCl₂ : glycyl-L-leucine, pH 10 (5mM CuCl₂)
□ 1:1 CuCl₂ : glycyl-L-leucine, pH 10 (10mM CuCl₂)
○ 1:1 CuCl₂ : glycylglycine, pH 10 (5mM CuCl₂)
△ 1:1 CuCl₂ : glycylglycine, pH 10 (10mM CuCl₂)
□ 1:1 CuCl : L-leucylglycine, pH 10
550
600
650
700
Wavelength in mμ

with IR and is different than the D-N(peptide) stretching frequency. The experiments must be performed with GG in the solid state since in solution (H_2O or D_2O) these stretching frequencies are masked. If an equimolar Cu(II)-GG D_2O solution was titrated to pH 10 with NaOD and then back titrated to pH 4 with DCl the H-N(peptide) absorption should be replaced by a D-N(peptide) absorption if the peptide proton has ionized. Due to difficulties in removing the H_2O and D_2O from the solid samples and in separating the Cu(II) from the GG, the region of the H-N and D-N absorptions was masked by strong absorptions from H_2O and D_2O molecules present.

2. Other Cu(II)-Peptide Complexes

In addition to the Cu(II)-GG complexes, complexes formed between Cu(II) and the following ligands were also studied:

a. glycylglycine methyl ester
b. glycylglycine ethyl ester
c. alanylalanine
d. leucylleucine
e. leucylglycine
f. glycylleucine
g. glycylnorvaline
h. glycylalanine
i. glycyl-∝-amino butyric acid
j. glycylvaline
k. glycylnorleucine
l. alanylphenylalanine
m. leucyltyrosine
n. glycyltryptophane
o. diglycylglycine
p. sarcosylglycylglycine
q. alanylglycylglycine
r. leucylglycylglycine
s. glycine
t. sarcosine
u. gycylsarcosine
v. triglycylglycine
w. chloroacetylglycylglycine
x. methionine
y. glycylethionine
z. alanylmethionine
a! glycylmethionine
b! cystiny-bis-glycine
c! arginylalanine acetate
d! alanine amide
e! bis-imidazole
f! histidylhistidine
g! histidylglycine
h! glycylhistidine

Those peptides which formed Cu(II) complexes which were spectrophotometrically and ESR spectrometrically identical with the glycylglycine-Cu(II) complexes are a, b, c, d, e, f, g, h, i, j, k, l, m, and n.

The complexes of Cu(II) and the peptides o, p, q, and r show the ESR spectra given in Fig. 48 under the conditions specified. They also show the same potentiometric titration curves and optical spectra.

The complexes of Cu(II) and the compounds s, t, and u are the same as judged by the potentiometric titration curves, optical spectra, and ESR absorption curves. The ESR specta of the Cu(II)-glycine complexes are shown in Fig. 49. The ESR spectrum of equimolar Cu(II) triglycylglycine at pH 10 is shown in Fig. 50.

The equimolar and 2:1 molar mixtures of chloracetylglycylglycine and Cu(II) form precipitates when the titration is carried above pH 6.5. These complexes were not characterized further.

Methionine, equimolar with Cu(II) formed a precipitate at pH 5.5 and was not characterized further. The complex formed follows the behaviour seen for the Cu(II)-glycine complexes.

The complexes of glycylethionine, alanylmethionine, and glycylmethionine with Cu(II) resemble those of glycylglycine-Cu(II) potentiometrically. The ESR spectra are virtually identical to these seen for the Cu(II)-GG complexes. The solutions are blue when first formed (absorption maxima at 6200 Å) and become blue green in color upon standing (absorption maxima at 565 mu with extinction coefficients = 120).

The peptide cystinyl-bis-glycine can bind two Cu(II) atoms per molecule since in a 1:2 molar mixture of Cu(II) and cysinyl-bis-glycine no precipitation of $Cu(OH)_2$ is formed when the pH is raised to 10. The first inflection in the titration curve occurs at 2 moles

FIG. 48

ESR SPECTRUM OF Cu(II)-LEUCYLGLYCYLGLYCINE COMPLEX

ESR spectra of 10 mM leucylglycylglycine with 10 mM $CuCl_2$ at pH 10.7, 4 equivalents of NaOH added. Curve A, 64° C; curve B, 24° C; curve C, -8° C; curve D, -14° C.

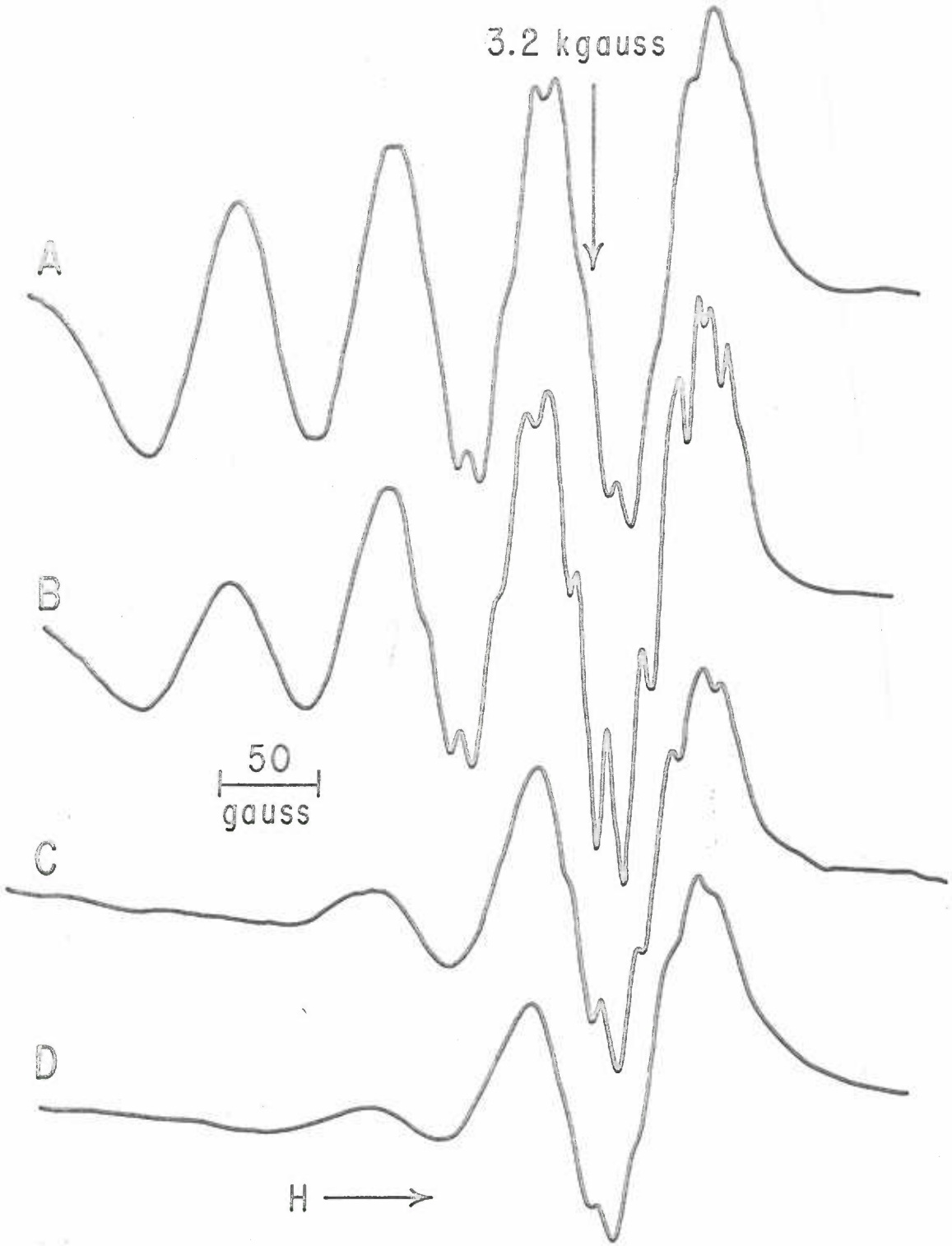
3.2 kgauss
A
B
50
gauss
C
D
H

FIG. 49

ESR SPECTRA OF Cu(II)-GLYCINE COMPLEXES

ESR spectra of 10 mM $CuCl_2$ at 20° C. Curve A, 40 mM glycine, pH 10.3; curve B, 10 mM glycine, pH 5.5. The ordinate for curve B is 1.2 times the ordinate for curve A. The 50 gauss distance refers to curve A.

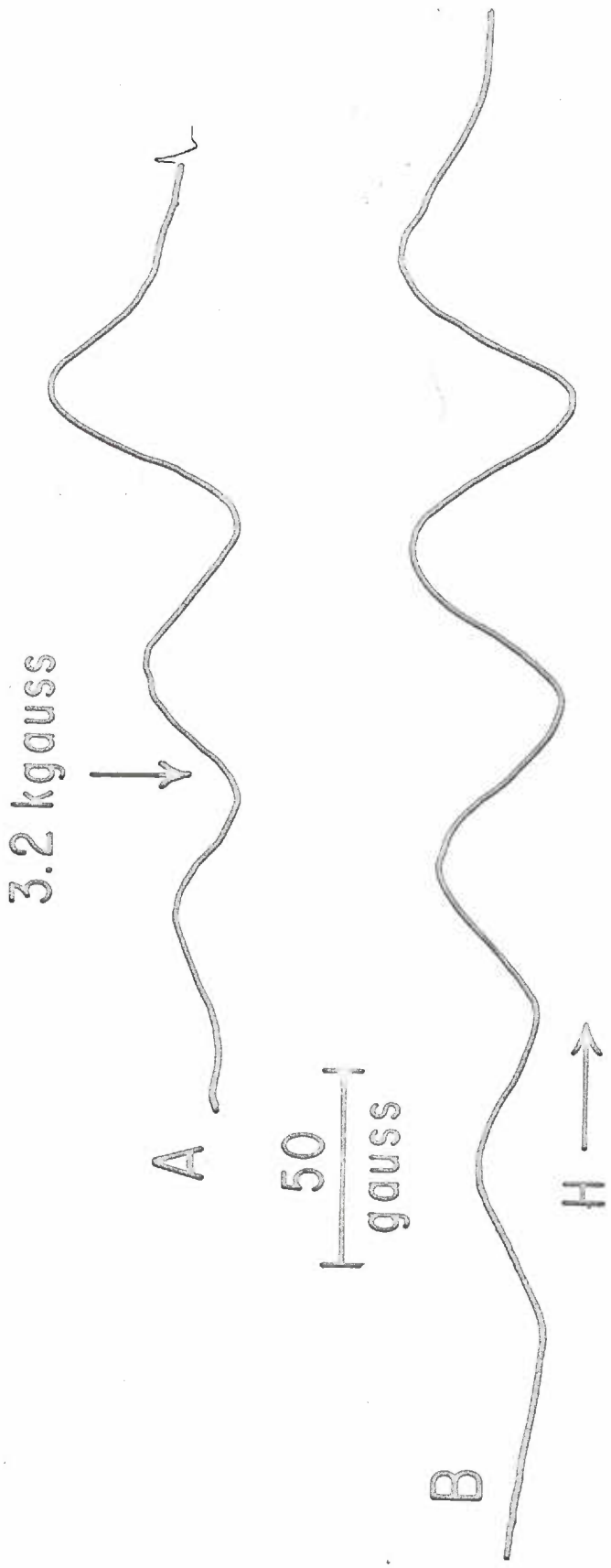
3.2 kgauss
A
50 gauss
H
B

FIG. 50

ESR SPECTRUM OF Cu(II)-TRIGLYCYLGLYCINE COMPLEX

ESR spectrum of 5 mM $CuCl_2$ and 5 mM triglycylglycine at 20° C, pH 10, 5 equivalents NaOH added. Ionic strength 0.16.

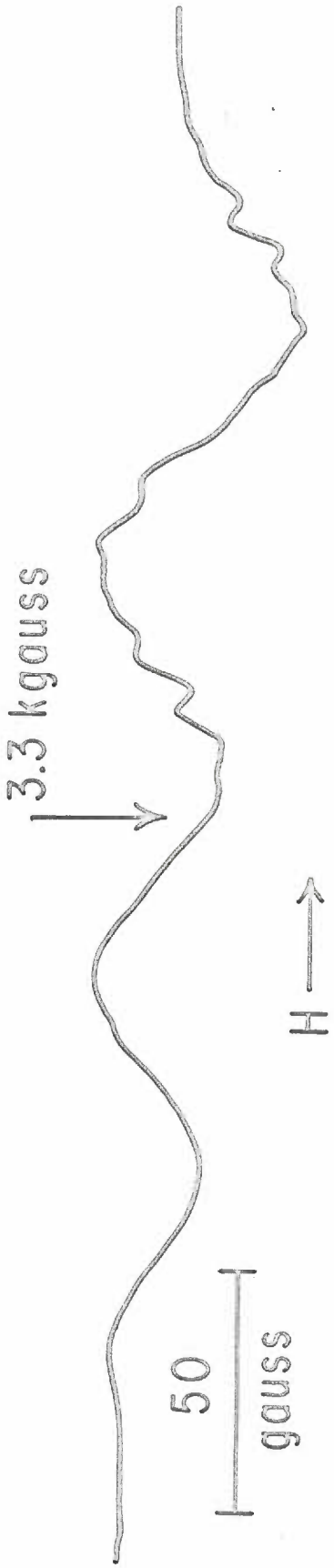
3.3 kgauss
H
50
gauss

NaOH/mole Cu(II) or 4 moles NaOH/mole cystinyl-bis-glycine in the 1:2 Cu(II):cystinyl-bis-glycine mixture. The solution is blue with an absorption maximum at 610 mu and an extinction coefficient of 100. The ESR spectra of 1:.5 and 1:2 molar solutions of cystinyl-bis-glycine and Cu(II) at pH 10 are shown in Fig. 51.

The ESR spectrum of the equimolar mixture of arginylalanine acetate at pH 10 is shown in Fig. 52. Potentiometrically and spectrophotometrically this solution resembles the glycylglycine-Cu(II) solution under these conditions. The ESR spectrum of the 2:1 alanineamide-Cu(II) solution at pH 11 is shown in Fig. 53. In an equimolar solution a precipitate of $Cu(OH)_2$ forms above pH 6.5.

The ESR spectrum of a solution containing the bisimidazole-Cu(II) complex described by Fruton (35) is given in Fig. 54. The spectrum was unchanged over the pH range 4 to 10.

The ESR spectra of the Cu(II) complexes of glycylhistidine, histidylglycine, and histidylhistidine are shown in Fig.'s 55, 56, and 57 respectively. All solutions are equimolar in Cu(II) and ligand and are at pH 10. The Cu(II)-glycylhistidine solution is purple with λ_{max}=560 mu; the Cu(II)-histidylglycine solution is blue with λ_{max}= 620 mu; the Cu(II)-histidylhistidine solution is purple with λ_{max}=560 mu.

3. Pseudomonas Aerugnosa Blue Copper Protein

The ESR spectrum of the Pseudomonas aeruginosa blue copper protein at liquid nitrogen temperatures was the same as that obtained previously by Mason (75). A room temperature ESR spectrum of the same sample was, within the limits of the error due to the decreased signal to noise

FIG. 51

ESR SPECTRA OF Cu(II)-CYSTINYLBISGLYCINE COMPLEX

ESR spectra, at -5° C, of 10 mM cystinyl-bis-glycine with $CuCl_2$ at pH 10. Curve A, 20 mM $CuCl_2$, 6 equivalents NaOH/Cu(II); curve B, 5 mM $CuCl_2$, 4 equivalents NaOH/Cu(II).

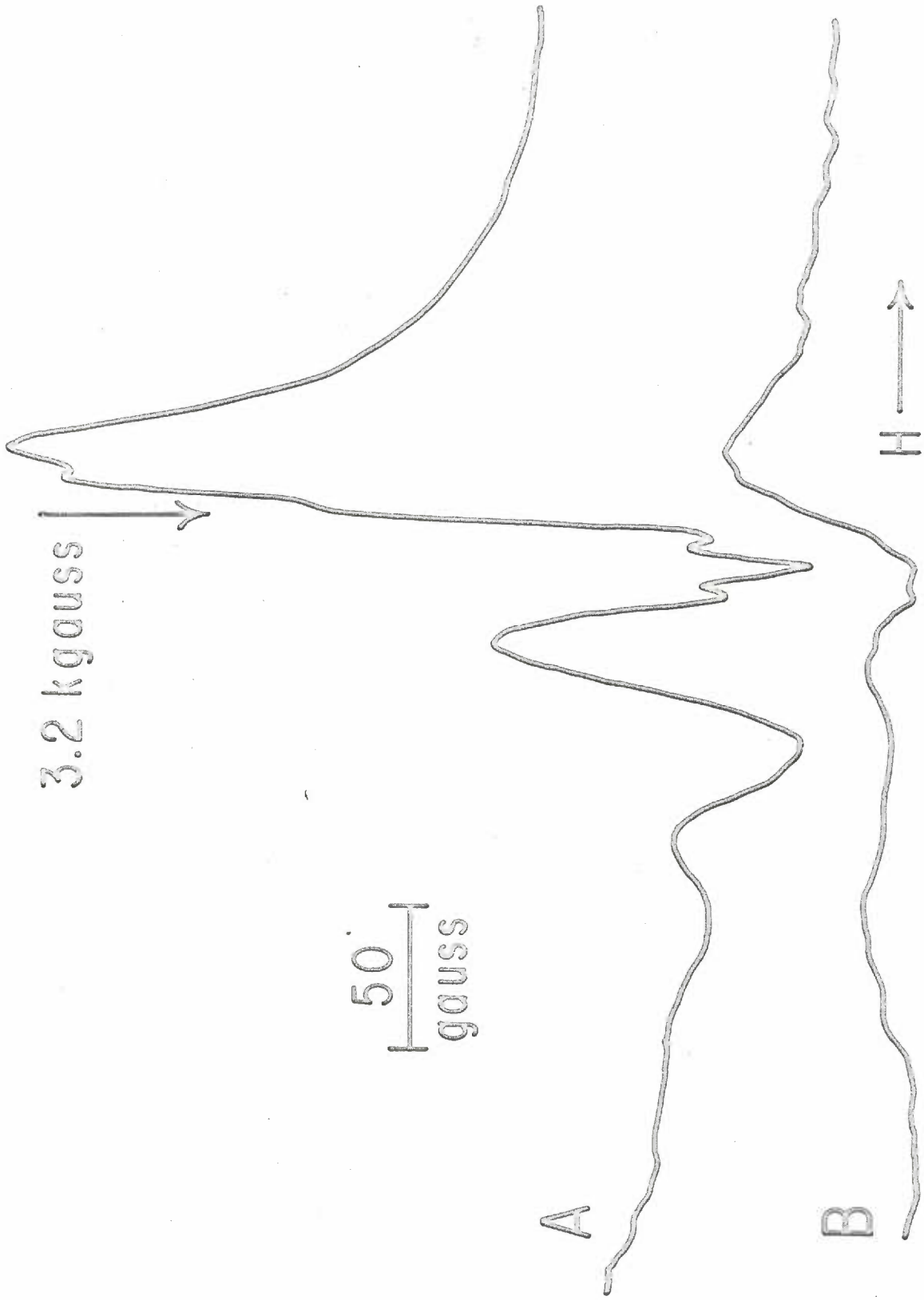
3.2 kgauss
50 gauss
A
B
H

FIG. 52

ESR SPECTRUM OF Cu(II)-ARGINYL ALANINE ACETATE COMPLEX

ESR spectrum of 10 mM $CuCl_2$ and 10 mM arginyl alanine acetate with 3 equivalents NaOH added, pH 10. Temperature - 10° C.

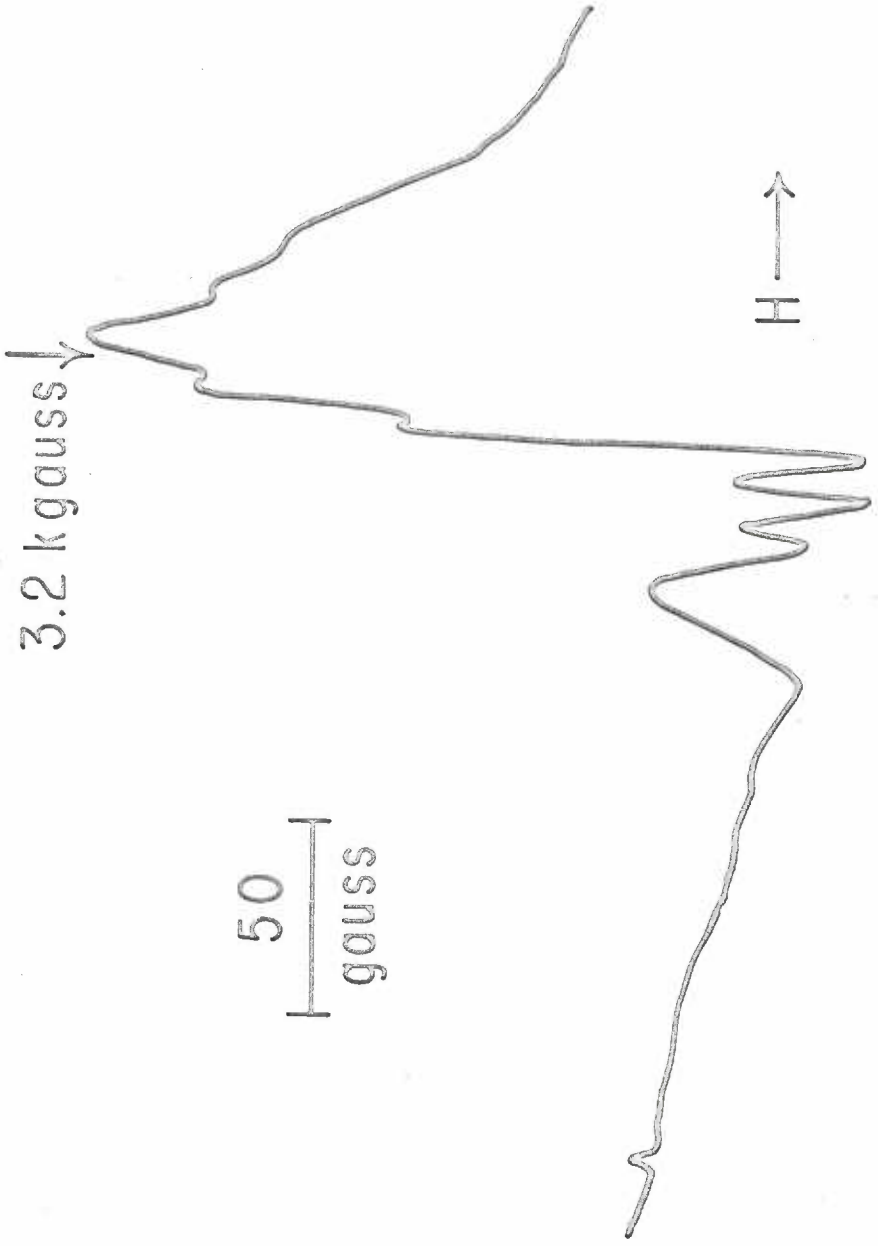
3.2 kgauss
H
50
gauss

FIG. 53

ESR SPECTRUM OF Cu(II)-ALANINE AMIDE COMPLEX

ESR spectrum, at -12° C, of 10 mM $CuCl_2$ with 20 mM alanine amide, pH 10, 4 equivalents NaOH added per Cu(II).

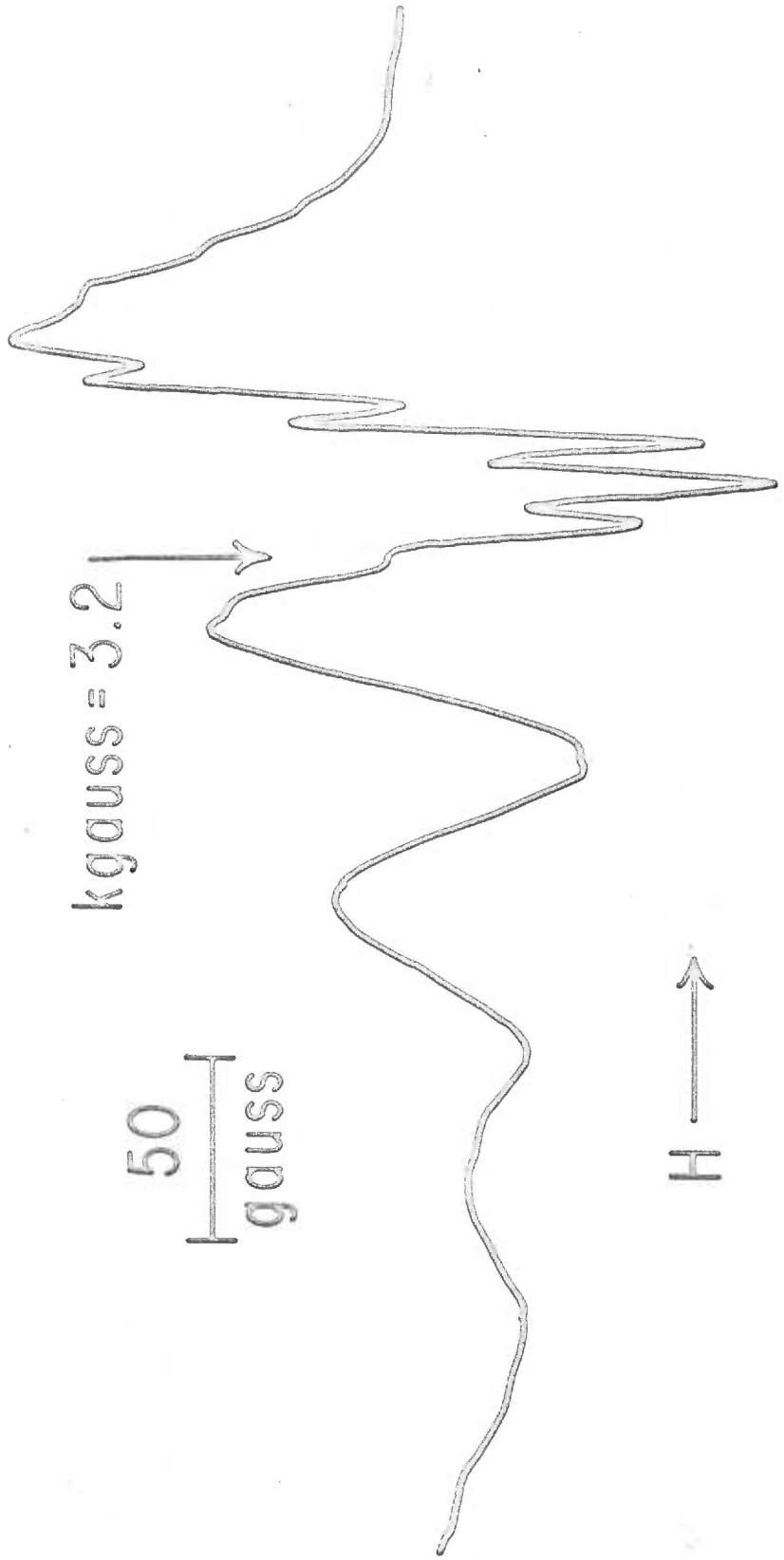
kgauss = 3.2
50 gauss
H

FIG. 54

ESR SPECTRA OF Cu(II)-BIS-IMIDAZOLE COMPLEX

ESR spectra of 10 mM $CuCl_2$ with mM bis-imidazole, at pH 7. Curve A, 60° C; curve B, 10° C; curve D, -5° C.

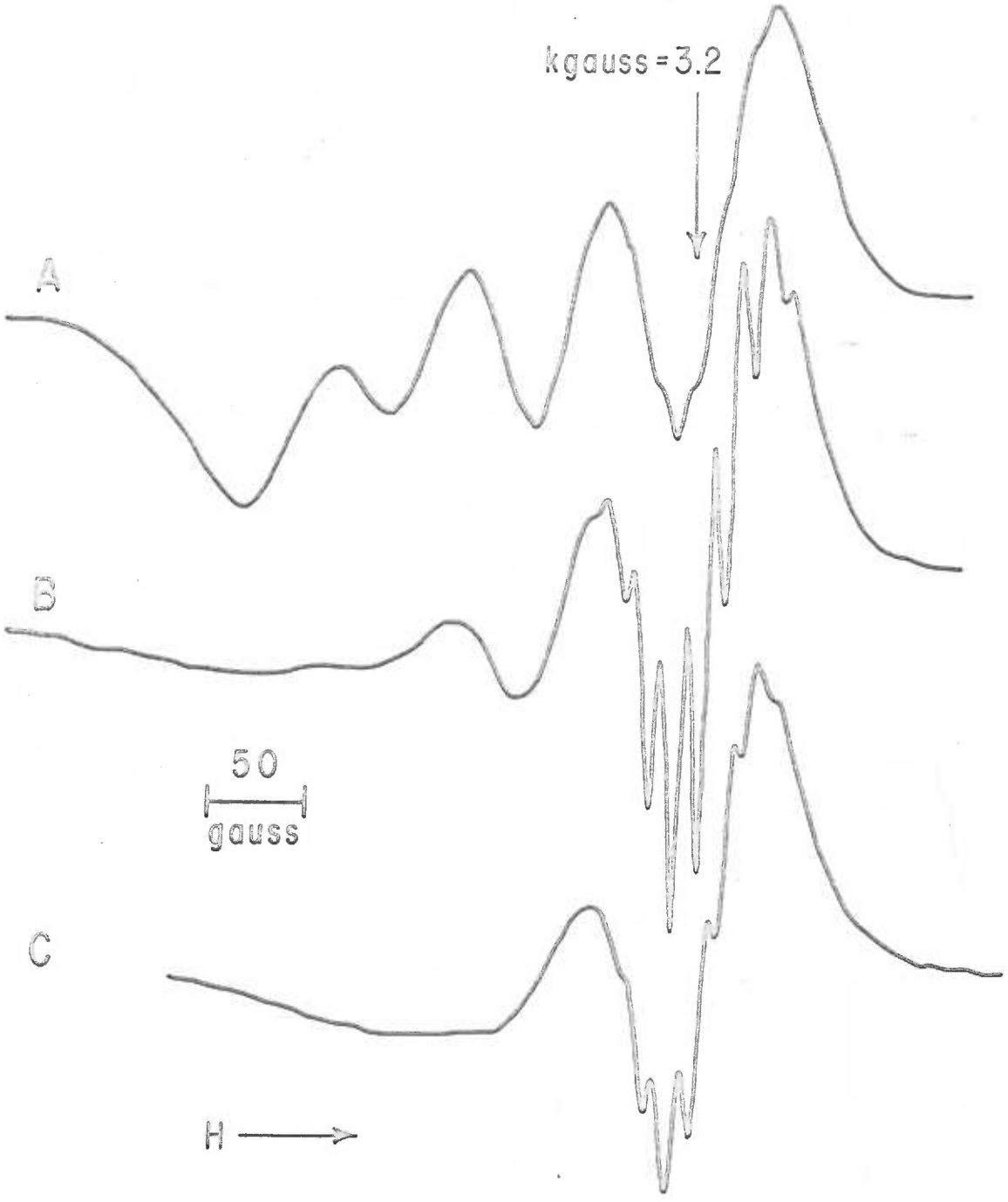
kgauss = 3.2
A
B
50
gauss
C
H

FIG. 55

ESR SPECTRA OF Cu(II)-GLYCYLHISTIDINE COMPLEX

ESR spectra of 10 mM $CuCl_2$ with 10 mM glycylhistidine at pH 10.8. Curve A, 33° C; curve B, 12° C.

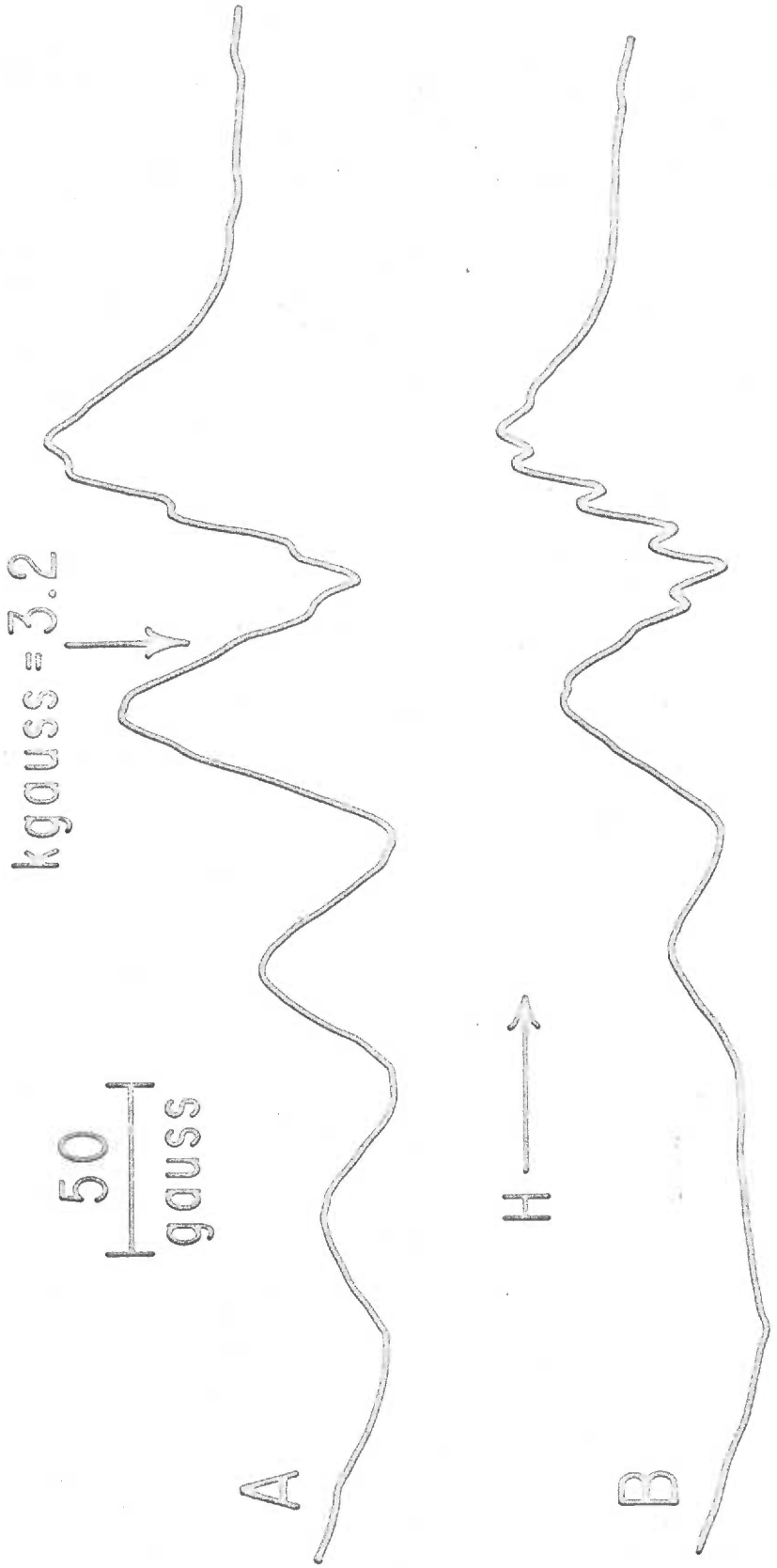
kgauss 3.2
50 gauss
H
A
B

FIG. 56

ESR SPECTRUM OF Cu(II)-HISTIDYLGLYCINE COMPLEX

ESR spectrum of 10 mM $CuCl_2$ with 10 mM histidylglycine at pH 10.5, temperature 11° C.

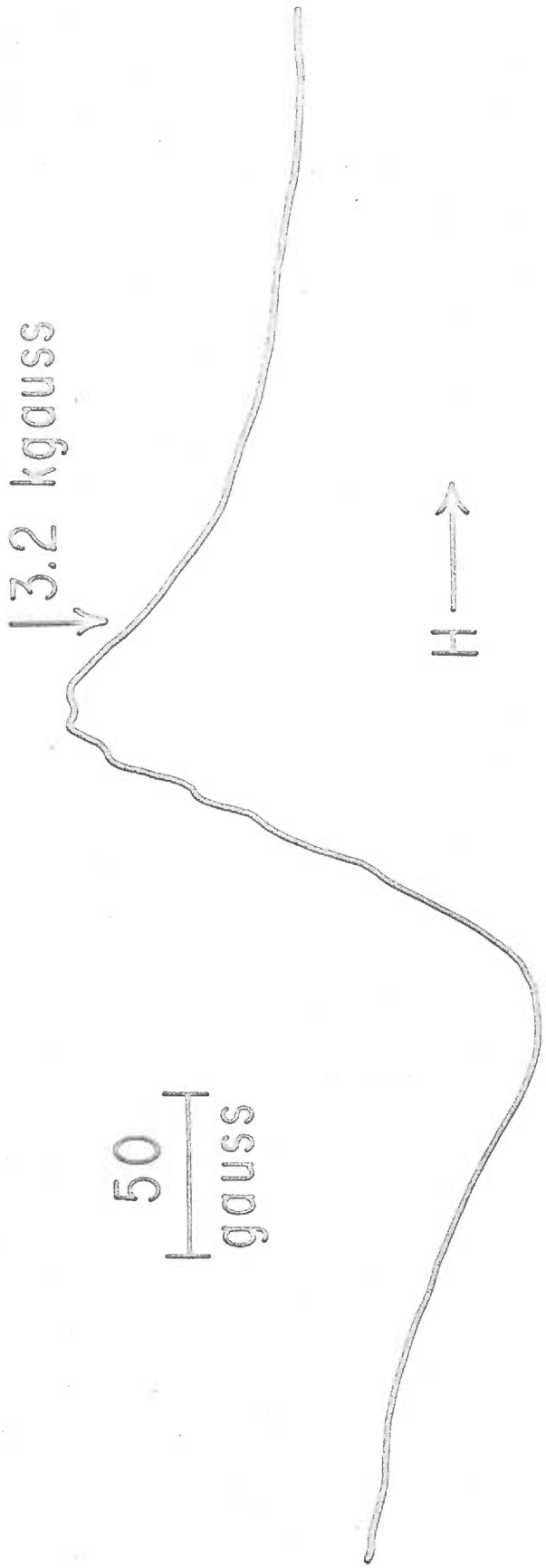
3.2 kgauss
50 gauss
H

FIG. 57

ESR SPECTRUM OF Cu(II)-HISTIDYLHISTIDINE COMPLEX

ESR spectrum of 10 mM $CuCl_2$ with 10 mM histidylhistidine, pH 10.5, temperature 11° C. The field position and ordinate scale is the same as in Fig. 56.

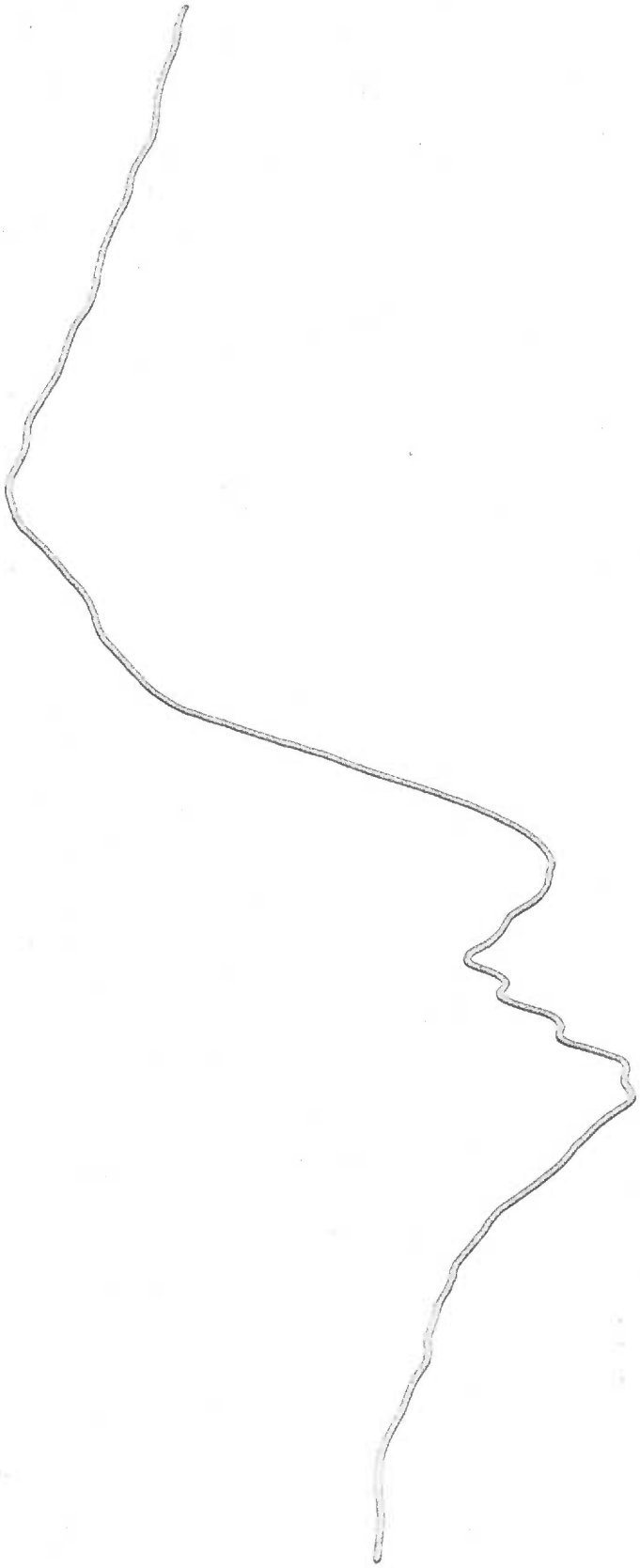

ratio, the same as the liquid nitrogen spectrum. ESR constants calculated were $g_{max} = 2.056$, $g_{//} = 2.26$ and the hyperfine splitting constants A were (low field to high) .006 cm^{-1}, .008 cm^{-1}, and .003 cm^{-1}. The extinction coefficient was $1.68X10^{3}$/ (mole Cu(II)). The ESR spectra of this copper protein at various pH values are given in Fig. 58. The pH was controlled by the use of buffers. An acetate buffer was used for the pH 4.0 solution. A phosphate buffer was used for the pH 6.5 and 7.8 solutions. A glycine buffer was used for the pH 9.5 and 10.5 solutions.

4. Preliminary Results

ESR spectra of a thiomalate-Cu(II) mixture in a .2M acetate buffer, pH 5.9, at thiomalate to Cu(II) ratios specified in the Fig. are shown in Fig. 59. The spectra were obtained at 20°C using an anaerobic quartz flat cell. Anaerobic ESR spectra at liquid nitrogen temperatures were virtually the same as those obtained at room temperature.

Addition of PCMB or PCMS to the 8:5 molar ratio of thiomalate to Cu(II) quantitatively abolished the strong absorption at 520 mu. Liquid nitrogen and room temperature ESR showed no signal for the solutions after PCMB treatment. Bubbling air through these solutions did not cause the appearance of an ESR signal.

Syringe drive flow experiments with the Cary spectrophotometer showed a transient brown colored complex with λ_{max}= 465 mu. The solution becomes clear on standing if the thiomalate/Cu(II) ratio is $> 8/5$ and becomes purple (λ_{max} = 520 mu) if the ratio is $\leqslant 8/5$.

$FeCl_3$ gave, when mixed in a molar ratio $< 8/5$ with thiomalate

FIG. 58

ESR SPECTRA OF PSEUDOMONAS COPPER PROTEIN

ESR spectra at -180° C of a copper protein from Pseudomonas aeruginosa. Protein concentration is approximately 10^{-3} M (10^{-3} in Cu(II)). Curve A, pH 10.5; curve B, pH 9.5; curve C, pH 7; curve D, pH 6.5; curve E, pH 4. The magnetic field increases from left to right. The discontinuity in the curves at the high field side of the 200 gauss marker represents a change in gain of $X10^{-1}$.

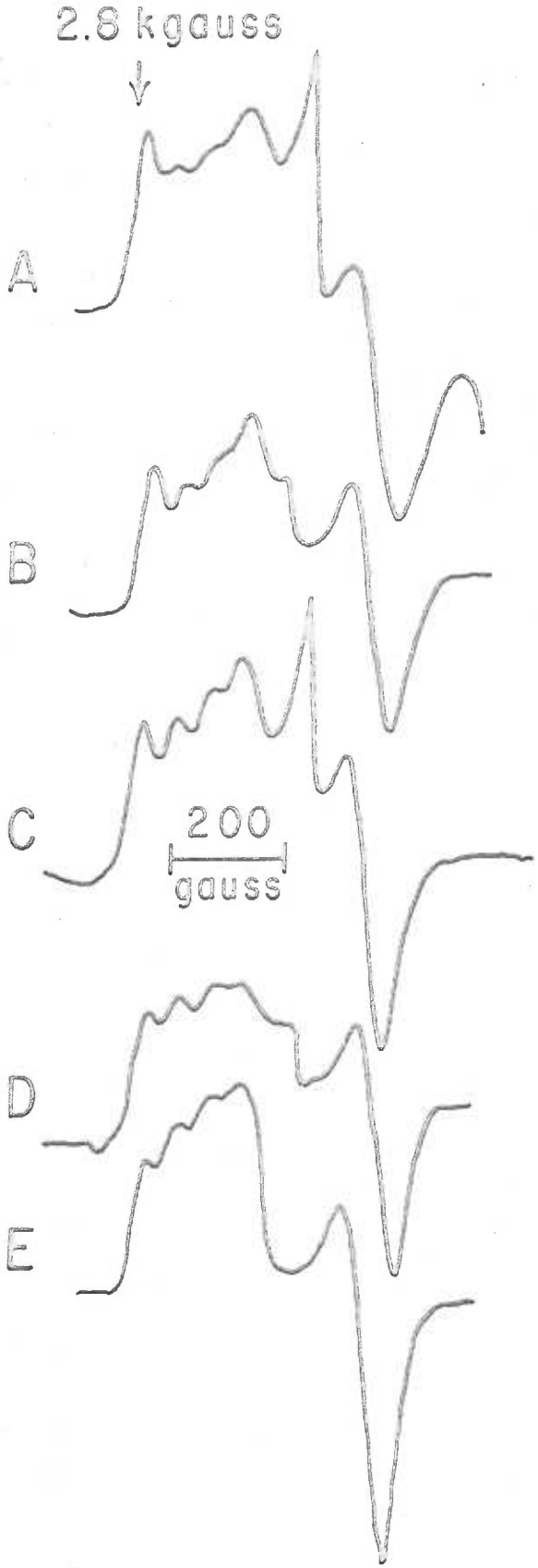
2.8 kgauss
A
B
C
200
gauss
D
E

FIG. 59

ESR SPECTRA OF Cu(II)-THIOMALATE COMPLEX

ESR spectra at 20° C of 10 mM thiomalate with $CuCl_2$ in .2 M acetate, pH 5.9. The spectra were obtained anaerobically. Curve A, 10 mM $CuCl_2$ only; curve B, 10 mM thiomalate, 7.5 mM $CuCl_2$; curve C, 10 mM thiomalate, 6.25 mM $CuCl_2$; curve D, 10 mM thiomalate, 2 mM $CuCl_2$.

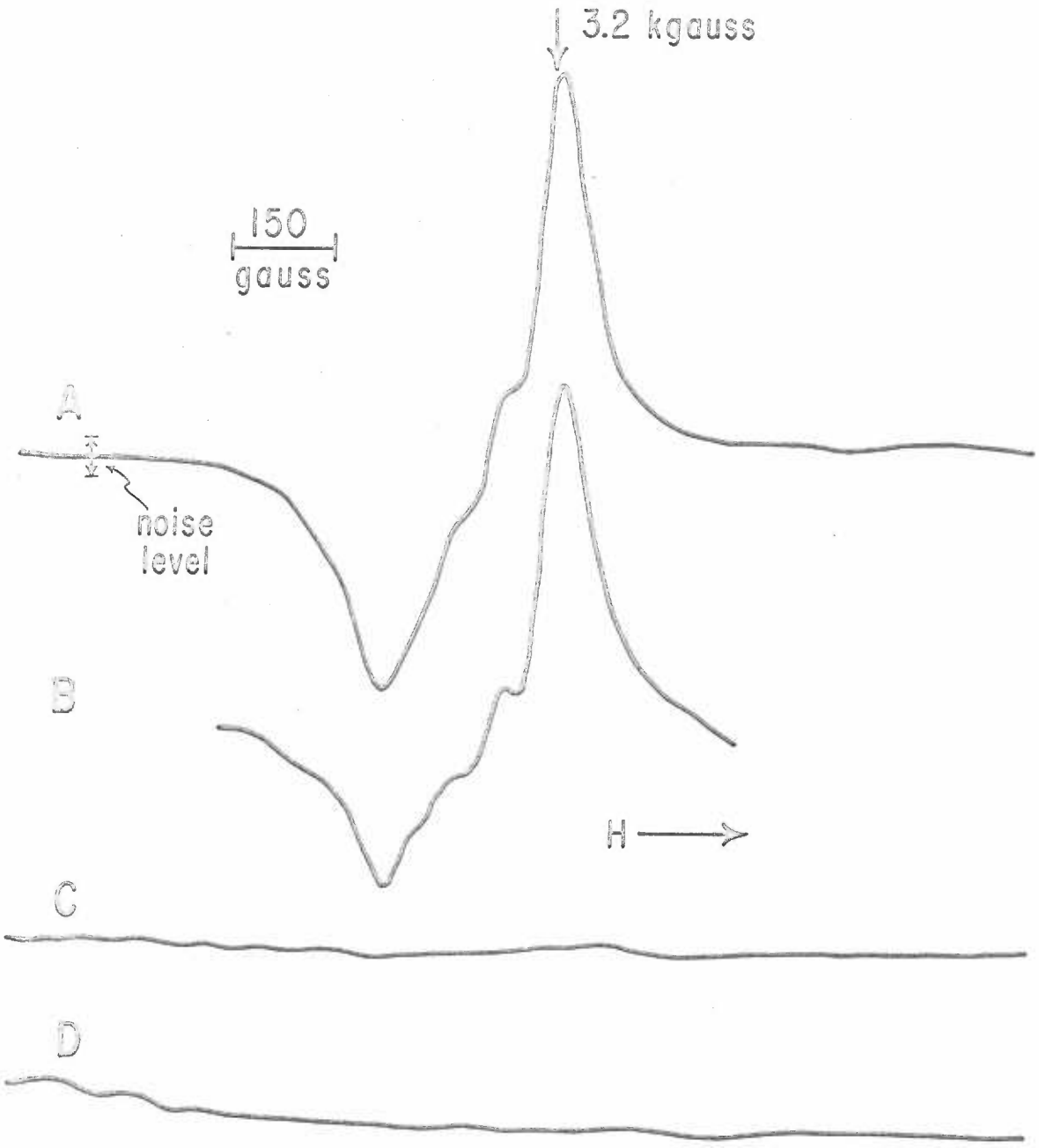
3.2 kgauss
150
gauss
A
noise
level
B
H
C
D

(thiomalate/$FeCl_3$), in a .2M acetate buffer, pH 5.9, a purple solution which rapidly became colorless upon standing. Flow experiments indicated that the λ_{max} was 560 mu. These same flow experiments indicated that the ratio of Fe(III) to thiomalate was 5 to 16 for the maximum color development. The use of buffers with a pH>5.9 caused a more rapid fading of the purple color.

Addition of H_2O_2 to an equimolar glycylglycine-Cu(II) mixture at pH 10 changes the blue solution to a green solution with an accompanying loss of the ESR signal ($T_{1/2}$= one minute).

IV. DISCUSSION

1. ESR Determination of the Different Forms of Cu(II)-Glycyl-glycine Complexes

$E=h\nu$ for the electron spin resonance experiments reported here is $\sim.3$ cm^{-1} or $\sim.86$ cal/mole. An absorption at 6,000 Å represents an energy of $1.7X10^4$ cm^{-1} or $4.7X10^4$ cal/mole. The energy of interaction between a nuclear and electronic dipole is $\sim10^{-2}$ cm^{-1} (12). If this interaction splits the ESR spectral line the energy levels differ by 3%. If the optical absorption line is split by this same interaction it represents a difference of $5X10^{-5}$%. Thus, ESR represents a more sensitive method for determining alterations in the environment about Cu(II) than does optical absorption measurements. On this basis it would be expected that changes in the form of the Cu(II)-GG* complex would be more easily detected by ESR than by optical absorption spectroscopy.

Malmstrom and Vanngard (71) determined the ESR spectra of several Cu(II) complexes (Table 3) at liquid nitrogen temperatures. A single pH (between 7 and 8) was chosen for each solution and an excess of ligand was used "since a change in the degree of coordination may otherwise occur during the freezing of the solutions."** They found that all complexes gave the asymmetric type absorption spectrum seen at low temperatures for Cu(II) complexes in general (Fig. 29).

* The abbreviation used is GG = glycylglycine.
** Malmstrom and Vanngard (71)

From the review of Cu(II)-peptide complexes it is seen that the pH of the solution affects the form of the complex; different complexes exist at different pH's. The -180° C ESR spectra of equimolar Cu(II) and glycylglycine at various pH values (Fig. 38) are only slightly different. The curve shape is consistent with Cu(II) in a site of axial symmetry. Using the method of Liehr and Ballhausen as given by Allen et al. (2) $g_{\parallel}$ and $g_{\perp}$ can be calculated for Cu(II) in a site of axial symmetry and compared with the experimentally determined values of $g_{\parallel}$ and $g_{\perp}$. The temperature dependence of the Cu(II)-GG ESR spectra (cf Fig. 38, -180° C and Fig. 43, 85° C) is as predicted by Liehr and Ballhausen for an octahedral complex with a tetragonal distortion (Fig. 28). At low temperatures the calculated g values are given by (87)

$$(1) \quad g_{\parallel} = 2 + 8|\lambda|/\Delta$$

$$(2) \quad g_{\perp} = 2 + 2|\lambda|/\Delta$$

where λ is the spin orbit coupling constant and Δ is the crystal-field splitting of the d-orbitals. At high temperatures (60° C) the vibrations of the ligands are assumed to average the distorted octahedral (axial) field (2). A single g value is then obtained

$$g = 2 + 4|\lambda|/\Delta$$

Using the g value for the symmetric 60° C curve the ratio $\frac{|\lambda|}{\Delta}$ can be obtained; this can then be used to calculate $g_{\parallel}$ and $g_{\perp}$ from equations (1) and (2).

For equimolar Cu(II)-GG, pH 10, at 85° C, a symmetric one line absorption with g = 2.09 is seen (Fig. 43). This gives $\frac{|\lambda|}{\Delta}$ =0.0225;

$g_{\parallel}$(calculated) = 2.20, $g_{\parallel}$ (observed) = 2.207 and $g_{\perp}$ (calc) =2.05, (obser)$_{\perp}$ = 2.054 (Fig. 38). This assumes that $g_{\perp}$ (obser) = g_{max}, undoubtedly an incorrect assumption. Why?

For equimolar Cu(II)-GG, pH 7, at 60° C a symmetric four line absorption with g = 2.18 is seen (Fig. 42). This gives $\frac{|\lambda|}{\Delta}$ = 0.045; $g_{\parallel}$ (calc) = 2.36, $g_{\parallel}$(obser) = 2.207 and $g_{\perp}$(calc) = 2.09, $g_{\perp}$(obser) =2.054 (Fig. 38).

A $CuCl_2$ solution (2.5 M in NaCl) at 90° C gives a symmetrical one line absorption with g = 2.18. Thus $\frac{|\lambda|}{\Delta}$=0.045 and $g_{\parallel}$ (calc) = 2.36, $g_{\parallel}$ (obser) = 2.22 and $g_{\perp}$ (calc) = 2.09, $g_{\perp}$ (obser) =2.074.

The agreement between calculated and observed g values for the equimolar Cu(II)-GG pH 10 complex is probably fortuitous for the following reasons. The expressions for $g_{\parallel}$ and $g_{\perp}$ were obtained assuming a d^9 atom in a cubic (octahedral) field with a tetragonal distortion (ligands at $\pm a$ on the z axis are displaced by equal amounts from the origin) (Fig. 28). The evidence for assuming that the Cu(II) occupies a site of distorted octahedral symmetry in these complexes is that the ESR spectrum resembles that calculated by Sands for Cu(II) in a site of distorted octahedral symmetry. However, the agreement between calculated and observed spectra is not precise since in the experimental curve the high field $g_{\parallel}$ absorption line is not resolved as it is in Sands' calculated spectrum. This absence of resolution of the high field $g_{\parallel}$ line is also seen in the spectra given by Allen et al. (2) for the phenanthroline and dipyridine-Cu(II) complexes. However, it has been found that in most Cu(II) complexes the Cu(II) does occupy a site of

tetragonal or square planar symmetry (16) so the assumption of such symmetry has experimental basis. A further assumption is that the complex which exists at -180° C is the same as that existing at 90° C; the difference in the ESR spectra being due only to the increased population of excited vibrational states.

It can be seen from Fig. 39 that the -180° C ESR spectra of the Cu(II)-GG complexes depend on NaCl concentration; the room temperature ESR spectra do not depend on NaCl concentration. The same behavior is seen for $CuCl_2$. While other explanations may be given*, it appears that the Cu(II)-GG complex that exists in aqueous solution is different from that which exists in the frozen state. For this reason all Cu(II)-peptide complexes were studied at temperatures above the freezing point of the solutions. The use of liquid nitrogen temperatures introduces an additional variable;-the structural changes of the water environment and of the complex associated with the solid state. This effect must be determined before interpretations of the -180° C specta can be made.

The ESR specta shown in Fig. 41, the -5° C ESR specta of 1:1 and 1:2 Cu(II)-GG mixtures at various pH's, can be interpreted as follows: only three spectra are present, one at equimolar Cu(II)-GG and pH 4 (0 equivalents NaOH), one at equimolar Cu(II)-GG and pH 7 (2 equivalents NaOH), and one at equimolar Cu(II)-GG and pH 10 (3 equivalents NaOH). The other spectra are either identical to these or can be obtained by combining two of these three spectra (eg. in Fig. 41, curve F is a combination of curves E and G). It is concluded that only two ESR distinct complexes of Cu(II) and GG exist under the conditions

* T. Vanngard, Personal Communication

specified. The spectrum at pH 4 is the same as the $CuCl_2$ spectrum (Fig. 40). A slight alteration of the $CuCl_2$ spectrum on the high field side of the pH 4 Cu(II)-GG spectrum can be ascribed to the formation of a small amount of complex in agreement with the IR data of Kim and Martell (51). Under these conditions Dobbie and Kermack (32) have calculated that 88% of the Cu(II) is present as free (hydrated) Cu(II) in agreement with the ESR results.

The conditions under which the pH 7 spectrum (Fig. 41, curve E) was obtained should give, from the work of Dobbie and Kermack, the complex CuGG in 98% concentration (Appendix III).

The pH 10 spectrum (Fig. 41 curve D) can be associated with the complex $CuGG(OH)^-$ as given by Dobbie and Kermack. Under the conditions specified the complex $CuGG(OH)^-$ should be present in 90% concentration.

The lack of ESR spectral evidence for the complex $CuGG^+$ can be attributed to its low concentration ($< 10\%$) or to the proposal that the Cu(II) binding with the displacement of two protons in the pH range 4 to 7 occurs as a single reaction

$$Cu(II) + GG = CuGG + 2H^+.$$

A careful synthesis of spectra between pH 4 and 7 from the pH 4 and 7 curves only and comparison with the experimental curves would be needed for detection of the $CuGG^+$ complex.

Addition of a fourth equivalent of NaOH to the equimolar Cu(II)-GG mixture may form the complex $CuGG(OH)^{-2}$ (60). As seen from curve C, Fig. 41, the addition of a fourth equivalent of NaOH does not alter the ESR spectrum over that of the curve obtained at 3 equivalents NaOH.

It is improbable that the inclusion of a second OH^- in the coordination sphere of the Cu(II) would not alter the ESR spectrum. The buffering effect in the region pH 11.5 to 13 is not, on this basis, attributable to the formation of a $CuGG(OH)^{-2}$ complex.

The IR data of Kim and Martell (51) show that no frequency changes occur in the IR specta of the Cu(II)-GG complexes above pH 7; this is seen since IR is "looking at" the glycylglycine molecule and no IR detectable change is occurring in the GG molecule above pH 7. The ESR data clearly show that a significant change occurs in the environment of the unpaired electron above pH 7.

The data of Dobbie and Kermack indicate that in 2:1 molar mixtures of GG and Cu(II), at pH's above 7, the Cu(II) should be distributed as $Cu(GG)_2^-$ and $Cu(GG)_2^{-2}$, and at pH 9 the complex $Cu(GG)_2^-$ should be present in 66% concentration and at pH 11 the complex $Cu(GG)_2^{-2}$ should account for 76% of the Cu(II) present (Appendix III). Kim and Martell (51) maintain that they can fit their proposed reaction schemes to the experimental data by assuming that the complex $Cu(GG)_2^-$ is the only 2:1 complex formed. It can be seen from the spectra in Fig. 41 that the ESR signals are unaltered under the conditions given by Dobbie and Kermack in which 2:1 GG-CU(II) complexes are to be formed (curves A and B). It would then appear that, as obtained by Kober and Sugiura, the Cu(II)-GG mixtures form only one to one complexes under the conditions specified. The consumption of 4 equivalents of NaOH in a 2:1 GG:Cu(II) mixture between pH 4 and 10 is due not to the formation of the complex $Cu(GG)_2^{-2}$ but to the formation of the complex $CuGG(OH)^-$ and

to the titration of one equivalent of the zwitterion form of glycylglycine (34).

2. ESR Determination of Certain Structural Features of the Cu(II)-GG Complexes

As pointed out in the section on ESR theory, ESR can be used to determine the "structure" of a transition metal chelate; "structure" referring to all the factors effecting the ESR spectrum. Since ESR detects only two complexes, the following discussion will be limited to these two spectra. We may refer to the "pH 7" complex (2 equivalents NaOH added to an equimolar Cu(II)-GG mixture) and the "pH 10" complex (3 equivalents NaOH added). A possible model giving the spatial arrangement of the atoms in the Cu(II)-GG complex will be considered first.

A. Calculation of the "Structure" of the Cu(II)-GG Complex

Using methods first proposed by Corey and Sneen (27) and later applied to the calculation of ring geometries for the Co(III)-ethylene diamine complexes by Corey and Bailar (28) the structure shown in Fig. 60 for the Cu(II)-GG complex was calculated. The method used is outlined as follows: The formation of a ring structure(s) is assumed. A tentative three-dimensional structure of the ring is drawn and coordinates (x_i, y_i, z_i) are assigned each atom. The bonds are then represented as vectors by the use of the unit vectors $\vec{i}$, $\vec{j}$, $\vec{k}$. Using standard vector relationships, of which the scalar product $\vec{ab}.\vec{ac} = BC\cos\Phi$ was the most useful, simultaneous equations in the unknown coordinates (x_i, y_i, z_i) are obtained. These are then solved to give

FIG. 60

PROPOSED MODEL FOR Cu(II)-GLYCYLGLYCINE COMPLEX

Calculated model for the Cu(II)-glycylglycine complex. Two positions are possible for the ring containing the peptide nitrogen atom and the terminal oxygen atom of the terminal carboxyl group as indicated in the Fig. The coordinates for the individual atoms are given in the Discussion.

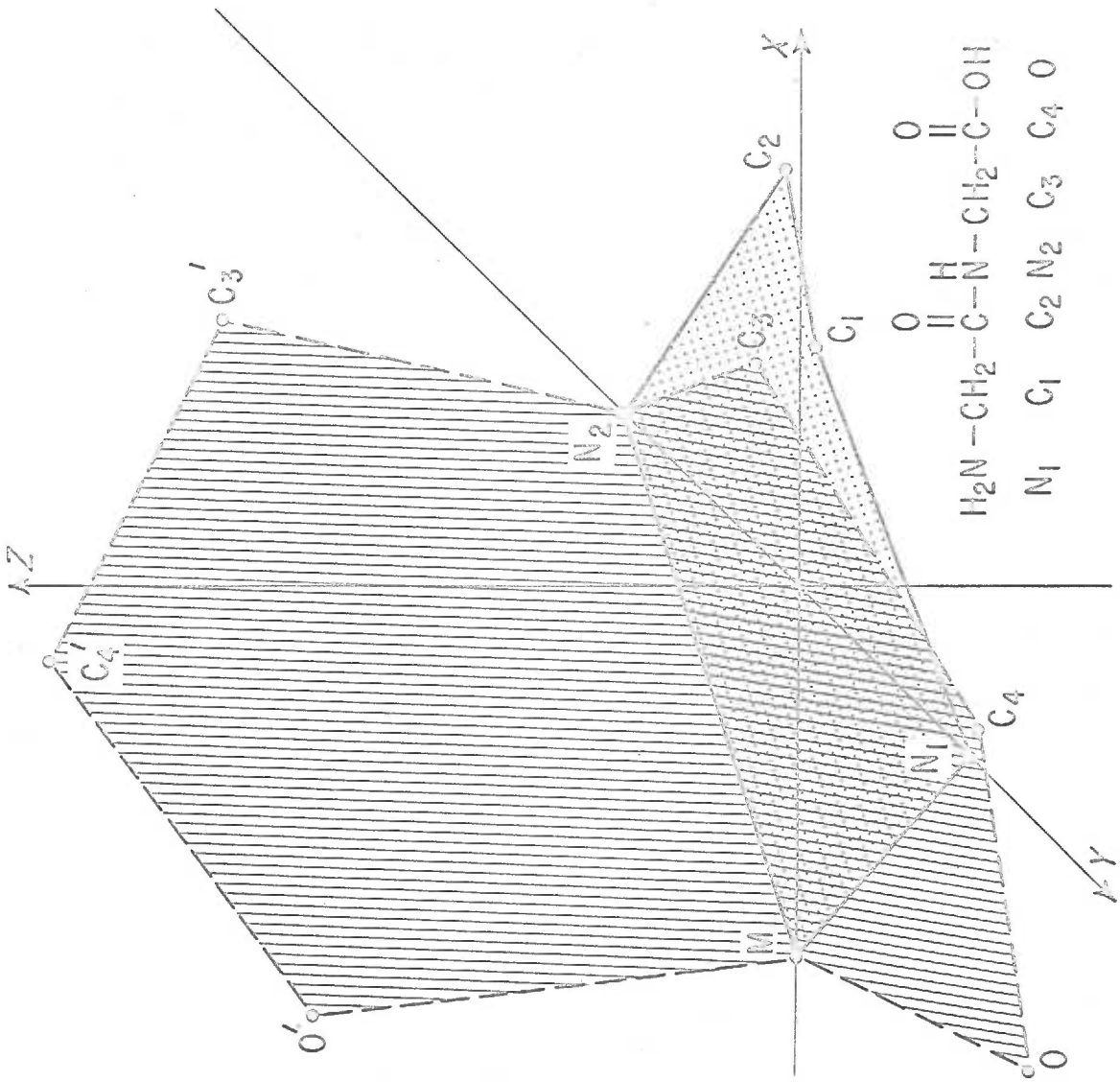
X
Z
Y
C2
C3'
C1
C3
N2
C4'
C4
N1
O'
O
H2N—CH2—C—N—CH2—C—OH
N1 C1 C2 N2 C3 C4 O

the coordinates of the atoms in the ring structure. The calculation is facilitated if the ring possesses elements of symmetry. The ring formed with the terminal amino and peptide nitrogen atom was assumed to have a mirror plane, the x-y plane (except that one C atom was +z above the X-Y plane and the other was -z below this plane). The ring containing the peptide nitrogen atom and the carboxyl oxygen atom was assumed to be planar.

Bond angles and lengths assumed were (28, 88) $\angle(CuN_2C_3, N_2C_3C_4, CuN_1C_1, N_1C_1C_2, C_2N_2C_3) = 109.5^o$, $\angle CuOC_4 = 110.4^o$, $\angle C_3C_40 = 120^o$; C-C = 1.54 Å, C-N = 1.47 Å, Cu-N = 2.0 Å, C_4-O = 1.43 Å. Cu-O = 1.83 Å. Angles calculated were $\angle N_2CuO = 91.5^o$ and $\angle N_1CuN_2 = 86.2^o$.

The coordinates calculated for the ring containing the terminal amino and peptide nitrogen atoms were, in Å, (28)

$Cu(-1.46,0,0)$; $N_1(0,1.37,0)$; $N_2(0,-1.37,0)$;

$C_1(1.28,0.74,0.30)$; $C_2(1.28,-0.74,-0.30)$.

The z-coordinates of C_1 and C_2 could be interchanged; the results are not qualitatively effected by this and the following discussion is based on the above coordinates.

Two sets of coordinates are obtained for the ring involving the terminal carboxyl oxygen atom and peptide nitrogen atom. They are

$C_3(-0.30,-2.40,-1.04)$; $C_4(-1.60,-2.05,-1.73)$

$O(-2.34,-.87,-1.36)$

and

$C_3'(0.06,-2.02,1.31)$; $C_4'(-1.01,-1.39,2.26)$

$O'(-1.88,-0.38,1.73)$

The Cu-O bond makes an angle of 137.7° with the N_1CuN_2 plane and the Cu-O' bond makes an angle of 109.9° with the N_1CuN_2 plane. On this basis, the complex does not possess square planar symmetry as was found for the Cu(II)-GG complex in crystalline form nor could it possess octahedral or distorted octahedral symmetry. The complex will assume a structure for which F is a minimum (dF = 0). As an approximation it can be assumed that S is the same for slightly different forms of the complex (84). The structure of the complex will then depend on which form minimizes E ($E \cong H$). Experimental evidence indicates that square planar Cu(II) is the stable form of Cu(II) (16).

As found for the Cu(II)-GG crystals, this involves a distortion of the normal bond angles of glycylglycine and would consequently increase the energy of the peptide. On the other hand, Cu(II) in a field of lower symmetry than square planar would have increased energy. A determination of the structure of the complex would involve evaluation of multiple factors effecting the energy of the Cu(II), the glycylglycine, and a determination of stabilizing energies of complex formation. The problem can be approached experimentally.

B. Optical Rotatory Dispersion

If neither a plane nor a center of symmetry exists at the center of gravity of the wave functions which determine the optical transition under consideration (the d-d transition at ~6,000 Å can be considered as centered at the Cu(II) nucleus), then there will be a differential absorption of left-handed and right-handed circularly polarized light (circular dichroism) (38). This will lead to a rotation of plane polar-

ized light (optical rotatory dispersion). If the rotation is determined as a function of wave length then a Cotton effect is seen in the resulting curve. Such an effect is seen in the 6,000 Å band of the Cu(II)-GG complex* (Fig. 47). A weaker Cotton effect is seen for the pH 7 complex.

The interpretation of this Cotton effect is uncertain. Piper and Karipides (48, 90) attribute the optical activity of the Co(ethylenediamine)$_3^{+3}$ complex to a distortion of the octahedral disposition of ligand atoms which abolished the plane or center of symmetry. For the Cu(II)-GG model calculated this would then explain the observed Cotton effect in the 6,000 Å absorption band. Mason and Norman (77, 78) have shown a deuterium effect on the circular dichroism of the Co(ethylenediamine)$_3^{+3}$ complex and have interpreted this in terms of a model in which the Co d-orbital wave functions extend to the carbon and hydrogen atoms as well as the nitrogen atoms of the ethylenediamine molecules. In this interpretation the nitrogen atoms could form a symmetric octahedral environment, with the asymmetry which gives rise to the Cotton effect being due to the carbon and hydrogen atoms. This interpretation could account for the Cotton effect seen when glycylleucine is used in place of glycylglycine to form the Cu(II) complex. The question of the symmetry about the Cu(II) in the Cu(II)-GG complex in solution remains unresolved.

* The Cotton effect is seen only if an optically active amino acid is used in place of glycine. When the Cu(II)-GG complex is formed equal amounts of d and l complexes would be expected**; when glycine is replaced by a d or l amino acid then a preferential formation of the d or l complex would be expected.

** P. Oriel, Personal Communication, 1963.

C. Cu(II) ESR Hyperfine Structure

The ESR spectrum of the pH 7 complex consists of four main lines (Fig. 42) with the high field lines showing further hyperfine structure. Since the complexes are in solution the anisotropic terms can be considered as "averaged out" (12) (the breakdown of this assumption will be considered later) and the spin Hamiltonian can be written (12)

$$\mathcal{H} = g\beta H_z \cdot S_z + a S_z I_z .$$

Off diagonal elements will be ignored (12). The spin wave functions can be written (ignoring, for now, the hyperfine structure on the high field lines)* $|1/2,3/2)$, $|1/2,1/2)$, $|1/2,-1/2)$, $|1/2,-3/2)$; $|-1/2,3/2)$, $|-1/2,1/2)$, $|-1/2,-1/2)$, $|-1/2,-3/2)$.

Diagonal elements have the form

$$E_{perturbation} = (3/2,1/2|g\beta H_z \cdot S_z + a S_z I_z|1/2,3/2) = 1/2 g\beta H_z + 3/4\, a$$

The selection rule for a transition from one state (energy) to another is $\Delta S_z = 1$ and $\Delta I_z = 0$. Therefore transitions will only occur between the $|1/2,3/2)$ state and the $|-1/2,3/2)$ state. The perturbation energy for the state $|-1/2,3/2)$ is $E_\rho' = -1/2 g\beta H_z - 3/4 a$. Thus a transition will occur when energy of the amount $\Delta E = E_\rho - E_\rho' = g\beta H_z + 3/2\, a$ is added to the system. For the state $|1/2,1/2)$ a transition to the $|-1/2,1/2)$ state gives $\Delta E = g\beta H_z + 1/2\, a$. Transitions between the remaining four states give $\Delta E = g\beta H_z - 1/2\, a$ and $\Delta E = g\beta H_z - 3/2\, a$. Four absorption curves are obtained, centered at $g\beta H_z$ and separated by a.

* The spin wave function notation follows that of Bleaney and Stevens (12). For $|1/2,1/2)$ the 1/2 on the left refers to S_z (an α spin state) and the 1/2 on the right gives I_z of the state under consideration. Further values of I_z are added on the right when multiple paramagnetic nuclei are present.

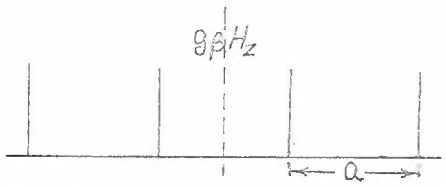

The wave functions and spin Hamiltonian used are those for a single unpaired electron interacting with a nucleus with I = 3/2. It is concluded that the four line spectrum of the pH 7 complex results from unpaired electron interaction with the Cu(II) nucleus.

The foregoing has assumed that, once the different energy levels and states belonging to these levels are established then transitions will occur between the levels. Actually, a further perturbation calculation must be made to determine which transitions will occur. The perturbation Hamiltonian is that due to the incident radiation (the microwave radiation). The calculation is made by first selecting a particular ground (low energy) state and then using the Hamiltonian of the perturbation to determine the wave function of the system after application of the perturbation (the microwave radiation) (38, 109) as in the discussion of perturbation theory. What is found is that the wave function, after application of the perturbation, is made up of not only the beginning ground state wave function but has higher energy states mixed in. This implies that there is a finite probability that some electrons are in the ground state and some are now in excited states as well; a transition between the ground and excited states has occurred. However, only certain high energy states are a part of this total wave function. For the situation under discussion the high energy states must be related to the low energy states by $Sz = 1$ and $\Delta\sum I_z = 0$. That is, the electron spin quantum number must change by one when a

transition occurs and the sum of the nuclear spin quantum numbers for the ground state must be the same as this sum for the high energy states. This is the origin of the selection rules used in this discussion.

D. Interpretation of Additional Hyperfine Structure

The proposed model shows Cu(II) binding by the terminal amino and peptide nitrogen atoms. The possibility of binding to the carbonyl oxygen exists (39). ^{14}N possesses a nuclear magnetic moment with I = 1; ^{16}O has a magnetic moment =0. Thus any unpaired electron interaction with a ^{14}N atom will result in a splitting of the ESR energy levels; unpaired electron interaction with a ^{16}O atom will not result in a splitting of the energy levels.

It is seen that the hyperfine splitting of the high field Cu(II) line consists of five hyperfine lines (Fig. 42). Considering only this high field Cu(II) line, using the assumption of "averaged out" anisotropies and zero values for off diagonal elements, and also assuming interaction with two paramagnetic nuclei an abbreviated spin Hamiltonian is obtained $\mathcal{H} = a S_z I_z + a' S_z I_z'$.

If it is assumed that the two paramagnetic nuclei are ^{14}N atoms then the spin wave functions are, for the lower energy levels $|\tfrac{1}{2},-1,-1\rangle$, $|\tfrac{1}{2},-1,0\rangle$, $|\tfrac{1}{2},0,-1\rangle$, $|\tfrac{1}{2},0,0\rangle$, $|\tfrac{1}{2},-1,1\rangle$, $|\tfrac{1}{2},1,-1\rangle$, $|\tfrac{1}{2},1,0\rangle$ $|\tfrac{1}{2},0,1\rangle$, $|\tfrac{1}{2},1,1\rangle$; the upper energy levels are given by replacing $S_z = \tfrac{1}{2}$ by $S_z = -\tfrac{1}{2}$. This will give, using the spin Hamiltonian given above, a five line hyperfine splitting if $a = a'$. The ESR spectrum of the pH 7 complex can thus be explained by assuming unpaired electron interaction with two ^{14}N nuclei. a =a' implies equal unpaired electron interaction with the two ^{14}N nuclei; this is to be considered further presently.

A further condition must be met; the intensity of the five lines must be in the ratio 1:2:3:2:1. This arises since the selection rule for the two nuclei is $\Delta(I_z+I_z') = 0$. For the central line this transition will involve the three low energy wave functions $|1/2, 0, 0\rangle$, $|1/2, 1, -1\rangle$, $|1/2, -1, 1\rangle$ and the three high energy wave functions $|-1/2, 0, 0\rangle$, $|-1/2, 1, -1\rangle$ $|-1/2, -1, 1\rangle$. These states are of equal energy and will be equally populated. The absorption line adjacent to the center line on the low field side is due to the transition between the states $|1/2, -1, 0\rangle$, $|1/2, 0, -1\rangle$ and the states $|-1/2, -1, 0\rangle$, $|-1/2, 0, -1\rangle$. These states and those giving rise to the central line are of unequal energy due to the difference in $\sum I_z$ for the two states. However, this difference is not large enough to produce a significantly unequal distribution of electrons in these states so that, as a first approximation, we consider all states to be equally populated. The outermost low field line is given by a transition between $|1/2, -1, -1\rangle$ and $|-1/2, -1, -1\rangle$. Thus, the ratio between the number of transitions occurring (the intensity of the signal) will be, low field to high, 1:2:3. Six further states exist which give the two high field lines and account for the intensity ratio 1:2:3:2:1. The overlapping of the hyperfine due to the copper nucleus and that due to the nitrogen nuclei has prevented an accurate determination of the intensities of the five lines.

The pH 10 complex also contains a five line hyperfine structure on the highfield Cu(II) line (Fig. 43). The alteration in the Cu(II) ESR spectrum will be considered later. As with the pH 7 complex, the hyperfine structure can be explained by unpaired electron interaction

with two ^{14}N nuclei. However, other interpretations may fit the data.

^{63}Cu and ^{65}Cu both give four line spectra since both have I = 3/2. However, in the spin Hamiltonian $\mathcal{H} = g\beta S_z H_z + aI_z S_z$, a(^{63}Cu) is < a(^{65}Cu) and the outermost line of ^{65}Cu will be displaced further from $g\beta H_z$ than will the outermost lines of ^{63}Cu. This will produce an overlapping of two spectra when the naturally occurring mixture of ^{63}Cu and ^{65}Cu is used and, as observed in the ESR spectra of the Cu(II) complexes of 1,10 phenanthroline and 2,2' dipyridine (2) can lead to anamalous nitrogen hyperfine structure. However, the use of ^{63}Cu only in the Cu(II)-GG pH 7 and pH 10 complexes gave no measurable alterations in the ESR spectra. The hyperfine structure is not, on this basis, anomalous.

Protons are the other nuclei present in the Cu(II)-GG system which possess a nuclear magnetic moment and could produce hyperfine structure. ESR spectra of the pD 7 and pD 10 complexes in D_2O were unaltered over those obtained using H_2O. This would rule out hyperfine structure due to protons in the hydration sphere of the Cu(II) and also to the protons attached to the terminal amino nitrogen atom, since these protons would be exchanged with deuterium in D_2O solution (55). Deuterium nuclei have a nuclear spin quantum number I = 1 compared to I = 1/2 for protons. These experiments do not, however, rule out the possibility of the unpaired electron wave function extending to the protons on the terminal amino nitrogen atom; if the unpaired electron does reside in an orbital that extends to the protons on the terminal amino nitrogen atom, the lack of observable proton splittings in the ESR spectra can be considered in terms of correlation times.*

* T. Shiga, Personal Communication, 1965.

If the rate of proton exchange between the solution and amino protons is rapid enough (if the correlation time for exchange is $< 1/\delta$, where δ is the splitting due to the proton(s)) then the unpaired electron will "see" an average I_z of the proton which will be zero, and which will not perturb the energy levels.

The deuterium experiments also do not rule out the possibility of splittings due to the protons attached to C atoms. However, covalent bonding with nitrogen atoms seems more likely so experiments were designed to test this hypothesis. ^{15}N has I=1/2 so that replacement of ^{14}N with ^{15}N atoms in glycylglycine will, if the postulate of nitrogen hyperfine structure is correct, alter the ESR spectra. As discussed earlier, in the approximation used, the hyperfine splittings are given by the Fermi contact term,

$$16\pi/3\, g\mu_0 \beta I_z S_z |\psi_i(0)|^2$$

The five line hyperfine could be explained in terms of the Hamiltonian

$$\mathcal{H} = a S_z I_z + a' S_z I_z'$$

if a' = a, which implies that

$$16\pi/3\, g\mu_0' \beta |\psi_i(0)|'^2 = 16\pi/3\, g\mu_0 \beta |\psi_i(0)|^2$$

or $$\mu_0' |\psi_i(0)|'^2 = \mu_0 |\psi_i(0)|^2 .$$

μ_0' (the nuclear magnetic moment) $= \mu_0$ since both nitrogen atoms are ^{14}N, so that

$$|\psi_i(0)|'^2 = |\psi_i(0)|^2$$

That is, the unpaired electron density at both nitrogen nuclei is the same. The Fermi contact term can also be written (46)

$$a = 16\pi/3\, \beta \left(\vec{\mu}/\vec{I}\right) |\psi(0)|^2 \quad , \quad \vec{\mu} = g\mu_0 \vec{I} ,$$

where $\vec{\mu}$ is the magnetic moment of the nucleus and $\vec{I}$ is the nuclear spin quantum number. Assuming $|\psi(0)|^2(^{14}N) = |\psi(0)|^2(^{15}N)$ (assuming the substitution of ^{15}N for ^{14}N does not effect the unpaired electron density at the ^{15}N nucleus) then

$$a(^{14}N)/a(^{15}N) = \left(\frac{\mu(^{14}N)}{I(^{14}N)}\right) \Big/ \left(\frac{\mu(^{15}N)}{I(^{15}N)}\right).$$

The nuclear magnetic moment of $^{14}N = 0.40357$ and of $^{15}N = 0.28304$. $I(^{15}N) = 1/2$ and $I(^{14}N) = 1$. From this $a(^{15}N) = 1.402\ a(^{14}N)$. The experimental value for the ratio $a(^{15}N)/a(^{14}N)$ is 1.398 (108). The ground state wave functions for two ^{15}N atoms are $|½, ½, ½\rangle$, $|½, -½, ½\rangle$, $|½, ½, -½\rangle$, $|½, -½, -½\rangle$. The two center functions are degenerate. The spin Hamiltonian is

$$\mathcal{H} = a I_z S_z + a' I_z' S_z .$$

Assuming that $a = a'$, application of the spin Hamiltonian to the spin wave functions gives eight energy levels, two of which are degenerate, leading to three absorption maxima. Curve A of Fig. 46 shows a three line absorption spectrum for the Cu(II)-u^{15}N glycylglycine pH 10 complex. Curve A, Fig. 45, which is the ESR spectrum of the pH 7 complex, also shows a three line hyperfine structure. Further, the separation of the five hyperfine lines for the Cu(II)-u^{14}N GG pH 7 and pH 10 complexes is 12.9 gauss. Since this separation is proportional to $a(^{14}N)$ then $a(^{15}N)$ should equal 1.4X 12.9 gauss = 18 gauss. The measured separation of the three line hyperfine is 17.6 gauss. Considering the inaccuracies inherent in estimating the miximum of a hyperfine line when several such lines are overlapping this is good agreement.

The use of ^{15}N-peptide, ^{14}N-terminal amino and ^{14}N-peptide, ^{15}N-

terminal amino glycylglycine to form the Cu(II) complex gives additional information about the origin of the hyperfine splittings. The Hamiltonian for these mixed ^{14}N-^{15}N peptides is

$$\mathcal{H} = a\, I_z(^{14}N) S_z + a' I_z(^{15}N) S_z$$

and assuming that the electron densities at the two nitrogen nuclei are the same, $a' = 1.4a$ so that

$$\mathcal{H} = 2.4a\, S_z (I_z(^{14}N) + I_z(^{15}N)) .$$

Using this spin Hamiltonian to determine the energies of the spin states (the spin states are non-degenerate) for the mixed ^{14}N-^{15}N glycylglycine-Cu(II) complexes and determining the allowed transitions between these states gives a six line hyperfine spectrum, all lines of equal intensity, with a spacing between lines of 13 gauss, 10 gauss, 16 gauss, 10 gauss, 13 gauss. Curve C, Fig. 46, is the ESR spectrum of the pH 10 complex of ^{14}N-terminal amino ^{15}N-peptide, glycylglycine-Cu(II). A four line hyperfine is seen with a spacing between lines of 14.8,13.4,14.8 gauss. If it is assumed that $a(^{15}N) = 1.16a(^{14}N)$ (ie. the electron density at the ^{15}N is slightly less than at the ^{14}N) then six hyperfine lines with a spacing 13, 2, 11, 2, 13 gauss results. The pH 7 Cu(II) complex of this peptide also has a four line hyperfine structure (curve C, Fig. 45).

The assumption of the equivalence of the nitrogen atoms implies that the ^{15}N-peptide, ^{14}N-terminal amino GG-Cu(II) complex would give the same hyperfine structure as the Cu(II) complexes of ^{14}N-peptide, ^{15}N-terminal amino glycylglycine since the spin Hamiltonian would be the same (in the approximation used here) as would the spin wave functions. The ESR spectrum of the pH 10 ^{15}N-terminal amino, ^{14}N-

peptide GG-Cu(II) complex shows a hyperfine structure consisting of three lines (curve B, Fig. 46); but the central line is asymmetric. At low modulation amplitudes (.16 gauss) there is an indication that the asymmetry in this central line is due to the presence of two overlapping lines which would then give a four line hyperfine structure. The pH7 Cu(II) complex of this peptide (curve B, Fig. 45) does show a four line hyperfine structure. However, the spectra for the ^{14}N-peptide, ^{15}N-terminal amino and ^{15}N-peptide, ^{14}N-terminal amino glycylglycine Cu(II) complexes are not identical.

Either the assumption that the unpaired electron density is the same at both nitrogen nuclei is incorrect or the errors due to the assumptions made to derive the simple spin Hamiltonians used here have finally become apparent. Since the assumption of equivalent nitrogens was consistent with the results obtained for the $u^{14}N$ and $u^{15}N$ glycylglycine-Cu(II) complexes the latter possibility will be considered.

Blumberg* gives the following spin Hamiltonian for the Cu(II)-GG ESR energy levels $g\beta \vec{H}\cdot\vec{S} + A\vec{I}(^{14}N)\cdot\vec{S} + A'\vec{I}(^{15}N)\cdot\vec{S} + g\vec{I}(^{14}N)\cdot\vec{H} + g'I(^{15}N)\cdot\vec{H} + J\vec{I}(^{14}N)\cdot\vec{I}(^{15}N)$.

The terms $\vec{I}.\vec{H}$ are those giving rise to nuclear magnetic resonance and, if the selection rule $\Delta\sum I_z = 0$ is applicable these terms will not alter the energy levels obtained with the simple spin Hamiltonians used. However, $\Delta\sum I_z = \pm 1$ transitions are observed (12) and will alter the spectra obtained with the simple spin Hamiltonian. The terms in $J\vec{I}\cdot\vec{I}$ will not alter the spectra obtained with the simple spin Hamiltonian if $\Delta\sum I_z = 0$ and if

* Blumberg, Personal Communication, 1965.

both nitrogen atoms are the same isotope of nitrogen. This term will give, for the states $|½,1,1\rangle$ and $|-½,1,1\rangle$, which are spin states for ^{14}N atoms, energies of $+J$ and $+J$ respectively. This gives, for the energy at which the transition occurs, $\Delta J = J - J = 0$ and will thus not alter the spectra over those obtained from the simple spin Hamiltonian. Since the selection rule is $\Delta \sum I_z = 0$, a transition can occur between the spin states $|½,1,-½\rangle$ and $|-½,½,0\rangle$; these are states associated with the mixed ^{14}N-^{15}N GG-Cu(II) complex. From the term $J\vec{I}\cdot\vec{I}$ perturbation energies of $-½J$ and 0 are obtained for the states $|½,1,-½\rangle$ and $|-½,½,0\rangle$. A transition between these states will then occur at an energy ΔE that differs by $-½J$ from the energy of the transition obtained with the simple spin Hamiltonian. Also, in the term $J\vec{I}\cdot\vec{I}$, $\vec{I}$ is equal to $I_x\vec{i} + I_y\vec{j} + I_z\vec{k}$. The diagonal elements which have been under consideration have the form $\langle 1,1,½|I_x+I_y+I_z|½,1,1\rangle$ and the terms $\langle 1,1,½|I_x|½,1,1\rangle$ and $\langle 1,1,½|I_y|½,1,1\rangle$ are zero. The off diagonal elements have the form $\langle 1,0,½|I_x+I_y+I_z|½,1,1\rangle$; the term $\langle 1,0,½|I_z|½,1,1\rangle$ is zero and the terms in I_x and I_y have been assumed to be zero. However, for an accurate analysis of the spectra these terms must be included.* The determination of the energy levels of the different spin states involves, using this spin Hamiltonian, the solution of twelve simultaneous equations with the energy of the various spin states as the unknowns. The solution has not yet been completed.

Thus, while the interpretation is not complete, the data presented here indicate that the hyperfine structure seen in the ESR spectra of the Cu(II)-GG complexes is due to the nitrogen atoms and that the un-

* W. Blumberg, Personal Communication, 1965

paired electron density at the nitrogen nuclei is the same for both nitrogen atoms. The presence of hyperfine structure at pH 7 for the Cu(II)-GG complex can also be interpreted in the same manner. The separation of the hyperfine lines alters very little (if at all) between pH 7 and pH 10 so it appears that the unpaired electron density at the nitrogen nuclei is essentially the same for the pH 7 and pH 10 complexes.

Evidence cited in the review section of this thesis indicates that the two nitrogen atoms in the Cu(II)-GG complexes (pH 7 and 10) are structurally inequivalent. Briefly, the peptide nitrogen atom is adjacent to a carbonyl carbon atom and IR indicates that it may form π bonds with the carbonyl carbon atom, the peptide nitrogen atom has ionized a proton and carries a (partial) negative charge, and the Cu-N (peptide) bond length is, from crystal structure analysis, less than the Cu-N (terminal amino) bond length. Yet, the ESR evidence is consistent with the assumption that the unpaired electron density at the nitrogen nuclei is the same for the peptide N atom as it is for the terminal amino N atom. This implies* that the covalent bonds between the Cu(II) and the nitrogen atoms are the same (52). The conclusion is that the observation of hyperfine which can be explained in terms of equivalent unpaired electron interaction with multiple nuclei does not imply that the atoms producing the hyperfine structure are structurally equivalent.

The calculation of the degree of covalency of the N-Cu bonds is dependent on many factors which have not been determined for the Cu(II)-GG complexes. However, Maki and McGarvey (67) calculated, from the

* Blumberg, Personal Communication, 1965

Fermi contact term, a value for α'^2 of 0.25 for the Cu(II)-bis-salicylaldehyde imine complex. This Cu(II) complex shows a nitrogen hyperfine splitting of 11.1 gauss. The Cu(II)-GG complexes show a splitting of 12.9 gauss so it is reasonable to assume that, for the Cu(II)-66 complexes, $\alpha'^2 \geq 0.25$. The electron can be said to spend 25% of its time in the region of the nitrogen nuclei.

3. Temperature Dependence of the ESR Spectrum of the pH 7 Cu(II)-GG Complex

The 10° C curve for the pH 7 complex (curve H, Fig. 44) resembles that discussed earlier in which the rate of rotation of the complex was such that the anisotropy in the low field lines was not averaged to zero (97). McConnell (79) has given a somewhat different interpretation. By a consideration of the anisotropic terms in the spin Hamiltonian he showed that the relaxation rate depends on I_z of the Cu(II) nucleus. He found, for a correlation time $\tau_c = 3X10^{-9}$ sec., for I_z =-3/2,-1/2,+1/2,+3/2, the values for the relaxation time T_2 = 0.9, 9.55, 0.4, $0.3X10^{-9}$. The line width of an absorption line is proportional to $1/T_2$. As the relaxation time decreases the absorption line is broadened. As the I = -3/2 line is the high field line, this interpretation is consistent with the experimental results.

Although the two interpretations given are somewhat different, the basis for each is the same; the rate of rotation is not sufficiently rapid to average the anisotropic components to zero when the asymmetric curves are obtained.

Rivkind (97) measured the ESR spectra of Cu(II)-ethylenediamine complexes at room temperature in solvents of varying viscosity. The

interpretation given above was applicable. As the solvent viscosity was increased the rate of rotation would be expected to decrease; it was found that the asymmetry of the curves became more pronounced as the rotational rate decreased (viscosity increased). Using glycerol water mixtures, the ESR spectrum of the pH 7 Cu(II)-GG complex also became more asymmetric as the viscosity of the solvent was increased. However, these experiments are somewhat ambiguous since glycerol is also a chelating agent of Cu(II) and in glycerol water solutions of the Cu(II)-GG complexes, glycerol-Cu(II) complexes will also exist.

An increase in the temperature would be expected to increase the rotational rate of the complex. Murphy and Martell measured the equilibrium constants for the reactions between Cu(II) and GG as a function of temperature. Their results are reproduced in Table 1. Over the temperature range 0^{o} C to 50^{o}C there is little variation in the equilibrium constants and thus it would be expected that the form of the complexes has also changed very little. The possibility exists that populating higher vibrational states produces the temperature variation seen in these curves. It would be expected that an increase in the size of the complex should alter the rotational rate of the complex without effecting the vibrational levels.

The peptide glycyltryptophane forms complexes with Cu(II) that are, potentiometrically, spectrophotometrically and on the basis of the hyperfine structure in the ESR spectra, identical with the Cu(II)-GG complexes. Fig. 44 is a comparison of the ESR spectra of the pH 7 glycyltryptophane and glycylglycine-Cu(II) complexes at several dif-

ferent temperatures. It appears that the ESR spectrum of the Cu(II)-glycyltryptophane complex is approximately 10°C "behind" that of the Cu(II)-GG complex. That is, the asymmetry of the Cu(II)-GG spectrum is the same at a temperature T as the Cu(II)-glycyltryptophane spectrum is at T-10°C. The low field line of the Cu(II)-glycyltryptophane complex at 0°C is broadened to the extent that it cannot be measured. These data are then consistent with the proposal that the asymmetric curves seen at low (10°C) temperatures and their conversion to symmetrical curves at higher (60°C) temperatures is due to the rotational rates of the complex ions.

From the spectra shown in Fig. 42, it can be seen that the five line hyperfine structure has a temperature dependence similar to that seen for the main four hyperfine lines. At 0°C the hyperfine lines are best resolved (narrowest) on the high field line. As the temperature is increased the hyperfine lines on the low field lines become somewhat apparent (narrow). However, as the temperature is further increased the high field lines begin to broaden until, at 60°C, no hyperfine structure due to the nitrogen atoms can be seen. Blumberg* has made the tentative proposal that this is due to a population of excited vibrational states at higher temperatures.

The ESR spectrum of the pH 10 Cu(II)-GG complex shows a similar temperature dependence. At high (60°C) temperatures a symmetrical absorption curve is obtained Fig. 43. However, at no temperature (0 to 60°C) is a four line hyperfine apparent. It is possible that at low temperatures the low field line is so broad that it is not apparent or

* W. Blumberg, Personal Communication, 1965.

that the two low field lines are broadened so that they appear as a single line. An interpretation of the lack of a four line hyperfine as is seen in the ESR spectrum of the pH 7 Cu(II)-GG complex has not been made. No conclusions regarding the presence of an OH^- in the coordination sphere of Cu(II) in the pH 10 Cu(II)-GG complex can be made from these data.

4. Other Cu(II)-Peptide Complexes

The Cu(II)-peptide complexes listed in the results which give ESR spectra identical to those shown by the Cu(II)-GG complexes can be assumed to form complexes identical to those discussed above. The differences which are seen in the spectra of these complexes can be attributed to the differing rates of rotation which would be expected as the dimensions of the side chains increase. The comparison of the Cu(II)-glycyltryptophane and Cu(II)-GG complexes illustrates these differences.

That the Cu(II)-leucyltyrosine and glycyltyptophane complexes are the same as the Cu(II)-GG complexes indicates that the terminal amino and peptide nitrogen atoms are stronger ligands towards Cu(II) than is the phenolic hydroxyl or the tryptophanyl residue. Dobbie and Kermack also found the lack of Cu(II) binding by the phenolic hydroxyl in the Cu(II)-glycyltyrosine complexes.

The Cu(II) complexes of the peptide di-glycylglycine and those resembling these complexes (listed in the results) have not been studied in detail. The four line hyperfine structure seen in the ESR spectra of these complexes (Fig. 48) can be attributed to the

unpaired electron interaction with the copper nucleus. It is found that the four line hyperfine is basically unchanged over the pH range 7 to 12. This is in contrast to the Cu(II)-GG complex in which a significant alteration in the four line hyperfine occurs between pH 7 and pH 10. The Cu(II) can fill four coordination positions by ligands supplied by the di-glycylglycine but can only fill three of these positions with ligands supplied by the glycylglycine molecule. The differences in the four line hyperfine structure in these complexes could then be due to the differences in the binding of the OH^- ions. The observation of Kober and Haw is applicable; the replacement of an oxygen ligand (the OH^-) in the Cu(II)-GG pH 10 complex by a nitrogen ligand in the Cu(II)-diglycylglycine pH 10 complex shifts the absorption towards shorter wave lengths (Fig.'s 15 and 16). That this shift must be determined on the basis of ligand field theory (covalent bonding) and not crystal field theory (electrostatic interactions) is shown by the presence of nitrogen hyperfine structure in the ESR spectra. The additional hyperfine structure seen on the high field lines of the ESR spectra of the Cu(II)-diglycylglycine complexes cannot be interpreted on the basis of unpaired electron interaction with three equivalent nitrogen atoms nor can it be interpreted on the basis of two equivalent and one inequivalent nitrogen atoms. A complete analysis of these spectra could best be made by utilizing the peptides synthesized with ^{15}N.

The Cu(II)-glycine, sarcosine, and glycylsarcosine complexes have ESR spectra showing the four line hyperfine structure (Fig. 49) which

can be attributed to unpaired electron interaction with the copper nucleus. At no point in the titration of these complexes is further hyperfine structure apparent. This could be due to the necessity for Cu(II) bonding by terminal amino and peptide nitrogen atoms for the Cu(II)-nitrogen atom bonds to be covalent. On this basis an isolated terminal amino group would not be expected to form covalent bonds with Cu(II). The ESR spectral equivalence of the glycine-Cu(II) and glycyl-sarcosyl-Cu(II) complexes confirms the potentiometric titration and optical spectral data. It appears that a proton on the peptide nitrogen atom is necessary for the formation of Cu(II)-nitrogen atom covalent bonds; the formation of five membered rings is a further requirement.

The Cu(II)-tri-glycylglycine complex has not been characterized in detail. As with the Cu(II)-di-glycylglycine complexes the four line hyperfine structure is apparent at all pH values above (Fig.50). The hyperfine structure on the high field copper lines is assumed to be due to nitrogen atoms but no analysis of this hyperfine structure has been made.

The sulfur containing peptides glycylethionine, alanylmethionine, and glycylmethionine form complexes which are identical to the Vu(II)-GG complexes indicating that the sulfur atoms are not involved in the binding of Cu(II). The slow change in the color of these solutions from blue to green is much the same as seen for Cu(II)-GG solutions when ascorbate is added, indicating that the Cu(II) may be reduced to Cu(I) in these solutions.

The ESR spectrum of the Cu(II)-cystinyl-bis-glycine complex indicates that, since the ESR spectra are alike (Fig. 51), this complex is similar to that of Cu(II)-GG. A five line hyperfine on the high field Cu(II) line is apparent in the spectrum.

While the ESR spectrum of the arginylalinine acetate-Cu(II) complex (Fig. 52) resembles that of the Cu(II)-GG spectrum there is further hyperfine structure present on the high field side of the spectrum indicating possible Cu(II) binding by the guanido group of arginine.

In titrating equimolar alanine amide-Cu(II), $Cu(OH)_2$ is formed at pH 6. Titration of a 2/1 ligand/Cu(II) mixture consumes four equivalents of NaOH/Cu(II) between pH 4 and 9 where the first inflection in the titration curve occurs. This is accompanied by the formation of a violet solution ($_{max}$=530). The consumption of NaOH is attributed to neutralization of protons from (30)

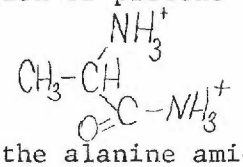

The ESR spectrum of the alanine amide Cu(II) 2/1 complex at pH 10 (Fig. 53) shows the typical four line hyperfine due to copper. The high field line is split by addition hyperfine lines. The splitting of these lines is of the order of 12.5 gauss so it seems attributable to nitrogen atoms. No assignment of specific interactions has yet been made to account for these hyperfine lines.

The ESR spectrum of the 2/1 Cu(II)-bisimidazole complex (Fig. 54) is the same over the pH range 5 to 10. This then confirms the interpretation given by Rising and Johnson (93) for the formation of the

biuret color with $Cu(OH)_2$ and acid imides without the further addition of base. Since the proton dissociation of the imidazole occurs at pH 6.5 the binding of Cu(II) would depress this dissociation below pH 5. Since further ionizations from the imidazoles would not be expected, and since the imidazoles fill the four Cu(II) coordination positions, the binding of a hydroxyl ion would not occur as it also does not for the diglycylglycine and triglycylglycine Cu(II) complexes. The ESR spectrum of the Cu(II) bisimidazole complex is identical with that of the Cu(II)-alanine amide complex. There are 7 hyperfine lines on the high field copper hyperfine line which indicates unpaired electron interaction with 3 equivalent nitrogen atoms. This does not seem likely if the structure for the complex is

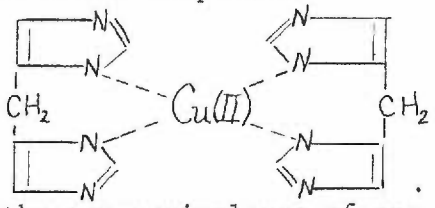

It is difficult to see the non-equivalence of one of the nitrogen atoms. The use of ^{15}N would possibly resolve this problem.

The ESR spectra of the Cu(II) complexes with glycylhistidine, histidylglycine, and histidylhistidine are all different on the basis of their ESR spectra (Fig.'s 55, 56, 57). The non-equivalence of the glycylglycine-and glycylhistidine-(or histidylglycine) Cu(II) ESR spectra would implicate the imidazole group in the binding of Cu(II). However, no conclusions as to the nature of the binding have yet been made. The reasons for the poor resolution seen in the ESR spectra of these complexes is not yet clear. Because of this poor resolution the number of hyperfine lines present has not been determined.

5. Pseudomonas Aeruginosa Blue Copper Protein

The interpretation of the ESR spectrum of the Pseudomonas aeruginosa blue copper protein was given in a preceding section. It was found that the signal is the same at -180°C as it is at 20°C. This is the expected result since the rate of rotation of the protein molecules is so low that there is no averaging of the anisotropies.

The ESR spectra of this copper protein at various pH values are shown in Fig. 58. While a rigorous interpretation requires a calculation of the curves, it can be seen that, as the pH is increased, the low field hyperfine lines narrow. That is, the g_{II} absorption as shown in Fig. 4 is narrowing since the low field hyperfine lines in the g_{II} region become better resolved. An alternative explanation is that the low field g_{II} hyperfine lines are becoming more intense. Whether this reflects a change in a ligand in the g_{II} (z-axis) direction or not cannot be determined from these data.

Any attempt to correlate these changes with a change in a ligand with a given pK can only succeed if the binding constant of the Cu(II) and the specific ligand is known. No conclusion about possible Cu(II) ligands in Pseudomonas aeruginosa blue copper protein can be drawn.

6. Preliminary Results

A complex formed between thiomalate ($COOHCH_2CH(SH)COOH$) and Cu(II) was first described by Klotz et al. (54). If a solution of thiomalate is titrated anaerobically with Cu(II), from 8/0 to 8/4 thiomalate/Cu(II) molar ratios, the addition of Cu(II) causes no detectable color changes (the solution remains colorless). Further addition

of Cu(II) (after the 8/4 ratio is reached) causes the formation of an intense absorption at 520 mu. The absorption reaches a maximum when the thiomalate/Cu(II) molar ratio is 8/5. Further addition of Cu(II) results in no increase in the absorption maximum. The extinction coefficient for the 520 mu absorption is 1200/MCu(II).

The reaction can be represented as

$$8RSH + 5\ Cu(II) \longrightarrow \text{colored complex}$$

Klotz et al. obtained polarographic evidence for the reduction of Cu(II) to Cu(I). They proposed the following reactions for the formation of the colored complex.

$$2RSH + Cu(II) \longrightarrow R\text{-}S\text{-}Cu(I) + 1/2\,R\text{-}S\text{-}S\text{-}R$$

which gave, in solution, for the 8/4 ratio,

$$4R\text{-}S\text{-}Cu(I) + 2R\text{-}S\text{-}S\text{-}R$$

This solution is colorless. The addition of Cu(II) to make the ratio 5/8 gives the complex,

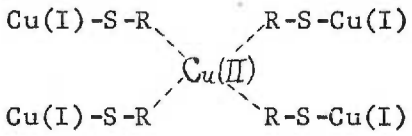

No spatial arrangement of atoms should be assumed. Only the stoichiometry is represented by the above "structure".

Fig. 59 shows the ESR spectra of solutions containing different thiomalate/Cu(II) ratios. At thiomalate/Cu(II) $\geq$ 8/4 no ESR spectrum is observed, both at -180°C and 20°C. This is consistent with the above reactions since Cu(I) is diamagnetic. At a ratio of 8/5 there is no ESR spectrum observed. For ratios $<$ 8/5 a Cu(II) ESR signal is observed, and the signal is identical with that seen for $CuCl_2$ (Fig.40). The 8/5 mixture, which forms the intensely colored solution, does not

possess an ESR spectrum. Hemmerich (45) attributes this lack of signal to a highly delocalized unpaired electron; the unpaired electron has a finite density at all 5 Cu nuclei. No definite mechanism has been given to explain how this would lead to a loss of the ESR signal. Since the electron is assumed to be unpaired the mechanism would seem to be one of line broadening.

Addition of PCMB or PCMS to a 8/5 thiomalate/Cu(II) solution, added stoichiometrically with the (presumably) four remaining thiogroups, abolished the 520 mu absorption in direct proportion to the added PCMB or PCMS. At no point during addition of sulfhydryl reagents could an ESR signal be detected. Aeration of the solutions produced no ESR signal. No interpretation of these results can be given at this time.

The abolishment of the ESR signal in the pH 10 Cu(II)-GG complex by H_2O_2 or ascorbate indicates that investigations of possible structure function correlations might be made in this way. The results are preliminary and no conclusions can be made at this time.

V CONCLUSION

Two ESR detectable forms of Cu(II)-glycylglycine complexes exist in solutions containing 1:1 to 1:4 molar ratios of Cu(II) to glycylglycine; one at pH 7 and another at pH 10. The complexes are 1:1 under these conditions. The structure of the complexes is altered over the structure that exists in aqueous solution when the solutions are frozen at -180°C.

The Cu(II) is bound through the terminal amino and peptide nitrogen atoms of the glycylglycine molecule. The ESR results can be interpreted by assuming that the Cu-N(peptide) and Cu-N(terminal amino) bonds are covalent and are equivalent. The equivalence of N-Cu bonds does not imply that the nitrogen atoms of these bonds are structurally equivalent.

The terminal amino and peptide nitrogen atoms are stronger ligands towards Cu(II) than the phenolic hydroxyl and tryptophanyl groups. The terminal amino and peptide nitrogen atoms must be capable of forming five-membered chelate rings for the formation of covalent N-Cu(II) bonds.

Cu(II) is bound to additional nitrogen atoms in the Cu(II)-diglycylglycine and triglycylglycine complexes but the Cu(II)-N bonds are inequivalent.

One or more of the Cu(II) ligands in the Pseudomonas aeruginosa blue copper protein is influenced by the hydrogen ion concentration. No definite assignment of possible ligands can be made at this time.

ACKNOWLEDGMENTS

I am very appreciative of the stimulation and insight provided by Dr. T. Shiga and I thank him for it. The gift of a sample of ^{15}N glycylglcycine from Dr. H. D. Hoberman is gratefully acknowledged. I also thank Dr. M. Cronyn for his advice during the glycylglcycine synthesis. Dr. B. Littman provided needed assistance in obtaining the ORD results. Assistance with the ESR theory given by Dr. B. Allen, Dr. T. Vanngard, and Dr. W. E. Blumberg was indespensible and is gratefully acknowledged.

The help of Dr. S. Duke of Durrum Instrument Company in obtaining the ORD curves is appreciated.

For the typing of the manuscript I thank my mother-in-law, Mrs. Agnes Barkdoll. Her assistance is fully appreciated.

APPENDIX I

CHEMICAL ANALYSIS OF THE PRECIPITATED SALTS OF Cu(II) AND AMINO ACIDS, PEPTIDES, AND PEPTONES

According to Kober and Sugiura (57)

Monobasic Amino Acids

Substance.		Weight of sample.	CuO in filtrate.	CuO in ppt.	Theoretical weight CuO calc. for this sample.	Per cent total CuO to theory.
		gm.	gm.	gm.	gm.	
Glycin	a	0.1015	0.0000	0.0563	0.0538	99.6
Glycin	a	0.1013	0.0000	0.0563	0.0537	99.3
Alanin	a	0.1008	0.0000	0.0454	0.0451	100.7
Alanin	a	0.1019	0.0000	0.0453	0.0455	99.6
Aminobutyric acid	a	0.1019	0.0005	0.0344	0.0394	87.3
Active valin	a	0.0944	0.0015	0.0301	0.0321	93.8
Isoleucin	a	0.1014	0.0011	0.0307	0.0308	103.2
Active prolin	a	0.1018	0.0078	0.0269	0.0352	98.6
Aminobutyric acid	b	0.1022	0.0004	0.0403	0.0395	102.0
Aminobutyric acid	b	0.1007	0.0007	0.0405	0.0383	104.4
Tyrosin [1]	b	0.1027	0.0007	0.0263	0.0226	116.4
Tyrosin	b	0.1011	0.0007	0.0269	0.0222	121.2
Tryptophan [2]	b	0.1022	0.0000	0.0183	0.0199	92.0
Tryptophan [2]	b	0.1017	0.0000	0.0183	0.0198	92.4
Tryptophan	b	0.0999	0.0000	0.0177	0.0195	90.8
Asparagin	b	0.1003	0.0005	0.0304	0.0302	100.7
Asparagin	b	0.1005	0.0006	0.0310	0.0303	102.3
Asparagin	b	0.1005	0.0005	0.0308	0.0303	101.7
Phenylalanin	b	0.1012	0.0000	0.0247	0.0244	101.2
Phenylalanin	b	0.1001	0.0000	0.0244	0.0242	100.8
Normal amino caproic acid	c	0.1006	0.0009	0.0297	0.0306	100.0
Normal amino caproic acid	c	0.1003	0.0003	0.0315	0.0305	105.7
Phenylglycin	c	0.1011	0.0000	0.0280	0.0266	105.3
Leucin	c	0.1003	0.0051	0.0246	0.0305	97.4
Leucin	c	0.1010	0.0054	0.0261	0.0307	102.6
Sarcosin hydrochloride [3]	n	0.1002	0.0021	0.0299	0.0315	101.6
Sarcosin hydrochloride	b	0.1017	0.0030	0.0308	0.0320	105.6
Arginin di-nitrate	a	0.1010	0.0011	0.0121	0.0134	98.5
Arginin di-nitrate	b	0.1006	0.0008	0.0139	0.0133	110.5
Arginin di-nitrate	a	0.1008	0.0011	0.0113	0.0134	92.5
Arginin di-nitrate	a	0.1022	0.0011	0.0134	0.0136	106.6
Histidin di-hydrochloride [4]	a	0.1000	0.0161	0.0005	0.0175	94.9
Histidin di-hydrochloride	b	0.1001	0.0173	0.0011	0.0175	105.1
Histidin di-hydrochloride	a	0.1014	0.0167	0.0005	0.0177	97.2
Lysin picrate	a	0.1006	0.0006	0.0097	0.0107	96.3
Lysin picrate	a	0.1011	0.0008	0.0109	0.0107	109.3

[1] The tyrosin copper solution has a greenish "complex" color.

[2] If more than 0.1 gm. tryptophan is used, method (c) must be added to this technique.

[3] All acid salts, such as hydrochlorides, nitrates, etc., are neutralized with N/10 alkali, using phenolphthalein as an indicator, before being treated with copper hydroxide as in method (a).

[4] Histidin forms a complex salt, as do the other monobasic amino acids, and on treatment with excess alkali, changes its color but little. Only on boiling the color changes towards a biuret. It is not a clear color, but smoky, and makes the solution look very dark. Characteristic is the deep red color to which the alkaline solution turns on the addition of acid. We expect to make this a basis for the colorimetric quantitative and qualitative estimation of histidin.

Dibasic Amino Acids

Substance.	Method of preparation.	Weight of sample.	CuO in filtrate	CuO in ppt.	Theoretical wt. CuO calc. for this sample.	Per cent total CuO to theory.
		gm.	gm.	gm.	gm.	
Cystin	c	0.1013	0.0000	0.0320	0.0332	96.4
Cystin	c	0.1000	0.0000	0.0324	0.0331	97.9
Cystin	c	0.1008	0.0000	0.0331	0.0334	99.1
Aspartic acid [1]	a	0.1022	0.0007	0.0575	0.0611	95.3
Aspartic acid	a	0.0997	0.0009	0.0579	0.0596	98.6
Glutaminic acid [1]	a	0.01002	0.0005	0.0500	0.0542	93.5
Glutaminic acid	a	0.01025	0.0004	0.0518	0.0554	94.9

[1] Before boiling, the copper salts are diluted to 150 c.c. with water.

Di-Peptides

Specimen.	Substance.	Weight of sample.	CuO in filtrate after adding 3 c.c. N NaOH (CO_2 free) and boiling.	CuO in ppt. after adding 3 c.c. N NaOH (CO_2 free) and boiling.	Total CuO.	Theoretical weight CuO calculated for this sample.	Per cent total CuO found to theory.
		gm.	gm.	gm.	gm.	gm.	
A	Glycyl-l-tyrosin	0.1015	0.0167	0.0073	0.0240	0.0340	70.6
B	Glycyl-l-tyrosin	0.1023	0.0267	0.0042	0.0309	0.0342	90.4
C	Glycyl-l-tyrosin	0.1017	0.0271	0.0016	0.0287	0.0340	84.4
D	Glycyl-l-tyrosin	0.1011	0.0268	0.0021	0.0289	0.0338	85.8
E	Glycyl-tyrosin	0.0545	0.0142	0.0043	0.0185	0.0181	102.2
A	D-leucyl-l-leucin	0.1011	0.0268	0.0003	0.0271	0.0330	82.1
B	D-leucyl-d-leucin	0.1007	0.0294	0.0013	0.0307	0.0328	93.6
C	L-leucyl-d-leucin	0.1016	0.0250	0.0004	0.0254	0.0331	76.7
D	D-leucyl-d-leucin	0.1010	0.0268	0.0037	0.0305	0.0329	92.7
E	R-leucyl-leucin	0.1006	0.0288	0.0014	0.0302	0.0328	92.1
F	L-leucyl-d-leucin	0.1004	0.0266	0.0021	0.0287	0.0327	87.8
A	L-alanyl-d-alanin [1]	0.1014	0.0320	0.0120	0.0440	0.0503	87.5
B	L-alanyl-d-alanin [1]	0.1010	0.0250	0.0217	0.0467	0.0502	93.0
C	D-alanyl-d-alanin	0.1016	0.0454	0.0035	0.0489	0.0454	107.7
D	D-alanyl-d-alanin	0.1018	0.0473	0.0048	0.0521	0.0506	103.0
E	D-alanyl-d-alanin	0.1001	0.0465	0.0041	0.0506	0.0497	101.8
F	D-alanyl-d-alanin [1]	0.1006	0.0282	0.0202	0.0484	0.0500	96.8
A	R-valyl-glycin	0.1005	0.0410	0.0059	0.0469	0.0459	102.2
B	R-valyl-glycin	0.1003	0.0085	0.0008	0.0093	0.0458	20.3
C	R-valyl-glycin	0.1003	0.0212	0.0018	0.0230	0.0458	50.2
D	R-valyl-g ycin	0.1001	0.0395	0.0052	0.0447	0.0457	97.8
E	R-valyl-glycin	0.1002	0.0047	0.0004	0.0051	0.0458	11.1
F	R-valyl-glycin	0.0521	0.0093	0.0016	0.0109	0.0238	45.8
A	Glycyl-valin (crude)	0.1012	0.0384	0.0052	0.0436	0.0462	94.4
B	R-glycyl-valin	0.1012	0.0400	0.0062	0.0462	0.0462	100.0
C	R-glycyl-valin	0.1020	0.0422	0.0006	0.0428	0.0466	91.8
D	Glycyl-d-valin	0.1015	0.0390	0.0059	0.0449	0.0464	96.8
E	Glycyl-d-l-valin	0.0654	0.0271	0.0011	0.0282	0.0299	94.3
A	R-glycyl-aminobutyric acid [1]	0.1022	0.0244	0.0263	0.0507	0.0508	99.8
B	R-glycyl-aminobutyric acid	0.1007	0.0437	0.0030	0.0467	0.0500	93.4
A	Amino-normal-caproic-glycin	0.0664	0.0257	0.0015	0.0272	0.0281	96.8
A	R-leucyl-glycin	0.0901	0.0344	0.0041	0.0385	0.0381	101.0
B	R-leucyl-glycin	0.1003	0.0398	0.0037	0.0435	0.0425	102.4
C	R-leucyl-glycin	0.1010	0.0398	0.0045	0.0443	0.0427	103.7
D	R-leucyl-glycin	0.1004	0.0378	0.0044	0.0422	0.0425	99.3
E	R-leucyl-glycin	0.1013	0.0397	0.0047	0.0444	0.0428	103.7
F	R-leucyl-glycin	0.1013	0.0381	0.0047	0.0428	0.0428	100.0

[1] This substance, judging from the heavy precipitate of CuO formed on adding alkali, is very impure; it is probably a mixture containing amino acids.

DI-PEPTIDES, *Continued*

Specimen.	Substance.	Weight of sample.	CuO in filtrate after adding 3 c.c. N NaOH (CO_2 free) and boiling.	CuO in ppt. after adding 3 c.c. N NaOH (CO_2 free) and boiling.	Total CuO.	Theoretical weight CuO calculated for this sample.	Per cent total CuO found to theory.
		gm.	gm.	gm.	gm.	gm.	
	Leucyl-aspartic acid [1]	0.1015	0.0175	0.0106	0.0281	0.0328	85.7
A	Glycyl-tryptophan	0.1016	0.0257	0.0010	0.0267	0.0310	86.1
A	Glycyl-d-alanin	0.1011	0.0524	0.0006	0.0530	0.0550	96.5
B	Glycyl-d-l-alanin	0.1006	0.0501	0.0049	0.0550	0.0548	100.4
C	Glycyl-d-alanin	0.1013	0.0494	0.0043	0.0537	0.0551	97.5
A	L-alanyl-glycin	0.1005	0.0496	0.0054	0.0550	0.0547	100.5
B	R-alanyl-glycin	0.1007	0.0516	0.0032	0.0548	0.0548	100.0
C	D-l-alanyl-glycin	0.0559	0.0285	0.0009	0.0294	0.0304	96.7
D	R-alanyl-glycin	0.1009	0.0512	0.0014	0.0526	0.0549	95.8
E	L-alanyl-glycin	0.1013	0.0492	0.0055	0.0547	0.0552	99.1
A	Glycyl-l-leucin	0.1006	0.0370	0.0036	0.0406	0.0425	95.5
B	Glycyl-d-l-leucin	0.0909	0.0357	0.0013	0.0370	0.0384	94.0
B	Glycyl-d-l-leucin	0.0720	0.0280	0.0010	0.0290	0.0305	95.1
C	Glycyl-leucin	0.1005	0.0380	0.0022	0.0402	0.0425	94.6
A	Glycyl-amino-normal-caproic	0.1004	0.0391	0.0026	0.0417	0.0425	98.1
B	Glycyl-amino-normal-caproic	0.1013	0.0368	0.0049	0.0417	0.0428	97.4
C	Glycyl-amino-normal-caproic	0.0963	0.0377	0.0014	0.0391	0.0407	96.1
A	Glycyl-asparagin	0.1028	0.0397	0.0031	0.0428	0.0433	98.8
A	Glycyl-asparagin	0.1009	0.0379	0.0024	0.0403	0.0425	94.8
A	Alanyl-asparagin [1]	0.0750	0.0026	0.0201	0.0227	0.0294	77.2
A	Alanyl-asparagin [1]	0.0551	0.0019	0.0144	0.0163	0.0215	75.5
A	Leucyl-asparagin	0.1016	0.0209	0.0006	0.0215	0.0330	65.2
A	Leucyl-asparagin	0.1004	0.0205	0.0010	0.0215	0.0326	66.0
A	Leucyl-asparagin	0.1013	0.0205	0.0009	0.0214	0.0329	65.0
A	Glycyl-phenylglycin	0.1021	0.0355	0.0030	0.0385	0.0390	98.7
B	Glycyl-d-phenylglycin	0.1022	0.0358	0.0010	0.0368	0.0391	94.1
A	Aminobutyl-glycin	0.1010	0.0467	0.0045	0.0512	0.0502	102.0
B	Aminobutyl-glycin	0.1005	0.0435	0.0059	0.0494	0.0499	99.0
A	Glycyl-glycin	0.1007	0.0519	0.0069	0.0588	0.0607	96.9
B	Glycyl-glycin	0.0123	0.0536	0.0070	0.0606	0.0616	98.4

[1] This substance, judging from the heavy precipitate of CuO formed on adding alkali, is very impure; it is probably a mixture containing amino acids.

TRI-PEPTIDES

Specimen.	Substance.	Weight of sample.	CuO in filtrate.	CuO in ppt.	Total CuO.	Theoretical weight CuO, calc. for this sample.	Per cent CuO in filtrate to theory.	Per cent total CuO to theory.
		gm.	gm.	gm.	gm.	gm.		
A	Glycyl-glycyl-alanin [1]	0.1008	0.0367	0.0163	0.0530	0.0395	92.9	134.2
B	Glycyl-glycyl-alanin	0.1021	0.0356	0.0064	0.0420	0.0400	89.0	105.0
A	Glycyl-glycyl-amino-butyric	0.1011	0.0382	0.0006	0.0388	0.0371	103.0	104.6
B	Glycyl-glycyl-amino-butyric	0.0820	0.0286	0.0012	0.0298	0.0333	85.9	89.5
A	R-glycyl-alanyl-glycin [1]	0.1013	0.0376	0.0207	0.0583	0.0397	94.7	146.9
B	R-glycyl-alanyl-glycin [1]	0.1016	0.0381	0.0211	0.0592	0.0398	95.7	148.8
C	Glycyl-d-alanyl-glycin	0.0323	0.0113	0.0009	0.0122	0.0127	89.0	96.1
A	Glycyl-amino-butyl-glycin [1]	0.1007	0.0350	0.0229	0.0579	0.0369	94.8	156.9
B	Glycyl-amino-butyl-glycin [1]	0.1016	0.0357	0.0197	0.0554	0.0372	96.0	148.9
C	R-glycyl-amino-butyl-glycin [1]	0.1003	0.0347	0.0209	0.0556	0.0368	94.3	151.1
A	Glycyl-valyl-glycin	0.0519	0.0047	0.0026	0.0073	0.0179	26.3	40.8
B	Glycyl-valyl-glycin	0.0639	0.0077	0.0032	0.0109	0.0220	35.0	49.5
C	Glycyl-valyl-glycin	0.0509	0.0046	0.0026	0.0072	0.0175	26.3	41.1
A	Gylcyl-leucyl-glycin	0.1013	0.0293	0.0004	0.0297	0.0329	88.5	90.3
A	Glycyl-leucyl-glycin	0.1010	0.0282	0.0002	0.0284	0.0328	86.0	86.6
A	Glycyl-leucyl-glycin	0.1005	0.0277	0.0002	0.0279	0.0326	85.0	85.6
B	Glycyl-leucyl-glycin	0.1003	0.0306	0.0052	0.0358	0.0327	93.6	109.5
A	Glycyl-glycyl-l-leucin	0.1020	0.0287	0.0024	0.0311	0.0331	86.7	94.0
B	Glycyl-glycyl-leucin	0.1010	0.0279	0.0044	0.0323	0.0328	86.4	98.5
A	L-leucyl-glycyl-glycin	0.1011	0.0284	0.0043	0.0327	0.0328	86.6	99.7
B	Leucyl-glycyl-glycin	0.1013	0.0283	0.0057	0.0340	0.0329	86.1	103.3
C	R-leucyl-glycyl-glycin	0.1007	0.0173	0.0019	0.0192	0.0327	52.9	58.7
A	Leucyl-alanyl-alanin	0.1017	0.0272	0.0050	0.0322	0.0296	91.9	108.8
B	L-leucyl-d-alanyl-d-alanin	0.1014	0.0262	0.0033	0.0295	0.0295	88.8	100.0
A	Glycyl-glycyl-valin	0.0757	0.0225	0.0020	0.0245	0.0261	86.2	93.9
B	Glycyl-glycyl-valin	0.1013	0.0284	0.0023	0.0307	0.0349	80.8	88.0
C	Glycyl-glycyl-valin	0.1007	0.0291	0.0037	0.0328	0.0347	83.9	94.5
D	Glycyl-glycyl-valin	0.0516	0.0155	0.0005	0.0160	0.0178	87.1	89.9
A	R-alanyl-glycyl-glycin [1]	0.1012	0.0370	0.0165	0.0535	0.0396	93.4	135.1
B	Alanyl-glycyl-glycin	0.0987	0.0254	0.0031	0.0285	0.0387	65.6	73.6
C	D-alanyl-glycyl-glycin	0.0492	0.0168	0.0014	0.0182	0.0193	87.0	94.3
A	Alanyl-leucyl-glycin	0.1012	0.0274	0.0037	0.0311	0.0311	88.1	100.0
A	Glycyl-glycyl-glycin	0.1000	0.0378	0.0010	0.0388	0.0421	89.8	92.2
A	Glycyl-glycyl-glycin	0.1003	0.0370	0.0006	0.0376	0.0422	87.7	98.0
A	Glycyl-glycyl-glycin [1]	0.1016	0.0409	0.0000	0.0409	0.0427	95.8	95.8
A	Glycyl-glycyl-glycin [1]	0.1020	0.0405	0.0000	0.0405	0.0429	94.4	94.4
A	L-leucyl-glycyl-d-alanin	0.0569	0.0161	0.0008	0.0169	0.0175	92.0	96.6
A	Leucyl-alanyl-glycin	0.1002	0.0289	0.0040	0.0329	0.0308	93.8	106.8
A	Amino-butyl-glycyl-glycin	0.1011	0.0350	0.0028	0.0378	0.0371	94.3	101.9
A	Valyl-glycyl-glycin	0.1023	0.0288	0.0027	0.0315	0.0352	81.8	89.5
A	Amino-normal-capronyl-glycyl-glycin	0.1003	0.0304	0.0035	0.0339	0.0325	93.5	104.3
A	Glycyl-d-alanyl-d-alanin	0.0536	0.0144	0.0001	0.0145	0.0192	75.0	75.5
A	Glycyl-d-alanyl-d-alanin	0.0507	0.0139	0.0001	0.0140	0.0186	74.7	75.3

[1] The copper salt in this case was formed in cold alkaline solution.

TETRA-PEPTIDES

Specimen.	Substance.	Weight of sample.	CuO in filtrate.	CuO in ppt.	Total CuO.	Theoretical weight CuO, calc. for this sample.	Per cent CuO in filtrate to theory.	Per cent total CuO to theory.
		gm.	gm.	gm.	gm.	gm.		
A	Normal-amino-caproic-di-glycyl-glycin [1]	0.1017	0.0202	0.0005	0.0207	0.0268	75.4	77.2
A	Normal-amino-caproic-di-glycyl-glycin	0.1006	0.0174	0.0004	0.0178	0.0265	65.7	67.2
A	R-aminobutyl-di-glycyl-glycin [1]	0.1050	0.0260	0.0037	0.0297	0.0305	85.2	94.1
A	R-aminobutyl-di-glycyl-glycin .	0.1006	0.0241	0.0022	0.0263	0.0292	82.5	90.1
A	R-alanyl-di-glycyl-glycin [1] . .	0.1012	0.0270	0.0040	0.0310	0.0309	87.4	100.3
A	R-alanyl-di-glycyl-glycin . . .	0.1008	0.0267	0.0017	0.0284	0.0308	86.7	92.2
A	Leucyl-di-glycyl-glycin [1] . . .	0.1008	0.0239	0.0030	0.0269	0.0265	90.2	101.5
A	Leucyl-di-glycyl-glycin	0.1015	0.0234	0.0024	0.0258	0.0267	87.6	96.6

[1] Filtered without boiling to decompose carbamino salts.

PEPTONES, ETC.

Substance.	Weight of sample.	CuO in filtrate.	CuO in ppt.	Molecular weight,[1] calc. from total CuO.
	gm.	gm.	gm.	
"Witte's" peptone . . .	0.1025	0.0041	0.0000	1990
"Witte's" peptone . . .	0.1046	0.0042	0.0000	1982
"Witte's" peptone . . .	0.1014	0.0039	0.0000	2070
"Roche" peptone	0.1110	0.0302	0.0173	186
"Merck" peptone	0.1020	0.0044	0.0002	1765
Meat peptone	0.1067	0.0000	0.0000	. . .
"Ereptone"	0.1005	0.0064	0.0133	406

[1] This calculation is based on the assumption that one molecule of peptone, as in the case of the peptides, combined with only one molecule of copper hydroxide.

APPENDIX II

OPTICAL SPECTRA OF Cu(II) AMINO ACID, PEPTIDE, AND PROTEIN COMPLEXES

According to Kober and Haw (58)

Copper ammonium complex. (0.063 g. CuO in 100 cc.)

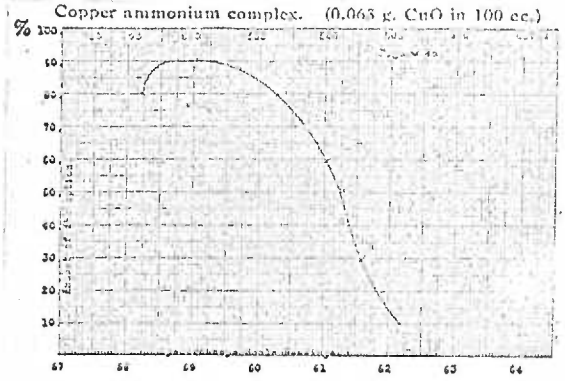

Amino acid copper complexes.

1. Histidin di-HCl (0.0637 g. CuO in 100 cc.)
2. Glutamic acid (0.0633 " " " " ")
3. Aspartic acid (0.0617 " " " " ")
4. Alanin (0.0635 " " " " ")
5. Glycin (0.0638 " " " " ")

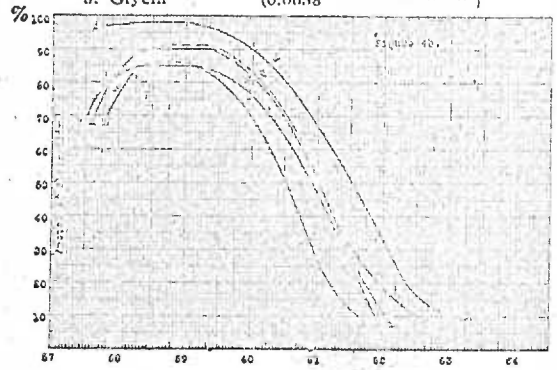

Dipeptide copper complexes.

1. Glycyl-tryptophane (0.0637 g. CuO in 100 cc.)
2. Glycyl-leucin (0.0640 " " " " ")
3. Amino-butyl-glycin (0.0636 " " " " ")
4. Alanyl-glycin (0.0635 " " " " ")

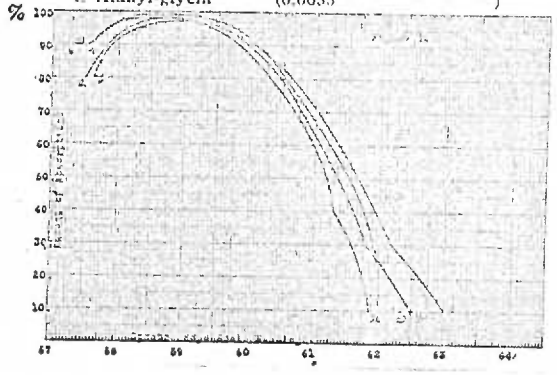

(1) *Tripeptide complexes.*

Alanyl-glycyl-glycin copper (neutral solution; 0.0640 g. CuO in 100 cc.)

Alanyl-glycyl-glycin copper (buffer solution; 0.0316 g. CuO in 100 cc.)

Alanyl-glycyl-glycin copper (alkaline solution; 0.0316 g. CuO in 100 cc.)

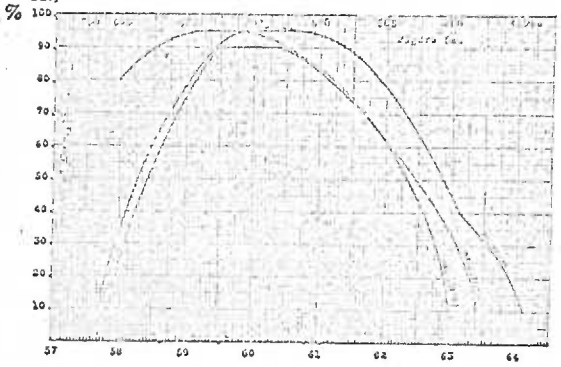

Di-glycyl-glycin copper (neutral solution; 0.0527 g. CuO in 100 cc.)
" " " (buffer solution; 0.0319 " " " " ")
" " " (alkaline solution; 0·0319 " " " " ")

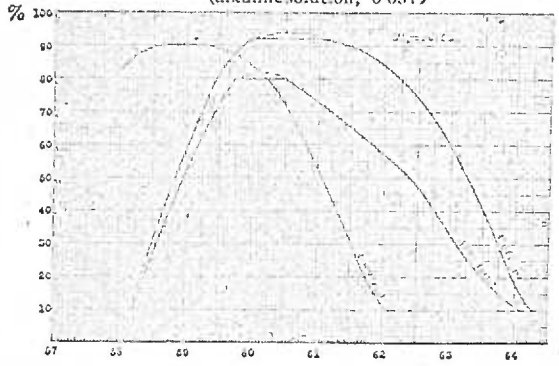

(2) *Tetrapeptide complexes.*

N-amino-caproyl-di-glycyl-glycin copper (neutral solution; 0.0629 g. CuO in 100 cc.)

N-amino-caproyl-di-glycyl-glycin copper (buffer solution; 0.0311 g. CuO in 100 cc.)

N-amino-caproyl-di-glycyl-glycin copper (alkaline solution; 0.0310 g. CuO in 100 cc.)

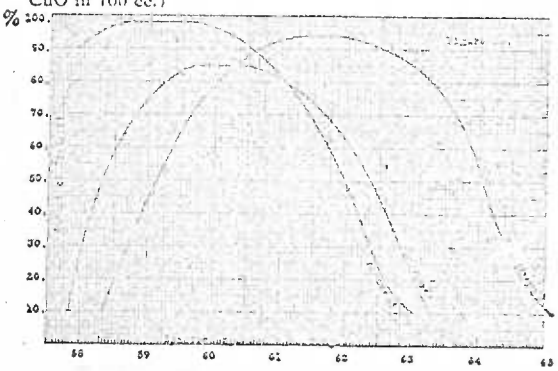

(2) *Tetrapeptide complexes.*

Alanyl-di-glycyl-glycin copper (neutral solution; 0.0630 g. CuO in 100 cc.)

Alanyl-di-glycyl-glycin copper (buffer solution; 0.0316 g. CuO in 100 cc.)

Alanyl-di-glycyl-glycin copper (alkaline solution; 0.0317 g. CuO in 100 cc.)

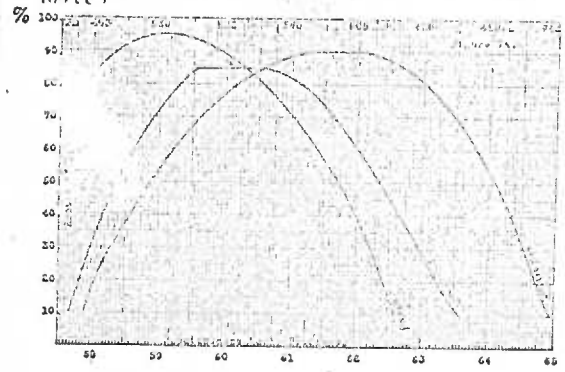

Egg albumin copper (alkaline solution; 0.0160 g. CuO in 100 cc.)

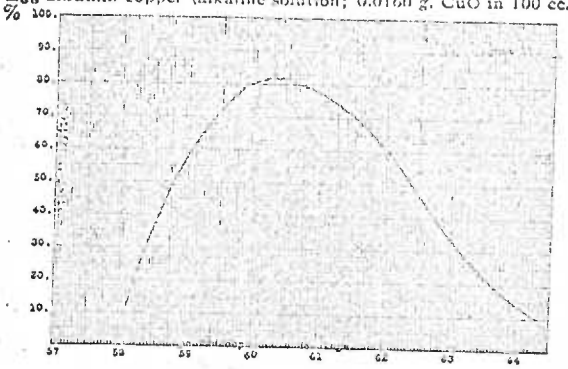

Edestin copper (alkaline solution; 0.0162 g. CuO in 100 cc.)

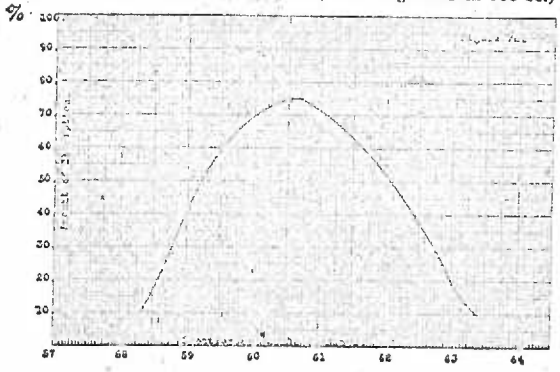

(1) *Tripeptide complexes.*

Amino-butyl-glycyl-glycin copper (neutral solution; 0.0633 g. CuO in 100 cc.)

Amino-butyl-glycyl-glycin copper (buffer solution; 0.0317 g. CuO in 100 cc.)

Amino-butyl-glycyl-glycin copper (alkaline solution; 0.0317 g. CuO in 100 cc.)

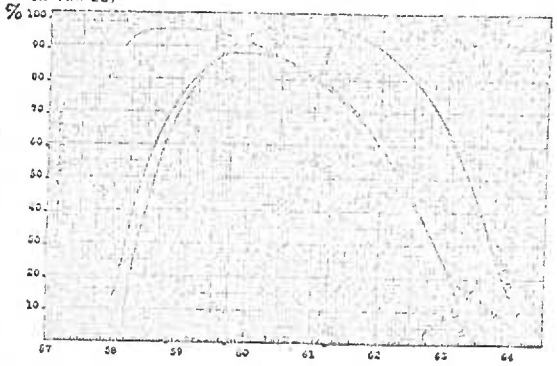

Leucyl-alanyl-glycin copper (neutral solution; 0.0639 g. CuO in 100 cc.)

Leucyl-alanyl-glycin copper (buffer solution; 0.0311 g. CuO in 100 cc.)

Leucyl-alanyl-glycin copper (alkaline solution; 0.0318 g. CuO in 100 cc.)

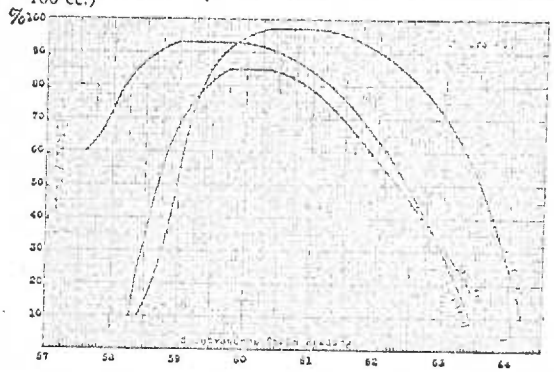

(2) *Tetrapeptide complexes.*

Amino-butyl-di-glycyl-glycin copper (neutral solution; 0.0634 g. CuO in 100 cc.)

Amino-butyl-di-glycyl-glycin copper (buffer solution; 0.0318 g. CuO in 100 cc.)

Amino-butyl-di-glycyl-glycin copper (alkaline solution; 0.0319 g. CuO in 100 cc.)

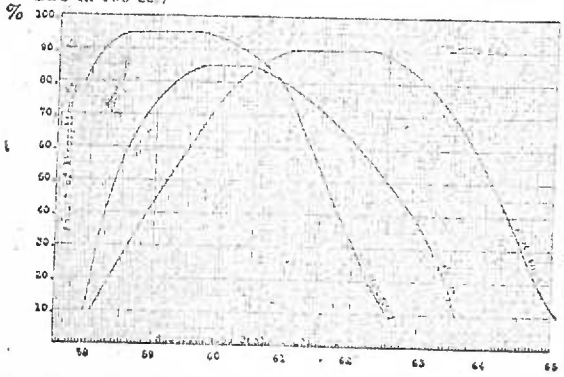

Casein copper (alkaline solution; 0.0162 g. CuO in 100 cc.)

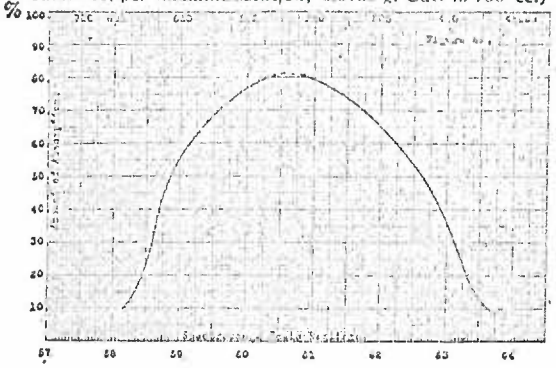

Witte peptone with copper ("semi-biuret") (alkaline solution; 0.0166 g. CuO in 100 cc.).
Witte peptone in excess ("biuret") (alkaline solution; 0.0162 g. CuO in 100 cc.)

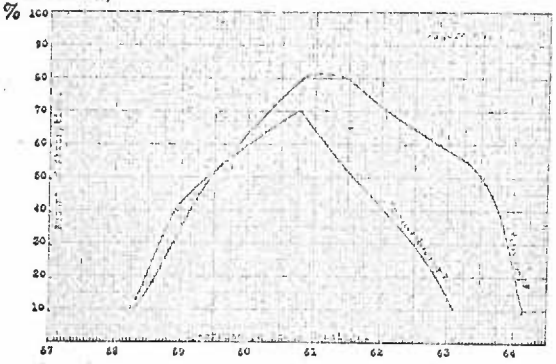

$Cu(biuret)_2$ ("biuret") (alkaline solution; 0.0628 g. CuO in 100 cc.)
$Cu(biuret)_1$ ("semi-biuret") (alkaline solution; 0.0628 g. CuO in 100 cc.)

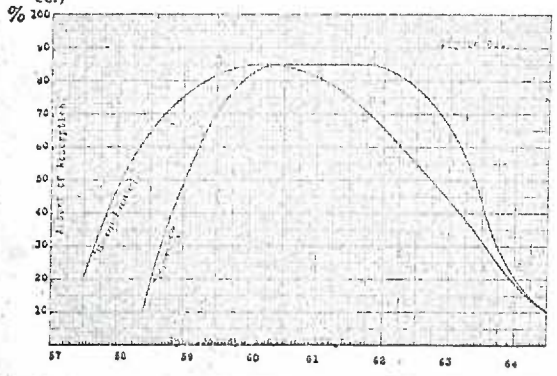

APPENDIX III

CALCULATED DISTRIBUTIONS OF Cu(II) IN GLYCINE, GLYCYL-GLYCINE, AND DIGLYCYLGLYCINE SOLUTIONS.

According to Dobbie, Kermack, and Lees (31)

According to Dobbie, and Kermack (32, and 33)

A: distribution of copper in form of cupric ions and copper–glycine complexes at various pH values in solutions containing 0·005M-$CuCl_2$, $2H_2O$ and different concentrations of glycine. *B*: comparison of observed and calculated optical densities of the solutions at various pH values. The figures are $\log I_0/I \times 10^3$ and have been adjusted to refer to a solution in which $[Cu_t] = 0{\cdot}005$M at each pH. G^- represents the glycine anion.

	A. Distribution of metal as			*B*. Optical densities at (mμ.)							
				600		650		700		750	
pH	Cu^{2+} (%)	CuG^+ (%)	CuG_2 (%)	Obs.	Calc.	Obs.	Calc.	Obs.	Calc.	Obs.	Calc.
				(*a*) Glycine concn., 0·005M (composition of solution as in Fig. 1)							
3·49	69·8	29·8	0·4	—	—	49	49	73	72	86	84
4·22	40·4	57·0	2·6	—	—	81	83	108	108	115	114
5·33	18·5	72·2	9·3	64	68	100	114	136	136	135	133
6·30	14·0	73·3	12·7	72	75	120	122	140	141	136	136
				(*b*) Glycine concn., 0·01M (composition of solution as in Fig. 2)							
3·35	58·6	40·5	0·9	—	—	62	62	88	86	97	96
4·41	13·7	73·3	13·0	74	76	122	122	141	142	135	136
5·25	2·5	56·0	41·5	122	124	160	161	155	156	130	131
6·51	0·1	19·0	80·9	181	181	201	201	158	159	108	109
				(*c*) Glycine concn., 0·02M (composition of solution as in Fig. 3)							
4·14	4·7	65·4	29·9	110	106	152	155	156	151	135	135
8·84	—	—	100·0	208	209	217	219	159	159	97	97
9·60	—	—	100·0	208	209	220	219	161	159	99	97

A: distribution of copper in form of cupric ions and copper–glycylglycine complexes at various pH values in solutions containing 0·005M-$CuCl_2,2H_2O$ and different concentrations of glycylglycine. *B*: comparison of observed and calculated optical densities of the solutions at various pH values. The figures are log $I_0/I \times 10^3$ and have been adjusted to refer to a solution in which $[Cu_0] = 0{\cdot}005$M at each pH. G^- represents the glycylglycine anion.

	A. Distribution of metal as				*B*. Optical densities at (mμ.)									
					550		600		650		700		750	
pH	Cu^{2+} (%)	CuG^+ (%)	CuG (%)	$CuG(OH^-)$ (%)	Obs.	Calc.	Obs.	Calc.	Obs.	Calc.	Obs.	Calc.	Obs.	Calc.
				(*a*) Glycylglycine concn., 0·005M (composition of solution as in Fig. 1)										
3·89	88·2	8·2	3·6	—	—	—	21	23	39	41	51	55	64	65
4·89	31·9	12·7	55·4	—	98	97	207	208	252	253	195	198	121	123
7·95	—	—	98·0	2·0	170	165	355	352	417	414	300	297	157	154
8·93	—	—	83·2	16·8	175	168	349	348	410	410	302	298	162	158
10·59	—	—	10·3	89·7	181	182	326	326	391	391	306	305	178	179

	A. Distribution of metal as					*B*. Optical densities at (mμ.)									
						550		600		650		700		750	
pH	Cu^{2+} (%)	CuG^+ (%)	CuG (%)	CuG_2^- (%)	CuG_2^{2-} (%)	Obs.	Calc.	Obs.	Calc.	Obs.	Calc.	Obs.	Calc.	Obs.	Calc.
					(*b*) Glycylglycine concn., 0·01M (composition of solution as in Fig. 2)										
4·12	64·5	20·4	15·1	—	—	—	—	75	73	103	102	105	103	94	92
5·16	4·3	10·4	84·8	0·5	—	144	146	307	311	368	369	270	273	148	150
6·90	—	0·2	80·1	19·7	—	180	178	361	364	408	410	284	286	137	140
7·83	—	—	49·3	50·5	0·2	203	199	382	383	402	401	264	271	139	143
9·00	—	—	29·6	66·2	4·2	216	211	388	390	395	398	254	262	137	140
10·43	—	—	18·6	30·2	51·2	198	196	350	351	382	381	274	276	155	155
11·00	—	—	12·0	12·0	76·0	188	189	330	331	375	372	282	282	163	162
					(*c*) Glycylglycine concn., 0·02M (composition of solution as in Fig. 4)										
4·06	51·4	29·5	19·1	—	—	—	—	90	95	127	130	131	127	112	106
5·60	0·2	4·1	91·5	4·2	—	150	163	330	341	401	402	304	289	163	158
7·23	—	—	40·3	59·6	0·1	199	205	380	388	401	402	272	266	141	141
8·67	—	—	7·2	90·2	2·6	222	227	402	405	390	394	252	250	133	135
10·07	—	—	3·0	55·7	41·3	216	211	378	370	381	381	256	263	138	143
11·07	—	—	0·6	11·8	87·6	194	191	331	327	364	366	275	281	156	164

A: distribution of copper in form of cupric ions and copper–diglycylglycine complexes at various pH values in solutions containing 0·005 M-$CuCl_2,2H_2O$ and different concentrations of diglycylglycine. *B*: comparison of observed and calculated optical densities of the solutions at various pH values. The figures are log $I_0/I \times 10^3$ and have been adjusted to refer to a solution in which $[Cu_0]=0{\cdot}005$ M at each pH. G^- represents the diglycylglycine anion.

	A. Distribution of metal as					*B*. Optical densities at (mμ.)									
						550		600		650		700		750	
pH	Cu^{2+} (%)	CuG^+ (%)	CuG (%)	CuG^- (%)	CuG_2^- (%)	Obs.	Calc.	Obs.	Calc.	Obs.	Calc.	Obs.	Calc.	Obs.	Calc.
						(*a*) Diglycylglycine concn., 0·005 M (composition of solution as in Fig. 1)									
5·06	58·0	24·2	17·5	0·2	0·1	—	—	59	60	102	100	113	116	107	110
5·93	15·1	12·3	65·9	5·6	1·1	118	113	218	213	288	282	257	255	174	176
6·95	1·3	0·9	51·3	45·8	0·7	415	426	413	417	328	331	224	223	131	127

	A. Distribution of metal as						*B*. Optical densities at (mμ.)											
							500		550		600		650		700		750	
pH	Cu^{2+} (%)	CuG^+ (%)	CuG (%)	CuG^- (%)	CuG_2^- (%)	CuG_2^{2-} (%)	Obs.	Calc.	Obs.	Calc.	Obs.	Calc.	Obs.	Calc.	Obs.	Calc.	Obs.	Calc.
							(*b*) Diglycylglycine concn., 0·01 M (composition of solution as in Fig. 2)											
4·83	52·5	33·1	14·1	0·1	0·2	—	—	—	—	—	—	—	—	—	94	95	115	116
5·78	1·9	17·9	68·1	4·1	5·4	—	—	—	115	111	227	225	306	303	276	275	186	190
6·86	—	0·9	41·7	30·2	26·3	0·9	171	167	342	338	380	376	327	329	228	228	133	132
7·88	—	—	7·1	53·9	28·3	10·7	294	294	527	529	463	464	280	288	143	143	59	59
10·36	—	—	—	61·7	0·3	38·0	272	273	616	617	476	475	236	234	86	87	—	—
							(*c*) Diglycylglycine concn., 0·02 M (composition of solution as in Fig. 3)											
4·53	53·2	38·5	8·2	0·1	—	—	—	—	—	—	—	—	83	78	114	104	119	111
5·82	1·3	15·4	64·1	4·2	15·0	—	—	—	124	125	236	243	303	315	271	276	184	187
6·82	—	0·6	27·0	17·9	52·7	1·8	116	120	264	273	337	345	313	320	218	220	128	129
7·97	—	—	2·8	26·5	48·2	22·5	194	198	369	373	371	372	264	268	148	149	79	77
9·22	—	—	0·2	29·9	7·5	62·4	276	277	445	445	360	358	193	196	83	86	—	—
11·31	—	—	—	30·4	0·1	69·5	286	290	454	456	361	356	186	184	73	76	—	—
							(*d*) Diglycylglycine concn., 0·03 M (composition of solution as in Fig. 4)											
4·65	34·9	50·4	14·2	0·1	0·4	—	—	—	—	—	62	61	112	111	144	137	143	136
5·53	2·5	26·7	57·0	1·9	11·9	—	—	—	92	94	194	207	268	283	253	261	182	187
6·87	—	0·4	17·5	13·0	66·6	2·5	103	104	246	251	329	334	308	314	215	211	126	123
8·18	—	—	1·1	17·3	46·4	35·2	179	180	327	331	334	336	243	246	139	139	75	73
9·44	—	—	—	19·0	5·4	75·6	255	252	390	391	315	316	170	175	79	79	—	—
11·28	—	—	—	19·3	0·1	80·6	261	261	397	399	316	313	166	166	71	72	—	—

BIBLIOGRAPHY

1. Albert, A. Quantitative Studies of the Avidity of Naturally Occurring Substances for Trace Metals 2. Amino-Acids Having Three ionizing Groups. Biochem. J., 1952. 690-698

2. Allen, H. C., Kokoszka, G. F., & Inskeep, R. G. The Electron Paramagnetic Resonance Spectrum of Some Tris-Complexes of Copper (II). J. Am. Chem. Soc., 1964. 86, 1023-1025.

3. Androes, G. M. & Calvin, M. Electron Paramagnetic Resonance in Biology. Biophys. L., 1962. 2 (No. 2, Pt. 2), 217-258.

4. Ballhausen, C. J. Introduction to Ligand Field Theory. New York; McGraw-Hill Book Company, Inc. 1962.

5. Beinert, H., Griffiths, D. E., Wharton, D. C. & Sands, R. H. Properties of the Copper Associated with Cytochrome Oxidase as Studied by Paramagnetic Resonance Spectroscopy. J. Biol. Chem., 1962. 237, 2337-2345.

6. Beinert, H. & Palmer, G. Oxidation-Reduction of the Copper Component of Cytochrome Oxidase. J. Biol. Chem., 1964. 239, 1221-1227.

7. Beinert, H. & Palmer, G. In King, T. E., Mason, H. S., and Morrison, M., (Eds.), Oxidases and Related Redox Systems, New York; Wiley, to be published.

8. Beinert, H. & Palmer, G. Contributions of EPR Spectroscopy to Our Knowledge of Oxidative Enzymes. In Nord, F. F., (Ed.) Advances in Enzymology, Vol. 27. New York; Interscience Publishers, 1965. pp. 105-198.

9. Beychok, S. & Blout, E. R. Optical Rotatory Dispersion of Sperm Whale Ferrihemoglobin. J. Mol. Biol., 1961. 3, 769-777.

10. Bjerrum, J. On the Tendency of the Metal Ions Toward Complex Formation. Chem. Rev., 1950. 46, 381-401.

11. Bjerrum, J., Ballhausen, C. J. & Jorgensen, C. K. Studies on Absorption Spectra I. Results of Calculations on the Spectra and Configuration of Copper (II) ions. Acta Chem. Scand., 1954. 8, 1275-1289.

12. Bleaney, B. & Stevens, K. W. H. Paramagnetic Resonance. Repts. Progr. in Phys., 1953. 16, 108-159.

13. Blumberg, W. E. In International Symposium on the Biochemistry of Copper. New York; Acedemic Press, 1966, to be published. personal communication).

14. Blumberg, W. E., Levine, W. G., Margolis, S. & Peisach, J. On the Nature of Copper in Two Proteins Obtained From Rhus Vernicifera Latex. Biochem. Biohys. Re. Comm., 1964. 15, 277-283.

15. Bond, A. D. Studies on Oxidative Phosphorylation - Oxidation of Quinol Phosphates. Unpublished doctor's dissertation, University of Oregon Medical School, 1964.

16. Bowers, K. D. & Owen, J. Paramagnetic Resonance II. Repts. Progr. in Phys., 1955. 18, 304-373.

17. Breslow, E. & Gurd, F. R. N. Interaction of Cupric and Zinc ions with Sperm Whale Metmyoglobin. J. Biol. Chem., 1963. 238, 1332-1342.

18. Brill, A. S. & Venable, J. H. Electron Paramagnetic Resonance in Single Crystals of Cupric Insulin. Nature, 1964. 203, 752-754.

19. Brill, A. S., Martin, R. B. & Williams, R. J. P. Copper in Biological Systems. In Electronic Aspects of Biochemistry (proceedings). Pullman, B. (Ed.), New York; Academic Press, 1964.

20. Broman, L., Malmstrom, B. G., Aasa, R. & Vanngard, T. The Role of Copper in the Catalytic Action of Laccase and Ceruloplasmin. Biochim. Biophys. Acta, 1963. 75, 365-376.

21. Carrington, A. The principles of electron-spin resonance. Endeavour, 1962. 51-57.

22. Chance, B. In International Symposium on the Biochemistry of Copper. New York; Acedemic Press, 1966, to be published. (personal communication).

23. Chouteau, J. Influence des fonctions ionisables sur la reactivite des liaisons peptidiques vis-a-vis des hydoxydes metalliques. C. R. Acad. Sci., Paris, 1951. 232, 2314-2315.

24. Chouteau, J. & Lenormant, H. Mise en evidence par spectrographie infrarouge de la fixation des ions bivalents sur la liaison peptidique. C. R. Acad. Sci., Paris, 1951. 232, 1479-1481.

25. Condon, E. U. & Shortley, G. H. The Theory of Atomic Spectra. Cambridge; Cambridge at the University Press, 1963.

26. Cooper, T., Freeman, H. C., Robinson, G. & Schoone, J. C. Model Compounds for Metal-Protein Interaction: Crystal Structures of Two Glycylglycylglycine-Copper Complexes. Nature, 1962. 194, 1237-1239.

27. Corey, E. J. & Sneen, R. A. Calculation of Molecular Geometry by Vector Analysis. Application to Six-membered Alicyclic Rings. J. Am. Chem. Soc., 1955. 77, 2505-2509.

28. Corey, E. J. & Bailar, J. C. The Stereochemistry of Complex Inorganic Compounds. XXII. Stereospecific Effects in Complex Ions. J. Am. Chem. Soc., 1959. 81, 2620-2629.

29. Curzon, G. Reversible decolorization of Caeruloplasmin under Acid Conditions. Biochim. Biophys. Acta, 1963. 71, 249-250.

30. Datta, S. P., Leberman, R. & Rabin, B. R. The Chelation of Metal Ions by Dipeptides and Related Substances Part 5.--Cupric Complexes of Sarcosyl and Leucyl Ligands. Trans. Faraday Soc., 1959. 55, 2141-2151.

31. Dobbie, H., Kermack, W. O. & Lees, H. Complex-Formation between Poly-peptides and Metals I. Application of Various Experimental Methods to the Glycine-Copper System. Biochem. J., 1955. 59, 240-246.

32. Dobbie, H. & Kermack, W. O. Complex-Formation between Polypeptides and Metals 2. The Reaction Between Cupric Ions and Some Dipeptides. Biochem. J., 1955. 59, 246-257.

33. Dobbie, H. & Kermack, W. O. Complex-Formation between Polypeptides and Metals 3. The Reaction Between Cupric Ions and Diglycylglycine. Biochem. J., 1955. 59, 257-264.

34. Doran, M. A., Chaberek, S. & Martell, A. E. Copper (II) Chelates of Histidylhistidine and Related Compounds. J. Am. Chem. Soc., 1964. 86, 2129-2135.

35. Drey, C. N. C. & Fruton, J. S. Metal Chelates of a Bis-imidazole. Biochem., 1965. 4, 1258-1263.

36. Ehrenberg, A. & Yonetani, T. Magnetic Properties of Iron and Copper in Cytochrome Oxidase. Acta Chem. Scand., 1961. 15, 1071-1080.

37. Eyring, H. & Urry, D. W., Biological Electron Transport. I. Imidazole Pump Model of Electron Transport: a Group Transfer Model. J. Theor. Biol., 1965. 8, 198-214.

38. Eyring, H., Walter, J. & Kimball, G. E. Quantum Chemistry. New York; John Wiley & Sons, Inc. 1960

39. Freeman, H. C. & Taylor, M. R. Model Compounds for Metal-Protein Interaction: The Crystal Structure of Disodium Glycylglycylglycylglycinocuprate (II) Decahydrate. Proceedings Chem. Soc., 1964. pp. 88-89.

40. Gersmann, H. R. & Swalen, J. D. Electron Paramagnetic Resonance Spectra of Copper Complexes. J. Chem. Phys., 1962. 36, 3221-3233.

41. Gomori, G. Preparation of buffers for use in enzyme studies. In Colowick, S. P., & Kaplan, N. O. (Eds.), Methods in Enzymology. Vol. I. New York; Academic Press, 1955, 138-146.

42. Greenstein, J. P. & Winitz, M. Chemistry of the Amino Acids. Vol. II. New York; John Wiley & Sons, Inc. 1961.

43. Griffiths, D. E. & Wharton, D. C. Studies of the Electron Transport System XXXV. Purification and Properties of Cytochrome Oxidase. J. Biol. Chem., 1961. 236, 1850-18 .

44. Gurd, F. R. N. & Breslow, E. Reaction of Sperm Whale Metmyoglobin toward Hydrogen Ions and p-Nitrophenylacetate. J. Biol. Chem., 1962. 237, 371-381.

45. Hemmerich, P. In International Symposium on the Biochemistry of Copper. New York; Acedemic Press, 1966, to be published. (personal communication).

46. Holton, W. C. & Blum, H. Paramagnetic Resonance of F Centers in Alkali Halides. Phys. Rev., 1962. 125, 89-103.

47. Ingraham, L. In King, T. E., Mason, H. S., and Morrison, M. (Eds.), Oxidases and Related Redox Systems, New York; Wiley, to be published.

48. Karipides, A. G. & Piper, T. S. Optical Activity of Coordination Compounds. II. A Molecular Orbital Model and an Analysis of Experimental Data for Complexes of Trigonal Symmetry. J. Chem. Phys., 1964. 40, 674-682.

49. Kauzmann, W. Quantum Chemistry. New York; Academic Press Inc. 1957.

50. Kendrew, F. C., Watson, H. C., Strandberg, B. E. & Dickerson, R. E. A Partial Determination by X-Ray Methods, and its Correlation with Chemical Data. Nature, 1961. 190,666-672.

51. Kim, M. K. & Martell, A. E. Copper (II) Complexes of Glycylglycine. Biochem., 1964. 3, 1169-1174.

52. Kivelson, D. & Neiman, R. ESR Studies on the Bonding in Copper Complexes. J. Chem. Phys., 1961. 35, 149-155.

53. Klotz, I. M., Urquhart, J. M., Klotz, T. A. & Ayers, J. Slow Intracolecular Changes in Copper Complexes of Serum Albumin. The Role of Neighboring Groups in Protein Reactions. J. Am. Chem. Soc., 1955. 77, 1919-1925.

54. Klotz, I., Czerlinski, G. H. & Fiess, H. A. A Mixed-valence Copper Complex with Thiol Compounds. J. Am. Chem. Soc., 1958. 80, 2920-2923.

55. Klotz, I. M. & Frank, B. H. Deuterium-Hydrogen Exchange in Amide N-H Groups. J. Am. Chem. Soc., 1965. 87, 2721-2728.

56. Kneubuhl, F. K. Line Shapes of Electron Paramagnetic Resonance Signals Produced by Powders, Glasses, and Viscous Liquids. J. Chem. Phys., 1960. 33, 1074-1077.

57. Kober, P. A. & Sugiura, K. The Copper Salts of Amino Acids, Peptides, and Peptones. 8th Intern. Congr. Appl. Chem., 1912. 6, 165-184.

58. Kober, P. A. & Haw, A. B. Spectrophotometric Study of Copper Complexes and the Biuret Reaction. J. Am. Chem. Soc., 1916. 38, 457-472.

59. Kolthoff, I. M. & Lingane, J. J. Polarography. New York; Interscience Publishers. 1952.

60. Koltun, W. L., Roth, R. H. & Gurd, F. R. N. Reactions of Glycine-containing Peptides with Cupric Ions and with p-Nitrophenyl Acetate. J. Biol. Chem., 1963. 238, 124-131.

61. Koltun, W. L., Ng, L. & Gurd, F. R. N. Reactivity of Peptide Imidazole, Amino, and Phenolic Groups towards p-Nitrophenyl Acetate. J. Biol. Chem., 1963. 238, 1367-1372.

62. Kubowitz, F. Spaltung and Resynthese der Polyphenoloxydase und des Hamocyanins. Biochem. Z., 1938. 299, 32-57.

63. Landau, L. D. & Lifshitz, E. M. Quantum Mechanics Non-Relativistic Theory. Reading, Mass.; Addison-Wesley Publishing Company, Inc. 1958.

64. Ley, H. & Werner, F. Salz- und Komplexsalz-Bildung bei Imidverbindungen. (10. Mitteilung uber innere Komplexsalze.) Ber. chem. Ges..1913. 46, 4040 in Kober, P. A. & Haw, A. B., J. Am. Chem. Soc., 1916. 38, 457-472.

65. Lindskog, S. & Malmstrom, B. G. Metal Binding and Catalytic Activity in Bovine Carbonic Anhydrase. J. Biol. Chem., 1962. 237, 1129-1137.

66. Maki, A. H. & McGarvey, B. R. Electron Spin Resonance in Transition Metal Chelates. I. Copper (II) Bis-Acetylacetonate. J. Chem. Phys., 1958. 32-34.

67. Maki, A. H. & McGarvey, B. R. Electron Spin Resonance in Transition Metal Chelates. II. Copper (II) Bis-Salicylaldehyde-Imine. J. Chem. Phys., 1958. 29, 35-38.

68.2 Malmstrom, B. G. In King, T. E., Mason, H. S., and Morrison, M. (Eds.), Oxidases and Related Redox Systems, New York; Wiley, to be published.

69. Malmstrom, B. G., Vanngard, T. & Larsson, M. An Electron-Spin-Resonance Study of the Interaction of Manganous Ions with Enolase and Its Substrate. Biochim. et Biohys. Acta, 1958. 30, 1-5.

70. Malmstrom, B. G., Mosbach, R. & Vanngard, T. An Electron Spin Resonance Study of the State of Copper in Fungal Laccase. Nature, 1959. 183, 321-322.

71. Malmstrom, B. G. & Vanngard, T. Electron Spin Resonance of Copper Proteins and Some Model Complexes. J. Mol. Biol. 1960. 2, 118-124.

72. Malmstrom, B. G. & Neilands, J. B. Metalloproteins. In Annual Review of Biochemistry. Snell, E. E., Lick, J. M., Boyer, P. D., & Mackinney, G. (Eds.), Vol. 33, Palo Alto; Annual Reviews, Inc., 1964.

73. Manyak, A. R., Murphy, C. B. & Martell, A. E. Metal Chelate Compounds of Glycylglycine and Glycylglycylglycine. Arch. Biochem. Biophys., 1955. 59, 373-382.

74. Martell, A. E. Metal Chelate Compounds. In Annual Review of Physical Chemistry. Rollefson, G. K. & Powell, R. E. (Eds.), Vol. 6, Stanford, Annual Reviews, Inc., 1955.

75. Mason, H. S. An ESR Study of Pseudomonas Copper-Protein. Biochem. Biophys. Re. Comm., 1963. 10, 11-13.

76. Mason, H. S. Oxidases. In Annual Review of Biochemistry, Vol. 34. Palo Alto; Annual Reviews, Inc., 1965. pp. 595-634.

77. Mason, S. F. & Norman, B. J. Origins of the Optical Activity of Coordination Compounds. Chem. Comm. 1965. No. 3, 48-49.

78. McCaffery, A. J., Mason, S. F. & Norman, B. J. The Effect of Ring Conformation on the Optical Activity of Transition-Metal Complexes. Chem. Comm. 1965. No. 3, 49-50.

79. McConnell, H. M. Effect of Anisotropic Hyperfine Interactions on Paramagnetic Relaxation in Liquids. J. Chem. Phys., 1956. 25, 709-711.

80. McGarvey, B. R. Paramagnetic Resonance in Copper Chelates. J. Phys. Chem., 1956. 60, 71-76.

81. Menzel, D. H. Mathematical Physics. New York; Prentice-Hall, Inc., 1953.

82. Milford, F. J. Hyperfine Interaction and the Knight Shift. Am. J. Phys., 1960. 28, 521-527.

83. Morrison, M., Horie, S. & Mason, H. S. Cytochrome c Oxidase Components II. A Study of the Copper in Cytochrome c Oxidase. J. Biol. Chem., 1963. 238, 2220-2224.

84. Murphy, C. B. & Martell, A. E. Metal Chelates of Glycine and Glycine Peptides. J. Biol. Chem., 1957. 226, 37-50.

85. Neiman, R. & Kivelson, D. ESR Line Shapes in Glasses of Copper Complexes. J. Chem. Phys., 1961. 35, 156-161.

86. Orgel, L. E. An Introduction to Transition-Metal Chemistry; Ligand Field Theory. London; Methuen and Co., Ltd., 1960.

87. Pake, G. E. Paramagnetic Pesonance. New York; W. A. Benjamin, Inc. 1962.

88. Pauling, L. The Nature of the Chemical Bond. Ithica; Cornell University Press. 1960.

89. Pauling, L. & Wilson, E. B. Introduction to Quantum Mechanics. New York; McGraw-Hill Book Company, Inc. 1935.

90. Piper, T. S. & Karipides, A. Optical activity of trigonal coordination compounds. Mol. Phys., 1962. 5, 475-483.

91. Pullman, B., Spanjaard, C. & Berthier, G. Features of the Electronic Structure of the Iron-Porphyrin Complexes with Special Reference to the Oxido-Reductive Properties of Cytochromes. Proc. Nat. Acad. Sci., 1960. 46, 1011-1020.

92. Rabin, B. R. Metal Peptide Complexes and Proteolytic Enzymes. Bull. Soc. Chim. Biol., 1960. 42, 1247-1261.

93. Rising, M. M. & Johnson, C. A. The Biuret Reaction. I. The Biuret Reaction of Acid Imides of the Barbituric Acid Type. J. Biol. Chem., 1928. 80, 709-722.

94. Rising, M. M. & Yang, P. S. The Biuret Reaction. III. The Biuret Reaction of Amino Acid Amides. J. Biol. Chem., 1933. 99, 755-765.

95. Rising, M. M., Parker, F. M. & Gaston, D. R. The Biuret Reaction. IV. (a) A Biuret Salt of the Tetrapeptide Triglycylglycine. (b) A Biuret Salt of Glycine Anhydride. (c) The Barium Biuret Salt of Succinimide. J. Am. Chem. Soc., 1934. 56, 1178-1180.

96. Ritthausen, H., J. prakt. Chem., 1873. 7, 361. In Rising, M. M. & Johnson, C. A., J. Biol. Chem., 1928. 80, 709-722.

97. Rivkind, A. I. Paramagnetic resonance in solutions of complex copper salts and the frequency of Brownian rotation of the complexes. Zhur. Fix. Khim., 1961. 35, 2099-2107.

98. Sands, R. H. Paramagnetic Resonance Absorption in Glass. Phys. Rev., 1955. 99, 1222-1226.

99. Schiff, H., Ber. chem. Ges., 1896, 24, 298. In Rising, M. M. & Johnson, C. A., J. Biol. Chem., 1928. 80, 709-722.

100. Schlichtkrull, J. Insulin Crystals. II. Shape of Rhombohedral Zinc-Insulin Crystals in Relation to Species and Crystallization Media. Acta Chem. Scand., 1956. 10, 1459-1464.

101. Sogo, P. B. & Tolbert, B. M. Nuclear and Electron Paramagnetic Resonance and Its Application to Biology. In Advances in Biological and Medical Physics. Lawrence, J. H. and Tobias, C. A. (Eds.), Vol. V. New York; Academic Press, Inc., 1957.

102. Strandberg, B., Lindqvist, I. & Rosenstein, R. The crystal structure of copper (II) monoglycylglycine trihydrate $Cu(NH_2CH_2CONCH_2COO) \cdot 3H_20$. Z. Krist., 1961. 116, 266-289.

103. Strickland, R. D., Freeman, M. L. & Gurule, F. T. Copper Binding by Proteins in Alkaline Solution. Anal. Chem., 1961. 33, 545-552.

104. Tanford, C. The Effect of pH on the Combination of Serum Albumin with Metals. J. Am. Chem. Soc., 1952. 74, 211-215.

105. Tanford, C. & Epstein, J. The Physical Chemistry of Insulin. II. Hydrogen Ion Titration Curve of Crystalline Zinc Insulin. The Nature of its Combination with Zinc. J. Am. Chem. Soc., 1954. 76, 2170-2176.

106. Tschugaeff, L. Ueber complese Verbindungen organischer Imide. Succinimidkupfer-Derivate. Ber. chem. Ges., 1905. 38, 2899.

107. Uhlenbeck, G. E. & Goudsmit, S. Spinning Electrons and the Structure of Spectra. Nature, 1926. 117, 264-265.

108. Ultee, C. J. Electron Spin Resonance of ^{15}N Atoms. J. Chem. Phys., 1965. 43, 1080-1081.

109. Venable, J. H. Magnetic Methods for Protein Single Crystals: Metal Binding to Insulin. Unpublished doctor's dissertation, Yale University, 1965.

110. Vogel, A. I. Practical Organic Chemistry. London; Longmans. 1961

111. Warner, R. C. & Weber, I. The Metal Combining Properties of Conalbumin. J. Am. Chem. Soc., 1953. 75, 5094-5101.

112. Wenaas, P. E. The Biuret Reaction of the Pentapeptide Tetraglycylglycine. J. Am. Chem. Soc., 1937. 59, 1353-1354.

113. Wertz, J. E. Nuclear and Electronic Spin Magnetic Resonance. Chem. Rev., 1955. 55, 829-955.

114. Wiedeman, G., Ann. Chem., 1848. 68, 323. In Rising, M. M. & Johnson, C. A., J. Biol. Chem., 1928. 80, 709-722.

115. Wiersema, A. K. & Windle, J. J. Electron Paramagnetic Resonance of Some Nitrogen-Bonded Copper Chelates. J. Phys. Chem., 1964. 68, 2316-2320.

116. Windle, J. J., Wiersema, A. K., Clark, J. R. & Feeney, R. E. Investigation of the Iron and Copper Complexes of Avian Conalbumins and Human Transferrins by Electron Paramagnetic Resonance. Biochem., 2, 1341-1345.

117. Yamazaki, I. & Piette, H. Mechanism of Free Radical Formation and Disappearance During the Ascorbic Acid Oxidase and Peroxidase Reactions. Biochim. Biophys. Acta, 1961. 50, 62-69.